ISSN **2960-9534**

JOURNAL OF THE GEORGIAN CERAMISTS' ASSOCIATION

CERAMICS, SCIENCE AND ADVANCED TECHNOLOGIES

Scientific, technical and industrial illustrated, registered, referral magazine

Vol. 25. 2(50).2023

Guidelines for submitting an article to the journal

- It is necessary to submit, one hardcopy of the article, as well as an electronic versionin English language, to editorial office.
- The length of the article is not limited to pages (including tables and images with appropriate numbering). Interval 1.5. Program-Sylfaen. Font size 12, the article must be accompanied by an abstract in Georgian of no more than 300 words.
- The article should use International System of Units (SI), as well as those units that are equated to this system.
- Mathematical and chemical formulas should be clearly indicated so that the difference between Capital (upper case) and Nuskhuri (Georgian script AD 800-1100) (lower case) letters, quality coefficient and co-multiplier can be easily discerned. All letter designations in the text of the article and formula are subject to decoding. Different concepts can not be represented by the same symbol.
- The literary source should be indicated at the end of the article as follows: for a book - indicating the author, title, title of publication, place of publication, year of publication and total number of pages;

  for a journal - indicating the author of the article, the name of the journal, year of publication, volume, number, beginning and end pages of the article;

  Foreign surnames, the title of the book and journal must be in the original language without abbreviation, it is not allowed to refer to unpublished work.
- When using a copyright certificate, it is necessary to refer to the bulletin of the invention (where the formula of the invention is published) indicating the number and year of publication.
- Pictures and drawings should be presented only in text in one copy in computerized form, they should not be overloaded with details and inscriptions. The position must be indicated by numbers and decoded by inscriptions under the picture;
- The article must be signed by one of the authors. It is necessary to indicate place of work, position, scientific degree, and telephone number.
- The publishing fee for foreign authors not residing in Georgia makes up 100 euros. It's free for authors residing in Georgia.

CONTENTS

UDC 543.42

DETERMINATION OF THE AMOUNT OF LEAD BY ATOMIC-ABSORPTION SPECTROPHOTOMETRY IN HYGIENIC AND COSMETIC PRODUCTS

N. Amashukeli. N.Rachvelishvili

Department of Chemical and Biological Technologies, Technical University of Georgia, Georgia, 0175, Tbilisi, Kostava Str. 69

E-mail: natamashukeli@mail.com

Resume: **Purpose**. Cosmetic and hygiene products are used by people of all ages on a daily basis. Of course, it is important for health to determine their safety. Continuous analytical express control at all stages of production is important in the technological processes of factories in order to make timely changes and eliminate complaints.

The aim of the research is to determine the amount of lead in toothpaste. People use toothpaste every day, so it is important to maintain the limit content of metals, in particular lead.

Method: the atomic-absorption spectrophotometric research method was chosen.

In the perfumery-cosmetics industry, the atomic-absorption method is used for the determination of metals in finished cosmetic products, semi-products of their synthesis, and raw materials. Metals belong to the number of toxic impurities, so it is very important to know the metal content, which should not exceed the permissible limit.

Results: during the conducted research, it was established that the atomic-absorption spectrophotometric research method determines the lead content in hygiene products with high accuracy.

Conclusion: It was found that the toothpaste meets the safe lead content set by the European Union. It does not exceed 0.0015%.

Key words: hygiene products, lead, atomic-absorption spectrophotometry.

1. INTRODUCTION

Cosmetic and hygiene products are products that serve to clean and beautify the human body. Some products are both cosmetic and medicinal substances. For example: Shampoo is a hair cleanser and this product contains anti-dandruff ingredients that are medicinal in nature. Toothpaste contains fluoride, which protects teeth from caries. The cosmetic function of the toothpaste is to whiten the teeth, and the fluoride content belongs to the group of non-prescription drugs. Deodorants mask odor, this product is also an antiperspirant. Mouthwashes are a remedy for inflammation of the gums. The foundation cream contains a protective factor against the harmful effects of the sun. The facial cleanser contains an active substance for treating or preventing acne. Hand soap contains antibacterial substances that kill disease-causing germs.

In the European Union, cosmetics are regulated by the 2009 regulation. This statute is aimed at

protecting the health of the user, through thorough informing and monitoring of the composition. According to the statute, a cosmetic product is a substance or solution of substances intended for contact with body parts: epidermis (skin), hair covering, nails and teeth. The same substances are considered to be curative and prophylactic. There are different types of such products, for example: cosmeceuticals, organic or natural cosmetics, hypoallergenic cosmetics. Cosmetics contain vitamins, antioxidants, proteins and others.

Consumer demand for products containing organic ingredients is increasing. It is believed that these ingredients are healthier and safer for the human body. This is not absolute truth. The source of their origin does not determine its safety. There are many toxins produced by animals and plants that are poisonous to the human body.

For many consumers, names such as aloe extract, lemon seed extract, chamomile extract sound safer. However, it should be noted that these ingredients can be synthesized in laboratories with the same chemical structure and physical properties.

Thus, the name of the ingredients does not mean that it is of natural origin. The problem with natural ingredients is that synthetic substances are used in the cultivation of the plants, which are also found in the products. In addition, there is no safety profile for a number of natural ingredients that can cause allergic reactions or other side effects. Therefore, people should be careful when using natural ingredients.

Hypoallergenic cosmetics are products that cause allergies less than other products. Users with hypersensitive skin may consider these cosmetics to be safer, although there is no standard that assigns this definition to the product. The manufacturer assigns this value, therefore, the allergic consumer should check the list of ingredients on the product label.

There are many physico-chemical methods of lead research, for example

1. Optical methods, namely: photocolorimetry and spectral analysis. 2. Electrical methods, for example: potentiometry, conductometry and others.

3. Chromatographic analysis methods and others

In the perfumery-cosmetics industry, the atomic-absorption method is used for the determination of metals in finished cosmetic products, semi-products of their synthesis, and raw materials. Metals belong to the number of toxic impurities, so it is very important to know the metal content, which should not exceed the permissible limit.

Atomic absorption spectrophotometry is based on the measurement of resonance absorption of unexcited atoms in the free state. When an atom is excited, the most possible energy level change is its transition to a level close to the initial energy state, i.e. resonance transition.

If we irradiate an unexcited atom with a resonant transition frequency, the atom will absorb a quantum and the radiation will decrease. This phenomenon is the basis of atomic absorption spectrophotometry. If the concentration of a substance in emission spectroscopy is related to the intensity of radiation, which is directly proportional to the number of excited atoms, in

atomic-absorption spectrophotometry the analytical signal (decrease in intensity of radiation) is related to the number of non-excited atoms, which in the flame are much more than excited atoms. Since the energies of absorption and emission are equal in the vapor state, the energy emitted by the same element is used as the source of excitation, that is, the so-called resonant waves. Theoretically, the width of this waveband is equal to 10-5 nm, no monochromator emits such a narrow band, and it must have a high energy to excite atoms in the vapor state.

This issue was solved when the so-called Resonant lamps. It represents lamps with a hollow cathode. The cathode is made of the same element that produces the determination. If the cathode is made of another element, then it is covered with a thin layer of the same element. A metal rod placed next to the cathode is used as the anode. Neon or argon is placed in the lamp. When the cathode is bombarded, it goes into an excited state and gives a powerful flow of resonant radiation.

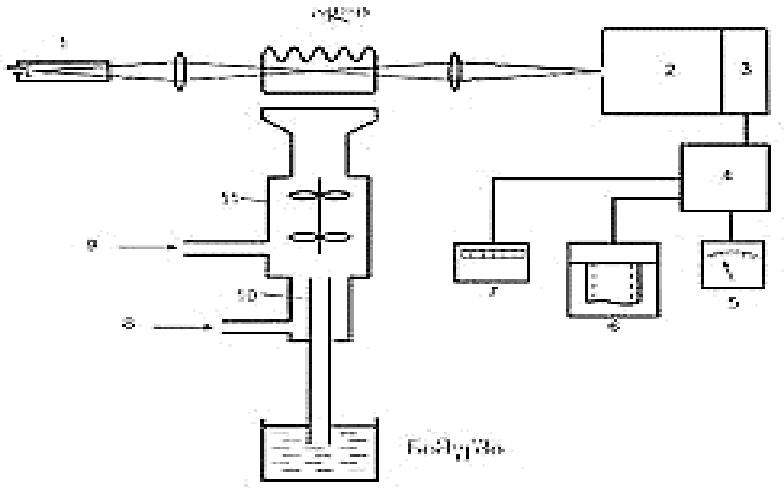

A light beam from the resonant radiation source (1) is directed into the flame, into which the finely dispersed aerosol of the analysis sample is sprayed. The resonant radiation lines in the spectrum are separated by a monochromator (2) and directed to a photoelectric detector (3) (a conventional photomultiplier). After the amplifier (4), the output signal from the detector is recorded by a galvanometer (5), a digital voltmeter, or a recording potentiometer (6). 11).

Resonance radiation is measured twice, first before and after spraying the test sample. The magnitude of the analyzed signal is determined by the difference between these two brightnesses.

In order to obtain a flame, various combinations of fuel gas and oxidizing agents are used, such as hydrogen, propane, acetylene mixture with air, or nitrous oxide. The mixture can be stoichiometric, more or less than that. If the mixture is less than stoichiometric, it is called depleted, and more than stoichiometric, it is called enriched.

Oxygen in its pure form as an oxidizing agent is almost never used, because when the fuel gas is mixed with it, the combustion takes place at a high speed and is not subject to control.

The laminar flame consists of three zones, the first reaction zone is 1 mm wide and the temperature is not less than 10000C. Hydrolysis of gasses takes place in this zone, atomization is insignificant and this zone is not used for analysis. There is an excess of fuel gasses in the inner cone zone. Therefore, negatively charged radicals and molecules that are characterized by reducing action prevail in it: C2, CN, CO, CH, H2, NH. In this zone, the temperature is maximum for the given gasses. In the inner zone, the absorption of elements that produce stable oxides or hydrogen oxides (aluminum, molybdenum, etc.) is observed.

In the second reaction zone, the oxidation of fuel gasses goes to the end with the formation of CO2 and H2O in the case of hydrocarbons. In this zone, the absorption of elements that do not produce thermally stable oxides (copper, silver, gold, zinc, manganese, etc.) is observed. Definitions are characterized by stability in this zone.

In atomic-absorption spectrophotometry, two types of flame are used: air-acetylene, and nitrogen (1) oxide-acetylene. The first is used in the determination of alkaline and alkaline earth elements. This impurity is characterized by high transparency in the 200 nm wavelength region, weak self-emission and provides highly efficient atomization of more than 30 elements.

A mixture of acetylene and nitrous oxide has a temperature of almost 900 K. The flame is characterized by high transparency in the entire wavelength range (190-850 nm). This gives the ability to determine more than 70 elements with a sensitivity of 10-4-10-10 g.

The second important block is the atomization block, which has a lot in common with flame photometry: atomizer, oxidizer, flame. The difference is that a more sophisticated system is used here. A smaller number is required. The flame plays the role of a cuvette, because in atomic-absorption spectrophotometry Berry's law is observed, the sensitivity of the method depends on the length of the absorbing layer of the flame. For this purpose, hole lamps have been introduced, which gives a thin flat lamp with a long absorbing layer, in the upper part of which there is a 12 cm long hole, it provides a laminar flow of gas. The premixed fuel and oxidizer mixture is separated from the reaction zone through this hole. When determining large concentrations, it is necessary to dilute the solution or turn the lamp by 900, as a result of which the length of the absorbing layer changes.

The atomization block includes a sprayer. When using conventional sprinklers, 5% of the useful signal comes, 95% of large drops condense and fall, due to which the solution consumption is high, 10 ml per minute is needed. Therefore, it is necessary to use more complex sprinklers, in which condensed drops return to the initial state, as a result of which the cost is reduced to 0.1-0.5 ml.

A monochromator is needed to remove the radiation of inert gasses, the flame's own radiation, and most importantly, the radiation produced by the excitation of the accompanying elements, which ensures the linear dependence of the solidified graph.

detector. An important problem of atomic-absorption spectrophotometry is the emission of atoms in a non-excited state in a flame. If it is not excluded, their emission creates a background when the concentration increases, which causes a deviation from Berry's law. This can be avoided by using two types of modulation: electronic and mechanical.

In electronic modulation, a relay is used, which turns off the resonant light for a few seconds in a certain period of time.

In mechanical modulation, to achieve the same effect, a rotating interrupter disk is placed between the lamp and the system, which measures the flame emission I1 at the moment of overlap, and when the interrupter is open, then the radiation received in the detector will be the total effect I1+I2. The detector emits a useful signal, the amplification of which is produced by means of a special amplifier block. Registration is done using a microammeter, the results are calculated using a microammeter, and the results are calculated on a more complex block where the results are printed.

2. MAIN PART

Quantification is done by constructing a non-scalable graph or by the method of additions.

When constructing a non-condensing graph, they measure the optical density of several standard solutions and construct a dependence graph in the optical density-concentration coordinates, after which they determine the optical density of the analytical solution under the same conditions and find its concentration using the graph.

When using the additive method, the optical density Ax of the analytical solution is first measured, then a standard solution is introduced into it in a certain volume and the optical density Ax+st is measured. If the concentration of the analytical solution is Cx, and Cst is the concentration of the standard solution, then

$$Ax = KhC$$

$$Ax+st= Kh(Cx + Cst)$$

Since K and h are constant, we get:

$$Ax/Ax+st = Cx/Cx+st \text{ hence } Cx=Cst.$$

$$Ax/Ax+st- Ax$$

The main source of error in the method is non-selective absorption, the extent of which increases with increasing the total concentration of the analyte solution. This is where the elements of turbidimetry come into play. Micro-droplets are included in the flame. If the concentration is high, solid particles are formed in the flame, which cannot absorb and scatter the resonant radiation. It is converted into a useful signal. This is non-selective absorption. To exclude this fact, it is necessary to dilute the solution or measure the non-selective absorbance and make an appropriate correction to the result.

Atomic-absorption spectrophotometry is a universal analysis method that can be used both at low element content and at high concentrations. As with atomic emission analysis, it is not necessary to remove the components of the mixture. Preliminary preparation of the sample is carried out only by opening it. It allows measuring more than 70 elements with a sensitivity of 10-4-10-6 g/ml, a repeatability of 3-5% if the excitation source is a flame, and 1-2% when using non-volatile atomizers.

Determination of lead in toothpaste.

The method is based on the absorption of resonance radiation of the 283.3 nm spectral line of lead ions in a propane-butane air flame, obtained from a hollow cathode lamp.

They prepare a toothpaste solution in advance. The weight of toothpaste weighed on an analytical scale (1 g) is treated with 15 cm3 of nitric acid (1:1) and heated. The solution is cooled, quantitatively transferred to a measuring flask with a capacity of 100 cm3 and filled to the brim with ethyl alcohol.

Reagents and equipment used

1. Lead nitrate

2. Nitric acid solution, diluted 1:1.

3. Atomic absorption spectrophotometer AAS-1 with a hole lamp

4. Atomizer: propane-butane-air.

5. Hollow cathode lamp.

They prepare a standard lead solution of 1000mg/ml: 1,559g of Pb (NO_3)_2 are dissolved in distilled water by adding 1ml of concentrated nitric acid, transferred to a liter measuring flask, brought to volume with distilled water and shaken well. The working solution with a concentration of 100 mg/ml is prepared as follows: transfer 10 ml of the basic solution to a measuring flask, bring the volume up to the mark with distilled water and shake well.

5, 10, 15, 20 and 25 ml lead solutions are placed in 5 100 ml measuring flasks, the volume is brought to the well with distilled water and shaken well.

They turn on the tool, put the hollow cathode lamp on the lead into working condition and warm up the electrical system for 15-20 minutes. With the maximum deviation of the galvanometer of the device, the analytical line of lead at 283.3 nm is taken out on the hole of the mono-chromator. The T meter on the conductivity scale is set to "100" or "0" when changing the hole width on the absorbance A scale. The width of the hole should not exceed 0.1 mm, otherwise the power of the photomultiplier or the degree of amplification will be increased. At the beginning of the test, the air consumption (480 l/h) is set according to the rotometer, then the propane-butane mixture and ignited. The fuel starts burning before the gas supply. They check the operation of the sprinkler and the stability of the flame. The inner cone of the flame should have a minimum height while maintaining a greenish-blue color. The zero adjustment on the instrument is carried out by spraying distilled water into the flame. Photometry of standard solutions is carried out at least 3 times and the obtained graph in coordinates: absorption-lead concentration, μg/ml

The analytical solution is transferred to a 100 ml measuring flask. They bring the volume to the well with distilled water and shake well. Photometry of the obtained solution is carried out in the same way as in the case of standard solutions, at least 6 times. The concentration of lead in the test solution is found by means of a non-cooling graph.

3. CONCLUSION

It was found that the toothpaste meets the safe lead content set by the European Union. It does not exceed 0.0015%.

REFERENCES

1. M. Tsintsadze, A. Mamulashvili, T. Giorgadze, N. Gegeshidze, N. Killasonia. Inorganic chemistry. First part. Tbilisi Technical University 2008.
2. M. Tsintsadze, A. Mamulashvili, T. Giorgadze, N. Gegeshidze, N. Killasonia. Inorganic chemistry. second part. Tbilisi Technical University 2008.
3. L. Bokuchava, N. Bokuchava, D. Jincharadze. Analysis of perfumery and cosmetic products and raw materials. Technical University, Tbilisi, 2013.
4. Ts. Physico-chemical methods of Ghudushauri analysis. Tbilisi 2008.
5. Bocca, B., Pino, A., Alimonti, A. and Forte, G., 2014. Toxic metals contained in cosmetics: A status report. Regulatory Toxicology and Pharmacology, 68(3), pp.447-467 https://pubmed.ncbi.nlm.nih.gov/24530804/
6. Celeiro, M., Rubio, L., Garcia-Jares, C. and Lores, M., 2021a. Multi-Target Strategy to Uncover Unexpected Compounds in Rinse-Off and Leave-On Cosmetics. Molecules, 26(9). https://www.mdpi.com/1420-3049/26/9/2504
7. Deconinck, E., Bothy, J., Desmedt, B., Courselle, P. and De Beer, J., 2014. Detection of whitening agents in illegal cosmetics using attenuated total reflectance-infrared spectroscopy. Journal of Pharmaceutical and Biomedical Analysis, 98, pp.178-185. https://www.sciencedirect.com/science/article/pii/S0731708514002519
8. Lee, S., Jeong, H. and Chang, I., 2009. Simultaneous determination of heavy metals in cosmetic products. J. Soc. Cosmet. Scientists Korea, 34(1), pp.57-62.
9. Greibrokk, T., & Andersen, T. (2003). High-temperature liquid chromatography. Journal of Chromatography A, 1000(1-2), 743-755.
10. Dugo, P., Cacciola, F., Kumm, T., Dugo, G., & Mondello, L. (2008). Comprehensive multidimensional liquid chromatography: theory and applications. Journal of Chromatography A, 1184(1-2), 353-368.
11. Vissers, J. P., Claessens, H. A., & Cramers, C. A. (1997). Microcolumn liquid chromatography: instrumentation, detection and applications. Journal of Chromatography A, 779 (1-2), 1-28.
12. Nawrocki, J. (1997). The silanol group and its role in liquid chromatography. Journal of Chromatography A, 779(1-2), 29-71.
13. Sawardeker, J. S., Sloneker, J. H., & Jeanes, A. (1965). Quantitative determination of monosaccharides as their alditol acetates by gas liquid chromatography. *Analytical Chemistry*, *37*(12), 1602-1604.
14. Sloneker, J. H. (1972). Gas–liquid chromatography of alditol acetates. In General Carbohydrate Method (pp. 20-24). Academic Press.
15. Moreno, P., & Salvado, V. (2000). Determination of eight water-and fat-soluble vitamins in multi-vitamin pharmaceutical formulations by high-performance liquid chromatography. Journal of chromatography A, 870(1-2), 207-215.
16. Taguchi, K., Fukusaki, E., & Bamba, T. (2014). Simultaneous analysis for water-and fat-soluble vitamins by a novel single chromatography technique unifying supercritical fluid chromatography and liquid chromatography. Journal of Chromatography A, 1362, 270-277.

უაკ 543.42

ტყვიის რაოდენობის განსაზღვრა ატომურ-აბსორბციული სპექტროფოტომეტრიით ჰიგიენურ და კოსმეტიკურ საშუალებებში

ნ. ამაშუკელი.ნ.რაჭველიშვილი

ქიმიური დაბიოლოგიური ტექნოლოგიების დეპარტამენტი,საქართველოს ტექნიკური უნივერსიტეტი,საქართველო, 0175, თბილისი,კოსტავას 69

E-MAIL: natamashukeli@gmail.com

რეზიუმე: მიზანი. კოსმეტიკურ და ჰიგიენურ საშუალებებს ყოველდღიურად ყველა ასაკის ადამიანი იყენებს. რა თქმა უნდა, ჯანმრთელობისთვის მნიშვნელოვანია მათი უსაფრთხოების დადგენა . ქარხნების ტექნოლოგიურ პროცესებში მნიშვნელოვანია უწყვეტი ანალიტიკური ექსპრეს კონტროლი წარმოების ყველა ეტაპზე, რათა დროულად მოხდეს ცვლილებების შეტანა და წუნის აღმოფხვრა.

კვლევის მიზანს წარმოადგენს კბილის პასტაში ტყვიის რაოდენობის განსაზღვა.კბილის პასტას ადამიანი ყოველდღიურად გამოიყენებს, ამიტომ მნიშვნელოვანია მეტალების, კერძოდ ტყვიის ზღვრული შემცველობის შენარჩნება.

მეთოდი. შეირჩა ატომურ-აბსორბციული სპექტროფოტომეტრიული კვლევის მეთოდი.

პარფიუმერიულ-კოსმეტიკურ დარგში ატომურ-აბსორბციულ მეთოდს იყენებენ ლითონების განსაზღვრისთის მზა კოსმეტიკურ ნაწარმში, მათი სინთეზის ნახევარპროდუქტებსა და გამოსავალ ნედლეულში. ლითონები მიეკუთვნება ტოქსიკური მინარევების რიცხვს, ამიტომ მეტად მნიშვნელოვანია ლითონის შემცველობის ცოდნა, რომელიც არ უნდა აღემატებოდეს დასაშვებ ზღვარს.

შედეგები. განხორციელებულიკვლევებისას დადგინდა რომ ატომურ- აბსორბციული სპექტროფოტომეტრული კვლევის მეთოდი მაღალი საზუსტით ადგენს ტყვიის შემცველობას ჰიგიენურ საშუალებებში.

დასკვნა. დადგინდა, რომ კბილის პასტაში დაცულია ევროკავშირის მიერ დადგენილი ტყვიის უსაფრთხო შემცველობა. იგი არ სცილდაბა 0,0015%-ს.

საკვანძო სიტყვები: ჰიგიენური საშუალებები, ტყვია, ატომურ-აბსორბციული სპექტროფოტომეტრია.

UDC 582.734.3

THE ROLE OF HERBAL MATERIALS IN BEAUTY PRODUCTS

K. Batsikadze, Kh. Mishelashvili

Georgian Technical University, Department of Pharmacy, Georgia, 0175, Tbilisi, Kostava Str. 69

E-mail: q.bacikadze@gtu.ge

Resume: **Goal**. Currently, the world is paying special attention to cosmetics containing antioxidants. Almost a century has passed since phenolic compounds became the focus of research attention. Flavonoids, a large group of phenolic compounds, are widely distributed in the plant world. They contain plant fruits, peel, leaf, pod, flower. One of the most valuable properties of flavonoids is their antioxidant activity.

Grapes are one of the most important sources of natural antioxidants. The use of grape seed extract as a biological additive in cosmetics is relevant and promising. Due to its universal properties, grape seed oil is used for all skin types. It has been proven that the addition of grape oil forms the functional and consumer properties of the developed sunscreen, affecting skin hydration and increasing the elasticity and firmness of the skin, as well as the correct change in its color under ultraviolet irradiation.

However, great importance is attached to improving oil extraction technologies while mitigating the technological impact on raw materials. Therefore, modern developers are paying increasing attention to technologies for processing grape seeds using the extraction method. The main objective of this work was to compare the extraction of grape seed oil with carbon dioxide and by mechanical extraction.

Method: The study was conducted to prepare high quality grape seed oils. Grape seed oils was obtained by two different extraction methods: mechanical extraction and extraction with carbon dioxide.

Results: Studies of the lipid complex of grape oil obtained by mechanical extraction and extraction with carbon dioxide showed that CO_2-extraction ensures the extraction of a much larger amount of biologically active substances, and maximum amount of oxidation products.

Conclusion: Grape seed oil is widely recognized throughout the world as one of the most powerful antioxidants and natural products, used for many years as an ingredient in cosmetics to treat damaged or aging skin. This is due to its regenerating properties, which provide more effective hydration; The oil quickly penetrates the skin and does not leave the skin feeling oily. Thanks to the high content of linoleic acid, which is quickly absorbed into the skin, thereby helping to reduce water loss and restore its elasticity.

Studies of the lipid complex of grape oil obtained by mechanical extraction and extraction with carbon dioxide have shown that CO2 extraction ensures the extraction of a much larger amount of biologically active substances, and the

maximum amount of oxidation products. We have developed a technology for obtaining grape oil and preparing it for use as a fatty raw material in cosmetic products.

Key words: cosmetics, skin, flavonoids, biologically active compounds, grape seeds, extraction.

1. INTRODUCTION

Any cosmetic product, be it anti-aging, sunscreen, for sensitive, problem skin or a simple day cream, contains plant extracts rich in phenolic compounds. The range of cosmetic effects of flavonoids is wide - they have the ability to protect the skin from premature aging, sunburn, rashes caused by microorganisms, can relieve inflammatory processes, and protect skin collagen.

The main value of grape seed extract is the presence of strong antioxidants - bioflavonoids, the so-called presence of proanthocyanidin. The coloring substances in grape seeds are in free form - anthocyanidins, and mainly in the form of glycosides associated with the rest of the sugar molecule - anthocyanins. Anthocyanins predominate in the skin of grapes, while catechins predominate in the pith and burgundy. The composition of anthocyanins depends on the grape variety and the place where it grows.

An innovation of the 21st century is that both scientists and cosmetologists started talking about the benefits of grapes, following traditional medicine. That is why today not only nets and medicines are made from grape seeds, but all cosmetic companies are trying to use it in their products.

2. MAIN PART

Over recent decades scientists have actively been studying plant originated biologically active compounds and refining the extraction methods of such compounds form plants. Biologically active compounds are represented by carbohydrates, proteins, lipids, vitamins, organic acids, alkaloids, glycosides phenolic compounds, terpenes and essential oils.

Modern cosmetics are being produced taking into consideration the skin anatomy and phisyology. Accordingly, they are used not only for visual effects and surface cleansing. The purpose of their consumption is broader. Normalizing skin homeostasis and increasing skin resistance, cosmetics become beneficial for preventing and healing skin pathological and aesthetic problems.

Cosmetics with antioxidant activities are becoming more and more popular among consumers. Fighting against viruses and bacteria, antioxidants delay the aging process. Since the last century they have rapidly gained popularity among beauticians, dermatologists, oncologists and gerontologists.

After the age of 25 the internal system responsible for protecting the body from free radicals weakens and gradually loses its effectiveness. Due to negative influence of external factors, the amount of ferments responsible for internal antioxidants proper working decreases. The body becomes unable to fight independently with free radicals that attack unprotected cells thus stemming into chain reactions of oxidation.

Scientists call the above mentioned process the oxidative stress that serves as the reason for inevi-

table aging. Fortunately, apart internal antioxidants there exist lots of external remedies fighting against free radicals. Some of them are acquired by the organism through food, biologically active supplements and synthesized vitamins consumption, while the others are penetrating the skin from the components of cosmetic creams, facial masks, or mesotherapy injections. The well-known antioxidants are vitamins A, C, E, co-enzyme q10 and bioflavonoids.

Phenolic compouns represent a significant interest of researchers for already a century. Number of scientific works have been dedicated to the studies of phenolic compound structure as well as working out and refining their research methods. Flavonoids or bioflavonoids, a large group of phenolic compounds, are widely spread in plants. They are found in plant fruits, skin, leaves, seeds and flowers. All flavonoids contain a benzene ring. Diverse combination of carbon, hydroxyl and methyl groups in this ring create various classes of flavonoids: flavonols, flavones, flavanones, catechins, anthocyanins and etc.

One of the valuable properties of flavonoids is their antioxidant activity. Binding free radicals, these compounds possess mighty antioxidant power. Phenolic compounds belong to widely spread large group of biologically active aromatic ring containing compounds. Due to their high biological activity and low toxicity, phenolic compounds attract high interest of researchers. Flavonoids, catechins and anthocyanins are able to reduce or avoid the radiation influence. Nowadays almost all beauty product including anti-aging, sun protection, sensitive skin or simple daily consumption cream contain herbal extracts reach in phenolic compounds.

Flavonoids possess a wide range of cosmetic properties from protecting the skin from aging, sun burn or avoiding bacterial rash to inflammation treatment. Flavonoids protect the skin collagen that helps to maintain the skin tone and elasticity. The most important property of flavonoids is their interaction with vitamins resulting in flavonoids antioxidation activity. In vitro research of flavonoids revealed that they represent much stronger antioxidants than vitamins C or vitamin E.

One of the most important natural source of antioxidants are grapes containing polyphenols: anthocyanins, phenolic acids, flavonoids, catechins, proanthocyanidins, tannins.

Using grape seed extract as a biological additive in beauty products is becoming very prospective. It contains a wide variety of nutrients and photochemical compounds that possess nutritional as well as healing and cosmetic properties. Grape seeds extract is used as oil, dye, etc. The main value of the grape seed extract is resulted from the fact that it contains mighty antioxidants, namely, bioflavonoids i.e. proanthocyanidins. Grape seed contains 95 % of proanthocyanidins, oligomers that are decomposed into monomers due to the biochemical reactions taking place in the body. The monomers serve as traps for free radicals resulting in pro-anthocyanidins antioxidant properties. The latter are mighty antioxidants behaving 50 times stronger than vitamin C or vitamin E. Proanthocyanidins are trapping free radicals formed due to inflammation or dystrophic changes in the human body, reinforcing blood vessels,

normalizing collagen level thus increasing the skin elasticity.

Nowadays from phenolic compounds there have been well studied catechins and their polymerization products. Grape berries contain dying compounds in the free form. These dying compounds are represented by anthocyanidins as well as by anthocyanins that form glucosides from sugar molecules and exist in the form of mono glycosides and diglycosides. The sugars met in anthocyanins are mainly glucose and rarely, galactose and rhamnose.

It has been stated that mono flavonoids, especially catechins and anthocyanins, possess P vitamin as well as strong bacteriocide effect. Anthocyanins dominate in grape skin while catechins are mainly obtained in grape stone and stalk. Anthocyanins amount in grape depends on vine species and the place where the vine is grown. Grape skin contains anthocyanin pigments of different color including pink, red, dark blue and violet in various shades coloring grape berries from pink to deep purple. Anthocyanins different colors can be explained by the peculiarities of their structure as well as by their complex made with different ions.

Molybdenium contained in anthocyanins gives violet color, iron forms dark blue, nickel and copper – white and potassium colors in purple. Anthocyanins color is also dependent on the medium pH. At pH<6, anthocyanins give red of different shade (sharp at pH=1–2), at pH=6 – violet, pH=8 – dark blue, pH=10 – green. In the acid environment anthocyanins become red altering the color with the presence of organic and inorganic compounds. The very property is used for making natural cosmetic products.

In this regard, an urgent area of research is the development of new and improvement of existing technologies for the production and processing of oil-containing plant raw materials, allowing to obtain oils of high nutritional and biological value.

The classic method of extracting grape seed oil is a press method. However, great importance is attached to improving oil extraction technologies while mitigating the technological impact on raw materials. Therefore, modern developers are paying increasing attention to technologies for processing grape seeds using the extraction method. Extraction with liquefied gases has certain advantages and disadvantages. The advantages include: low temperature of the main process and process of separation from the extract. This main advantage ensures the safety of biologically active substances in their original – natural form. Table 1 shows the physicochemical parameters extracts obtained by solvent extraction in comparison with oil obtained by pressing.

Grape seed excellent properties were well known in ancient Greece and Egypt. The properties were widely used in cosmetology. Bioflavonoides contained in grape seeds resemble estrogen, female sex hormone in structure and aid hair growth, regulate collagen synthesis, prevent aging, feed dried, moisturize greasy and recover aged skin. All the above mentioned caused the use of herbal materials, including grape, in the modern beauty products.

As a base product, grape seed oil has been widely used in cosmetic products. Besides rejuve-

nating effect, it possesses anti-inflammation, nutrition and moisturising properties, removes couperose problems; it is used for preventing skin cancer and pigment spots. For its universal properties, the grape seed oil is used for the skin of any type.

Table 1

Quality indicators of grape seed oil

Indicators quality	Indicator value	
	Extraction methods	
	Liquid CO_2	mechanical extraction
Density (g/cm^3)	0,9129	0,9190
Refractive index	1,4730	1,4782
Acid value (KOH mg/g)	10,42	2,2
Saponification value	470,55	250,53
Iodine value (g/100g)	115,10	136,10
Technological output	13,42	5,30

The fact that alongside the folk medicine, scientists and cosmetologists confirm the benefits of grape, can be considered as innovation of XXI century. Grape seeds are used not only in production of biological additives and medical products. Almost all cosmetic companies are including them in their products. It is impossible not to pay attention to beauty product made with "youth elixir". After all such cosmetic products were preferred even by Cleopatra, the queen of Egypt. And as it is well aware everything new is actually well-forgotten old.

3. CONCLUSION

Grape seed oil is widely recognized throughout the world as one of the most powerful antioxidants and natural products, used for many years as an ingredient in cosmetics to treat damaged or aging skin. This is due to its regenerating properties, which provide more effective hydration; The oil quickly penetrates the skin and does not leave the skin feeling oily. Thanks to the high content of linoleic acid, which is quickly absorbed into the skin, thereby helping to reduce water loss and restore its elasticity.

Studies of the lipid complex of grape oil obtained by mechanical extraction and extraction with carbon dioxide have shown that CO2 extraction ensures the extraction of a much larger amount of biologically active substances, and the maximum amount of oxidation products. We have developed a technology for obtaining grape oil and preparing it for use as a fatty raw material in cosmetic products.

REFERENCES

1. Bruno Burlando, Luisella Verotta, Laura Cornara, Elisa Bottini-Massa Herbal Principles in Cosmetics: Properties and Mechanisms of Action, 2010, 462 p.

2. Vimaladevi M. Textbook of Herbal Cosmetics, 2022, 144 p.
3. Dr. Vivek V Byahatti, Dr. Arpita Singh, Mr. Gireesh Tripathi, Dr. Kamal Jeet A text book of Herbal Cosmetics, 2020
4. Daniel Franco Ruiz, José Manuel Lorenzo Rodríguez Grape Seeds: Nutrient Content, Antioxidant Properties & Health Benefits, 2016, 231 p.
5. Марголина А., Эрнандес Е., Зайкина О., "Новая косметология", Косметика и медицина, 2001, 204 с
6. Дрибноход Ю. Введение в косметологию Санкт-Петербург : Питер, 2003. – 352 с
7. Boelsma E., Hendriks H.F.J., Roza L. Nutritional skin care: health effects of micronutrients and fatty acids. Am J Clin Nutr., 2001. Vol. 73. - p. 853
8. Chunmeng S., Tianmin C., Yongping S., et al. Effects of dermal mulripotent cell transplantation on skin wound healing. J Surg Res. - 2004. -Vol. 121. p. 13 - 19
9. Dell'Angelica E.C. Melanosome biogenesis: shedding light on the origin of an obscure organelle. Trends Cell Biol., 2003. Vol. 13. - p. 503-505
10. Griffiths C.E.M., Wang T.S., Hamilton T.A., Voorhees J.J., Ellis C.N. A photonumeric scale for the assessment of cutaneous photodamage. Arch Dermatol., 1992.Vol. 128. - p. 347-3.
11. Влияние режимов предобработки растительного сырья на эффективность экстракционных процессов. / К.Г. Восканян,А.Ю. Кривова, Т.А. Шакер // Глобальный научный потенциал. - 2013. - №8 - с. 69-71. 51
12. Здоровенина А.О., Фридман И.А. О точности измерения перекисного числа методом настаивания. Часть 1. Оценка источников погрешности. Масложировая промышленность, 2006, № 2 - с. 22-24
13. Зуева Т.А. Разработка малоотходной технологии переработки семян винограда и получение на их основе лекарственных и косметических средств. Дисс.... канд. фарм. наук. - Пятигорск, 2004. - 161 с
14. Габлаев Ш.А. Совершенствование технологии получения высококачественных виноградных семян из выжимки для производства пищевого масла. Дисс.... канд. техн. наук. - Ялта, 1990. - с. 158
15. Бондакова (Кривченкова), М.В. Растительные флавоноиды как функциональные добавки в косметических и пищевых продуктах [Текст] / М.В. Бондакова (Кривченкова), Е.В. Клышинская, М.А. Ильиных, С.Н. Бутова // Вестник РАЕН. - 2012. - 3. - С. 47-51
16. Бондакова, М.В. Экстракт винограда - антиоксидант для косметических изделий [Текст] / М.В. Бондакова, Е.В. Клышинская, С.Н. Бутова // Известия Иркутского государственного университета. Серия «Биология. Экология». - 2013. - Выпуск 3 (3). - Том 6
17. Babiarz-Magee L., Chen N., Seiberg M., Lin C.B. The expression and activation of protease-activated receptor-2 correlate with skin coloyr. Pigment Cell Res., 2004. Vol. 17. - p. 241-251
18. Berardesca E., Maibach H.i. Sodium lauryl sulphate induced cutaneous irritation: comparison of White and Hispanic subjects. Contact Derm., 1988. Vol. 18. - p. 136-140
19. Doherty M., Ashton B., Walsh S., et al. Vascular pericytes express osteogenic porential

of vitro and in vivo. J Bone Miner Res. - 1998. Vol. 13. - p. 828-838.
20. Глущенко В.Т., Березовский Ю.С. Виноград. - М.: АСТ, 2008. - 108 с
21. Камышан Е.М., Малышкин Б.Ю. Стабильность масел и жиров. Качественное отбеливание для обеспечения длительного срока хранения масел и жиров. // Масла и жиры, 2004, № 10. - с. 4-5.

უაკ 582.734.3

მცენარეული ნედლეულის როლი კოსმეტიკურ პროდუქციაში

ქ. ბაციკაძე, ხ. მიშელაშვილი

საქართველოს ტექნიკური უნივერსიტეტი, ფარმაციის დეპარტამენტი

E-mail: q.bacikadze@gtu.ge

რეზიუმე: დღეისათვის მსოფლიოში განსაკუთრებული ყურადღება ექცევა ანტიოქსიდანტების შემცველ კოსმეტიკას. თითქმის უკვე საუკუნეა, რაც ფენოლური ნაერთები მკვლევართა ყურადღების ცენტრში მოექცა. ფლავანოიდები, ფენოლური ნაერთების დიდი ჯგუფი, ფართოდ არის გავრცელებული მცენარეულ სამყაროში. მათ შეიცავს მცენარეთა ნაყოფი, კანი, ფოთოლი, წიპწა, ყვავილი. ფლავანოიდების ერთ-ერთი ყველაზე ღირებული თვისება არის მათი ანტიოქსიდანტური აქტივობა.

ბუნებრივი ანტიოქსიდანტების ერთ-ერთ ყველაზე მნიშვნელოვან წყაროს წარმოადგენს ყურძენი. ყურძნის წიპწის ექსტრაქტის, როგორც ბიოლოგიური დანამატის, გამოყენება კოსმეტიკურ საშუალებებში, აქტუალური და პერსპექტიულია. ყურძნის წიპწის ზეთი უნივერსალური თვისებების გამო გამოიყენება ყველა ტიპის კანისთვის. დადასტურებულია, რომ ყურძნის ზეთის დამატება აყალიბებს მზისგან დამცავი კრემის ფუნქციურ და სამომხმარებლო თვისებებს, გავლენას ახდენს კანის დატენიანებაზე და ზრდის კანის ელასტიურობასა და სიმტკიცეს, ასევე ულტრაიისფერი გამოსხივების ქვეშ მისი ფერის სწორ ცვლილებას.

თუმცა, დიდი მნიშვნელობა ენიჭება ზეთის მოპოვების ტექნოლოგიების გაუმჯობესებას. ამიტომ, თანამედროვე მეცნიერები სულ უფრო მეტ ყურადღებას უთმობენ ყურძნის თესლის გადამუშავების ტექნოლოგიას ექსტრაქციული მეთოდით. ამ სამუშაოს მთავარი მიზანი იყო შედარება ყურძნის თესლის ზეთის ექსტრაქციის მექანიკური გზით და ნახშირორჟანგის გამოყენებით.

საკვანძო სიტყვები: კოსმეტიკა, კანი, ფლავონოიდები, ბიოლოგიურად აქტიური ნივთიერებები, ყურძნის წიპწა, ექსტრაქცია.

UDC 669.01

HIGH-STRENGTH CAST IRONS WITH MICRO-ADDITIVES OF BORON - AN INNOVATIVE STRUCTURAL MATERIAL FOR AUTOMOTIVE COMPONENTS

S. Gvazava[1], N. Khidasheli[2], Z. Rusishvili[1], M. Chikhradze[2], T. Badzoshvili[1], G. Zakharov[1], R. Tabidze[1]

[1]F. Tavadze Metallurgy and Materials Science Institute

[2]Georgian Technical University

E-mail: salomegvazava@gmail.com

Resume: ***Goal.*** In the presented work, important functional indicators of boron microalloyed high-strength cast iron were studied, such as - tribotechnical characteristics and features of corrosion cracking. The object of research was high-strength cast irons with different structures, which differed by the type of bainite and the difference in the ratio of structural components.

It is determined that cast irons with a lower bainitic structure are characterized with more stable tribotechnical characteristics and high corrosion resistance in sliding under dry friction conditions, which is due to the dispersity of the structure and the homogeneity of the phase components.

Methods:

The study of the structural components and phase composition of the material was carried out with a Neophot-32 microscope and an X-ray structural diffractometer (X-RAY). On tribometer СМЦ-2, the current changes in the process of frictional interaction of the studied alloy were studied, in particular, the evolution of the coefficient of friction. The resistance to corrosion cracking of the experimental cast irons was determined by the electrochemical method (Tafel curves) on the potentiostat "Ivium CompactStat CS350". The frequency exponents (Fourier series) of horizontal oscillations developed during the wear process of the contact layers of high-strength cast irons were determined by means of a UNI-T UT315A vibration-analyzer. Determination of the distribution of elements in the frictional layers of the experimental material was carried out based on the method of energy-dispersive spectroscopy - using a scanning electron microscope Hitachi TM3030Plus.

Results:

The resistance to corrosion cracking of boron microalloyed high-strength cast irons has been established. The influence of the change in the isothermal hardening temperature of the experimental alloys on the evolution of the friction coefficient under the conditions of dry sliding friction is studied.

Conclusions:

- Microalloying with boron (0.03%) increases the corrosion resistance of bainitic cast irons by 20-22%, which is related to the dispersity of the metallic base of the material and the formation of borides and nitrides in the structure.

❖ The coefficient of friction of boron microalloyed high-strength cast iron ranges from 0.38 to 0.49 and it maintains its stability in sliding dry friction conditions.

❖ Decreasing the isothermal tempering temperature from 400^{0}C to 280^{0}C results in a 10% reduction in the coefficient of friction of boron microalloyed high-strength cast irons.

Key words: High strength cast iron, heat treatment, corrosion cracking resistance, wear intensity, friction coefficient, bainite type, structure optimization.

1. INTRODUCTION

For the effective operation of the responsible systems of road and railway vehicles in extreme conditions, it should be taken into account that the materials used for their production should be characterized with high mechanical strength, thermal resistance, corrosion and wear resistance, and an optimal friction coefficient. These requirements can be met by managing the alloy structure formation processes, optimizing the ratio of structural components and regulating the distribution of phase components [1-6].

At present, high-strength spheroidal cast iron belongs to one of the most promising groups of constructional innovative materials. High-strength bainitic cast iron is distinguished by technological diversity, and the use of details made from it allows reducing economic characteristics [7-11].

For the stable formation of bainitic structure in the above-mentioned alloys, it is necessary to alloy high-strength cast irons with expensive elements such as Cu, Mo and Ni [11-16]. The high cost and necessary quantity of these elements (up to 2%) determines the high cost of the manufactured products. Therefore, it is relevant to replace the above-mentioned elements with multi-factor influence and relatively cheap ones.

According to the data of various researchers, boron microalloying of high-strength cast irons has a positive effect on the processes of formation of structure and operational properties [17-19]. In particular, when high-strength cast iron is microalloyed with boron, boron nitrides are formed in the metal base of the material, which have a positive effect on the tribophysical properties of the material [20-23].

Besides, boron microalloying of alloy in the metallic base of the material increases the speed of carbon diffusion and structure stiffness, dispersity of eutectic grain and graphite inclusions, inhibits coagulation of phases, as a result of which the technological plasticity of iron-carbon alloys increases [24-26].

It should be noted that the temperature of the contact zone can reach 300-450^{0}C during the frictional loading of the material under conditions of dry friction with sliding and as a result there is an intensification of the oxidative processes, accordingly, there is the degradation of the surface layers and corrosive breakdown. Based on this, the study of wear and corrosion resistance of the material has great scientific and practical importance.

At the same time, it should be noted that the functional characteristics of this group of materials remain practically not-investigated, which limits the wide production use of these alloys.

2. MAIN PART

Boron microalloyed high-strength cast iron with 2.0-2.1% silicon content was selected as the research object, which, as it is well-known [10], is characterized by high crack resistance, which is very important to prevent the danger of micro cracks in the bainitic structure. A high-frequency induction furnace with a capacity of 50 kg was used to melt the experimental samples. Cast iron with the following composition (C - 4.0-4.2%, Si - 2.1-2.3%, Mn - 0.25-0.30%, S - 0.06%, P - 0.05% and steel scrap (5-8%) was used as furnace materials for melting the base alloy. The chemical composition of the experimental cast irons is given in Table 1.

Table 1

Chemical composition
of experimental cast irons

High strength cast iron	Chemical composition of test cast irons, wt.%						
	C	*Si*	*Mn*	*S*	*P*	*B*	*Mg*
basic	4.0-4.2	2.1-2.3	0.25	0.006	0.005	-	0.040
micro-alloyed with boron	3.45	2.20	0.25	0.003	0.06	0.03	0.045

For spheroidization of graphite inclusions in the structure of cast iron, the lower layers of liquid metal were processed through magnesium vapor at 1320-1350°C. After that, alloy microalloying was carried out ФБ0-0.15%. The resulting liquid metal was poured into preliminary prepared casting molds. Various research experimental samples were prepared from the obtained basic preparation.

To obtain different bainitic structures, the experimental cast irons were subjected to a two-step heat treatment process: austenitization at 900°C with a controlled time delay of 60 minutes and further isothermal tempering at 280 and 400°C with appropriate delay to obtain different types of bainitic structure (lower and upper bainitic structure) Fig.1.

Fig. 1. Mode of heat treatment of experimental cast irons

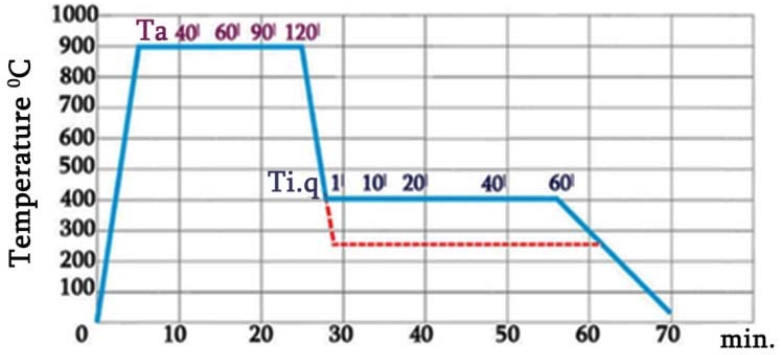

In order to control the stability of retained austenite in the base metal, either the austenitization time or the duration of isothermal quenching was varied. Isothermal tempering was carried out in a molten metal bath (Sb-8%, Sn-5%, Pb-87%). Metallographic microscope Neophot-32 and x-ray structural (X-RAY) diffractometer ДРОН-4 were used to study the structure of the obtained cast irons and the ratio of phase components.

Brake pad-shaped research samples were tested for wear resistance by sliding under dry friction conditions to determine the tribotechnical characteristics of the material. To determine the intensity of wear of experimental cast irons, tribometer СМЦ-2 Fig.2 was used, which provided computer registration of tribotechnical parameters (friction moment) of the material.

Cyclic tests consisting of five stages were carried out under conditions of constant rotation number - 1000 rpm, contact load force was 50N and the total distance of vector sliding - 6.280m.

Fig. 2. Testing samples on a tribometer

A roller made of (0.9%C) tempered steel У8 with a diameter of 40 mm was used as a counterbody, with hardness of 64-HRC unit on the Rockwell scale. The kinetics of change in the friction coefficient and mass loss during wear of high-strength cast irons with different structures were studied. As a friction pair, the following was used: a stationary ball (test sample) - a rotating disk (counter body) Fig. 3.

Fig. 3. Scheme of the tribosystem

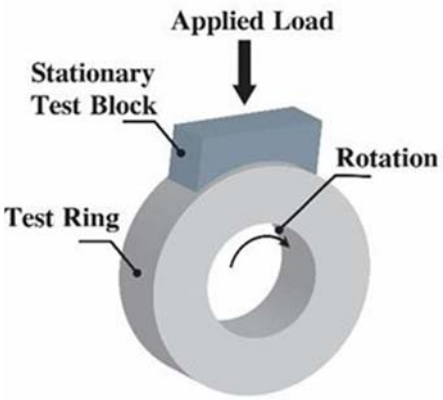

Electrochemical research was carried out on Ivium CompactStat CS350 potentiostat.

To determine the corrosion rate of high-strength bainitic cast irons with different structures, Tafel potentiodynamic curves were taken in a 3% NaCl aqueous solution, ± 0.3V from the standard potential of the mentioned sample. Platinum was used as an auxiliary electrode; The reference electrode was Ag/AgCl. The reference electrode was placed in a supersaturated KCl solution connected to the bath by a Lugin capillary.

- ***Obatained results and discussions:***

According to metallographic analysis, micro-alloying high-strength cast iron with boron by 0.03% increases the dispersity of the metal base and the disorientation of structural elements. Iron borides are formed in the structure and ultra-disperse (≤1μm) particles, probably boron or carbides, are observed in the grinding plane.

The hardness of samples microalloyed with boron with upper bainitic structure reaches 45-48HRC, and the hardness of bainitic cast iron isothermally tempered at 280^{0}C increases to 57-60HRC, which is explained by the structure of finely dispersed metallic base and the formation of dispersed boron carbides and nitrides.

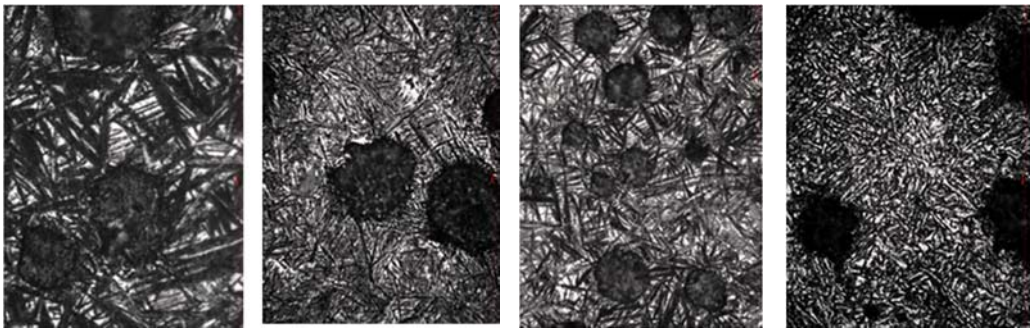

a b c d

Fig. 4. Typical microstructures of experimental cast irons isothermally tempered at 280⁰C, base cast irons – a and b x1000 c, d micro-alloyed with boron

To determine the tribotechnical characteristics (wear resistance, friction coefficient, temperature in the contact zone) of boron microalloyed cast irons by sliding under dry friction conditions, two types of samples were prepared: high-strength boron microalloyed cast irons isothermally annealed at 400⁰C and 280⁰C.

Fig. 6-a presents the kinetics of the change of the friction coefficient of high-strength cast irons with a lower bainitic structure. According to the obtained results, the coefficient of friction of the samples of the mentioned group ranges from 0.25 to 0.40 and it maintains its stability during the experiment, Fig. 6a.

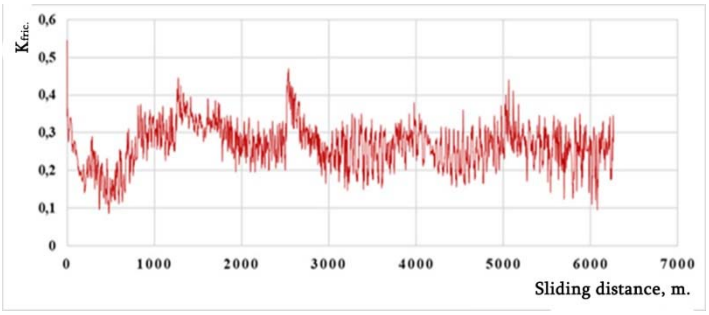

Fig. 5-a. Kinetics of change of friction coefficient of boron microalloyed cast irons with lower bainitic structure under 50N contact load conditions

When determining the tribotechnical characteristics of isothermally tempered cast irons at 400⁰C, a low intensity of wear of the surface layers is observed, there is no selective transfer of individual phases and covering of graphite inclusions, which perform the function of a lubricant for a long time. The coefficient of friction of

experimental cast iron ranges from 0.38 to 0.49 (Fig. 5-b.).

According to the energy dispersive analysis (EDX) of the frictional surfaces of the experimental samples, the upper bainitic structures under 50N contact load undergo oxidation processes and on their surface 52% more oxygen is observed, which is equally distributed on the friction surface (Fig. 6).

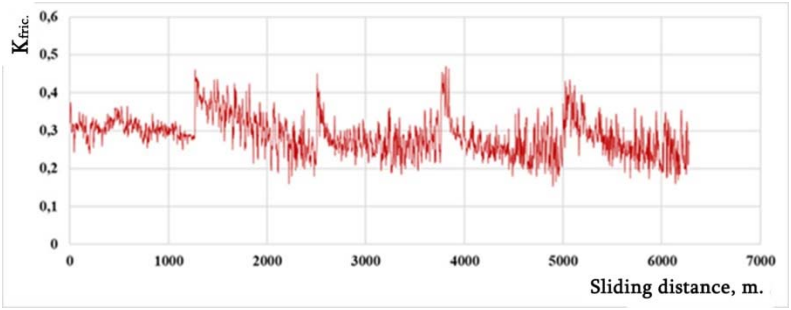

Fig. 5. b. Kinetics of change of friction coefficient of boron microalloyed cast irons with upper bainitic structure under 50N contact load conditions

Spectrum: Point

Element	AN	Series	norm. C [wt.%]	Atom. C [at.%]
Iron	26	K-series	76.20	45.16
Oxygen	8	K-series	13.67	28.27
Carbon	6	K-series	9.28	25.58
Silicon	14	K-series	0.85	1.00
Total:			100.00	100.00

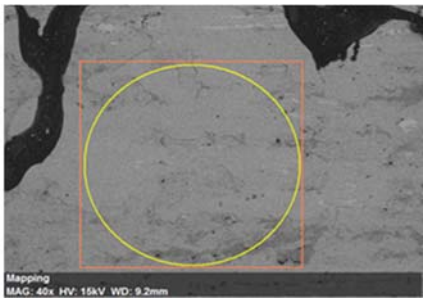

Spectrum: Point

Element	AN	Series	norm. C [wt.%]	Atom. C [at.%]
Iron	26	K-series	60.78	30.28
Oxygen	8	K-series	33.67	58.55
Carbon	6	K-series	4.29	9.93
Silicon	14	K-series	1.26	1.25
Total:			100.00	100.00

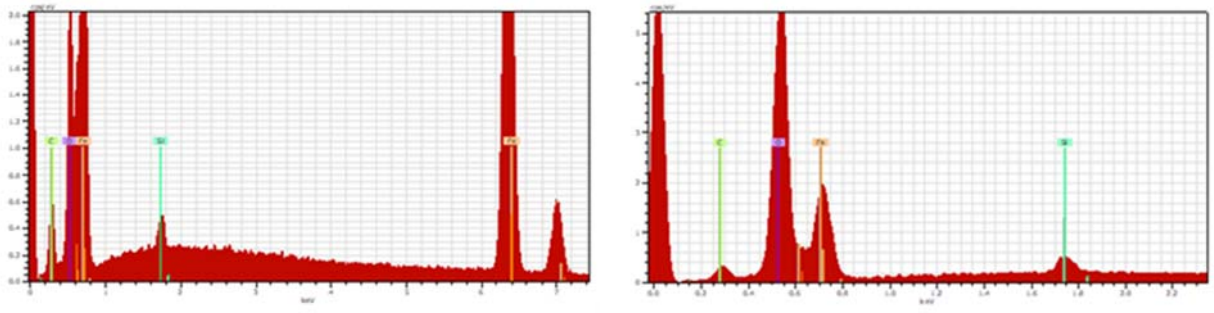

a b

Fig. 6. Energy-dispersive analysis of frictional surfaces of bainitic cast iron microalloyed with boron; a- isothermally calcined at 280 ^{0}C; b- isothermal melting at 400^{0}C;

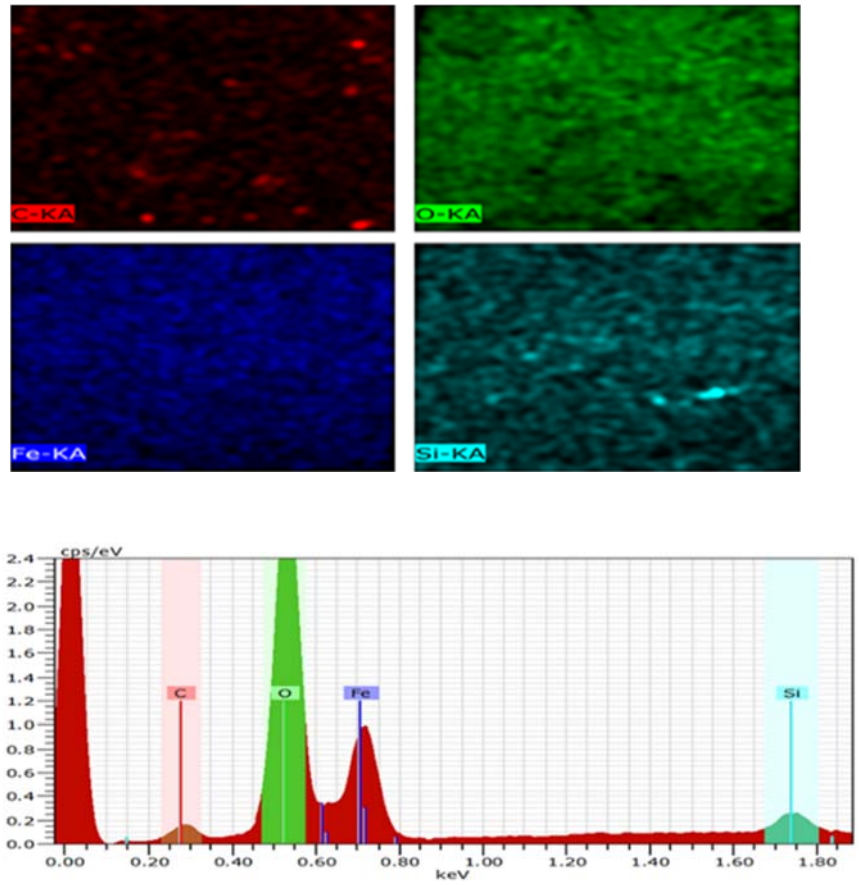

Fig. 7. Distribution of elements on frictional surfaces of experimental cast irons (mapping)

In the process of frictional interaction of the contact layers, there is a change in the wear mechanism, which is accompanied by an amplitude oscillation. The study of the frequency characteristics of horizontal oscillations decomposed into Fourier series (Fig. 8) showed that under dynamic loading, samples with a lower bainitic structure are characterized by a low amplitude of frictional oscillations and a noise level (7-9 dB).

This is explained by the fact that the dispersed inclusions of borides, carbides and nitrides located on the grain surfaces strengthen the metal base and increase their resistance to plastic deformation.

In addition, the optimal amount of metastable residual austenite ensures the strengthening of the frictional surfaces as a result of contact loading, which prevents the generation of internal stresses. This leads to stable tribotechnical characteristics during long-term frictional interaction of surfaces.

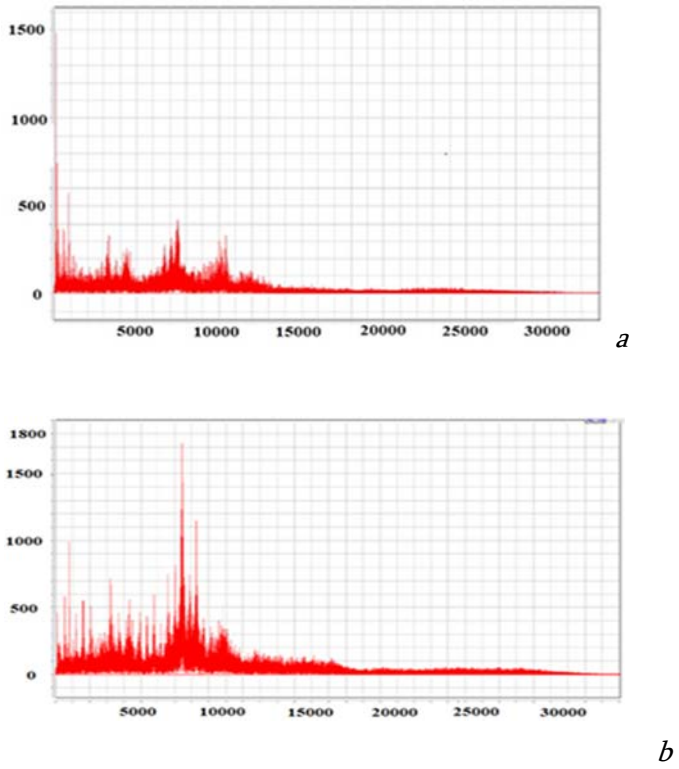

Fig. 8. Frequency characteristics of horizontal oscillations of samples with different bainite structures: a- upper bainite; b- lower bainite;

In the course of the experiment, the resistance to corrosive breakdown of basic and boron microalloyed bainitic cast irons was determined by means of the potentiodynamic method. By extrapolating the anodic and cathodic areas of the Tafel, the corrosion rates of the base and microalloyed samples were determined. The data presented in Fig. 10 show the corrosion potentials of basic and boron microalloyed bainitic cast irons.

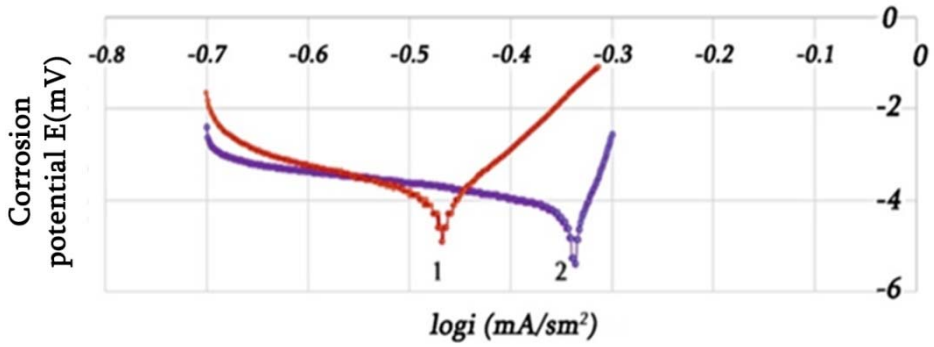

Fig. 9. Tafel potentiodynamic curves of bainitic cast irons. (0.5M NaCl) 1-basic cast iron; 2- micro-alloyed with boron;

Tafel curves characteristic of boron microalloyed bainitic cast irons have similar polarization characteristics and no passivation regions are observed. Based on this, it can be concluded that a protective layer of corrosion products does not form on the sample.

In addition, the corrosion potentials and current densities of the samples are significantly different, which indicates the increased susceptibility of cast irons to corrosion. It is estimated that boron microalloying (0.03%) increases the corrosion resistance of bainitic cast irons by 20-22%.

3. CONCLUSION

❖ Microalloying with boron (0.03%) increases the corrosion resistance of bainitic cast irons by 20-22%, which is related to the dispersity of the metallic base of the material and the formation of borides and nitrides in the structure.

❖ The coefficient of friction of boron microalloyed high-strength cast iron ranges from 0.38 to 0.49 and it maintains its stability in sliding dry friction conditions.

❖ Decreasing the isothermal tempering temperature from 400^{0}C to 280^{0}C results in a 10% reduction in the coefficient of friction of boron microalloyed high-strength cast irons.

REFERENCES

1. Konca, E., Tur, K., & Koç, E. (2017). Effects of Alloying Elements (Mo, Ni, and Cu) on the Austemperability of GGG-60 Ductile Cast Iron. Metals, 7(8), 320.
2. Mrzygłód, B., Kowalski, A., Olejarczyk-Wożenska, I., Adrian, H., Głowacki, M., & Opaliński, A. (2015). Effect of Heat Treatment Parameters On the Formation of ADI Microstructure with Additions of Ni, Cu, Mo. Archives of Metallurgy and Materials, 60(3), 1941–1948.
3. Górny, M., Tyrała, E., & Lopez, H. (2014). Effect of Copper and Nickel on the Transformation Kinetics of Austempered Ductile Iron. Journal of Materials Engineering and Performance, 23(10), 3505–3510.
4. D. Aubakirov (2022). Modifying Effect of a New Boron-Barium Ferroalloy on the Wear Resistance of Low-Chromium Cast Iron. MDPI *Metals, 12* (7), 1153; DOI:10.3390/met 12071153
5. B. Białobrzeska, R. Dziurka (2023). Effect of Boron Accompanied by Chromium, Vanadium and Titanium on the Transformation Temperatures of Low-Alloy Cast Steels. Arch. Metall. Mater. 68 (2023), 1, 257-267. DOI:10.24425/ amm.2023.141502.
6. G. Zakharov, N. Khidasheli, Z. Aslamazashvili, G. Gordeziani, M. Chikhradze, S. Gvazava, I. Maisuradze. (2021). Wear behaviour of austempered, ductile iron microalloyed with boron under different contact load by dry sliding wear conditions. WMMES, World Symposium on Mechanical - Materials Engineering & Science, Prague (Czech Republic).
7. B. Białobrzeska (2022). Effect of boron accompanied by chromium, vanadium and titanium on kinetics of austenite grain growth. Ironmaking & Steelmaking, Volume 48, 2021 - Issue 6. DOI:10.1080/03019233.2021.1889894.

8. : Gontijo, M.; Chakraborty, A.; Webster, R.F.; Ilie, S.; Six, J.; Primig, S.; Sommitsch, C. Thermomechanical and Microstructural Analysis of the Influence of B- and Ti-Content on the Hot Ductility Behavior of Microalloyed Steels. Metals 2022, 12, 1808. https://doi.org/10.3390/met12111808.
9. Tavadze, G., Khidasheli, N., Tabidze, R., Gordeziani, G., Gvazava, S. (2020). Influence of hot plastic deformation on austenization process during austempering of ductile iron Bulletin of the Georgian National Academy of Sciencesthis link is disabled. 14(3), pp. 80–84.
10. J. Mallia & M. Grech (1997). Effect of silicon content on impact properties of austempered ductile iron, Materials Science and Technology, 13:5, 408-414 To link to this article: http://dx.doi.org/10.1179/mst.1997.13.5.408.
11. A.V. Kolubaev, E.A. Kolubaev, O.V. Sizova. Structure, deformation, and fracture of hard coatings during sliding friction Russian Physics Journal. T. 62. № 8. C. 1363-1397. 2019.
12. B. Wang, F. Qiu, G.C. Barber, Y. Pan, W. Cui, and R. Wang. Microstructure, wear behavior and surface hardening of austempered ductile iron. Journal of Materials Research and Technology, 9(5), 9838–9855, 2020.
13. J. K. Kaleicheva, and V. Mishev. Wear Resistance of Austempered Ductile Iron with Nanosized Additives. IOP Conference Series: Materials Science and Engineering, 295, 012034, 2018.
14. T. Sarkar, and G. Sutradhar. Investigation on mechanical properties and wear behavior of Cu-
15. alloyed austempered gray cast iron (AGI). Sādhanā, 43(10), 2018.
16. B. Wang, X. Han, G.C. Barber, and Y. Pan. Wear Behavior of Austempered and Quenched and Tempered Gray Cast Irons under Similar Hardness. Metals, 9(12), 1329, 2019.
17. A. Bedolla-Jacuinde, F.V. Guerra, M. Rainforth, I. Mejía, and C. Maldonado. Sliding wear behavior of austempered ductile iron microalloyed with boron. Wear, 330-331, 23–31, 2015.
18. P. Sellamuthu, D. Samuel, D. Dinakaran, V. Premkumar, Z. Li, and S. Seetharaman. Austempered Ductile Iron (ADI): Influence of Austempering Temperature on Microstructure, Mechanical and Wear Properties and Energy Consumption. Metals, 8(1), 53, 2018.
19. A. Bedolla-Jacuinde, F.V. Guerra, M. Rainforth, I. Mejía, and C. Maldonado. Sliding wear behavior of austempered ductile iron microalloyed with boron. Wear, 330-331, 23–31, 2015.
20. R. Kumar, R.K. Dwivedi, and S. Ahmed. Influence of Multiphase High Silicon Steel (Retained Austenite-RA, Ferrite-F, Bainite-B and Pearlite-P) and Carbon Content of RA-Cγ on Rolling/Sliding Wear. Silicon, 2020.
21. A. Bedolla-Jacuinde, F.V. Guerra, M. Rainforth, I. Mejía, and C. Maldonado. Sliding wear behavior of austempered ductile iron microalloyed with boron. Wear, 330-331, 23–31, 2015.
22. S. Yazdani, and M.A. Rahimi. Wear Behavior of an Austempered Ductile Iron Containing Mo- Ni-Cu. Materials Science Forum, 475-479, 199–202, 2005.

23. B. Li, and Z. Rui. Friction and wear behaviours of YG8 sliding against austempered ductile iron under dry, chilled air and minimal quantity lubrication conditions. Advances in Mechanical Engineering, 11(5), 168781401984706, 2019.
24. G. Oniashvili, G. Tavadze, G. Zakharov, and Z. Aslamazashvili. Self-propagating High-temperature Synthesis of Ferroalloys. LAP Lambert Academic Publishing. 2018.
25. J.S. Sokolan. Effect of external friction on deformational aging of steel taking into consideration its thermal treatment. Problems of Tribology, № 4,з.73-80, 2014.
26. A.P. Cheiliakh. Ekonomnolegirovannye metastabil'nye splavy i uprochniaiushchie tekhnologii. [Economically alloyed metastable alloys and the strengthening technologies]. Mariupol': PGTU, 483 p., 2009.

უაკ 669.01

ბორით მიკროლეგირებული მაღალმტკიცე თუჯი როგორც ინოვაციური კონსტრუქციული მასალა მანქანათმშენებლობაში

ს. გვაზავა[1], ნ. ხიდაშელი[2], ზ. რუსიშვილი[1], მ. ჩიხრაძე[2], თ. ბაძოშვილი[1], გ. ზახაროვი[1], რ. ტაბიძე[1]

[1.]სსიპ ფერდინანდ თავაძის მეტალურგიისა და მასალათმცოდნეობის ინსტიტუტი

[2.]საქართველოს ტექნიკური უნივერსიტეტი

E-mail: salomegvazava@gmail.com

რეზიუმე. მიზანი: წარმოდგენილ ნაშრომში შესწავლილ იქნა ბორით მიკროლეგირებული მაღალმტკიცე თუჯის ისე მნიშვნელოვანი ფუნქციონალური მაჩვენებლები, როგორებიცაა - ტრიბოტექნიკური მახასიათებლები და კოროზილი რღვევის თავისებურებანი. კვლევის ობიექტს წარმოადგენდა სხვადასხვა სტრუქტურის მქონე მაღალმტკიცე თუჯები, რომლებიც განსხვავდებოდნენ ბეინიტის ტიპითა და სტრუქტურული მდგენელების თანაფარდობის სხვაობით.

დადგენილია, რომ ქვედა ბეინიტური სტრუქტურის მქონე თუჯები ხასიათდებიან უფრო სტაბილური ტრიბოტექნიკური მახასიათებლებითა და მაღალი კოროზიამედეგობით სრიალით მშრალი ხახუნის პირობებში, რაც განპირობებულია სტრუქტურის დისპერსულობითა და ფაზური კომპონენტების ჰომოგენურობით.

მეთოდი: მასალის სტრუქტურული კომპონენტებისა და ფაზური შემადგენლობის შესწავლა განხორციელდა მიკროსკოპით Neophot-32-ის და რენტგენო-სტრუქტურული დიფრაქტომეტრის (X-RAY) საშუალებით. ტრიბომეტრზე СМЦ-2-ზე შესწავლილ იქნა საკვლევი შენადნობის ფრიქციული ურთიერთქმედების პროცესში მიმდინარე ცვლილებები, კერძოდ- ხახუნის კოეფიციენტის ევოლუცია. ექსპერიმენტული თუჯების კოროზიული რღვევისადმი მედეგობა განისაზღვრა ელექტროქიმიური მეთოდით (ტაფელის მრუდები) პოტენციოსტატ Ivium CompactStat CS350 -ზე. მაღალმტკიცე თუჯების საკონტაქტო შრეების ცვეთის პროცესში განვითარებული ჰორიზონტალური რხევების სიხშირის მახასითებლების (ფურიეს მწკრივები) დაფიქსირება განხორციელდა ვიბროანალიზორ UNI-T UT315A საშუალებით. ექსპერიმენტული მასალის ფრიქციულ შრეებში ელემენტების განაწილების დადგენა განხორციელდა ენერგო-დისპერსული სპექტროსკოპიის მეთოდის საფუძველზე - მასკანირებელი ელექტრონული მიკროსკოპის Hitachi TM3030Plus-ის გამოყენებით.

მიღებული შედეგები: დადგებილია ბორით მიკროლეგირებული მაღალმტკიცე თუჯების კოროზიული რღვევისადმი მედეგობა. შესწავლილია ექსპერიმენტული შენადნობების იზო-თერმული წრთობის ტემპერატურის ცვლილების გავლენა ხახუნის კოეფიციენტის ევოლუციაზე სრიალით მშრალი ხახუნის პირობებში.

დასკვნები: ნადნობის ბორით (0.03%) მიკროლეგირება ზრდის ბეინიტური თუჯების კოროზიული რღვევისადმი მედეგობას 20-22%-ით, რაც დაკავშირებულია მასალის ლითონური ფუძის დისპერსულობითა და სტრუქტურაში ბორიდების და ნიტრიდების ფორმირებით.

- ბორით მიკროლეგირებული მაღალმტკიცე თუჯების ხახუნის კოეფიციენტი მერყეობს 0.38-დან 0.49-მდე და იგი ინარჩუნებს თავის სტაბილურობას სრიალით მშრალი ხახუნის პირობებში.
- იზოთერმული წრთობის ტემპერატურის შემცირება 400^{0}C-დან 280^{0}C-მდე იწვევს ბორით მიკროლეგირებული მაღალმტკიცე თუჯების ხახუნის კოეფიციენტის 10%-ით შემცირებას.

საკვანძო სიტყვები: მაღლმტკიცე თუჯი, თერმული დამუშავება, კოროზიული რღვევისამდი მედეგობა, ცვეთის ინტენსიობა, ხახუნის კოეფიციენტი, ბეინიტის ტიპი, სტრუქტურის ოპტიმიზაცია.

UDC 666.946.6

PREPARATION OF HETERO-MODULAR NANOCOMPOSITES BASED ON THE B_4C-SIC-BN-TIC-AL_2O_3 SYSTEM FOR TURBINE DISKS AND WINGS, BALLISTIC ARMOR, FOR WORKING IN HOT NODES OF FLYING MACHINES

Ts. Danelia

Department of Chemical and Biological Technologies, Institute of Bionanoceramics and Nanocomposites Technology. Georgian Technical University. Kostava 69. Tbilisi. Georgia

E-mail: Tsddental@gmail.com

Resume: **Goal.** Purpose. Preparation of hetero-modular nanocomposites with high operational properties based on B4C-SiC-BN-TiC-Al_2O_3 systems.

Method: Structural research was carried out on the X-ray structural analysis device DRON 3, optical-microscopic research was carried out on the AC100 microscope, electron-microscopic research - on the OPTON device. Micro and macro mechanical properties were measured.

Results: nanocomposites with high modular properties were obtained based on the B4C-SiC-BN-TiC-Al_2O_3 system. According to the structural research, it was determined that the shape of the grains is mostly spherical and the size of the largest grain does not exceed 3 μm, the structure is mostly homogeneous

Physical and technical properties of composites, under high temperature conditions, are studied. The viscosity of the obtained composites at 800^0C is 11-13 GPa, the limit of bending strength at 1000^0C is almost the same as at room temperature - 340-390 MPa.

Conclusion: the obtained composites withstand thermal shocks without deformation and cracks: 800^0C - water, more than 20 cycles. The properties of composites make it possible to use them for operation under high temperature and wear conditions, for example, in dry friction bearings of space vehicles and other similar machines, the so-called Self-lubricating bearings. Composites #20 and K6 are recommended due to their low density and relatively high strength for the manufacture of individual and aircraft cabin armor, while composites #19; #22 and K5, for making the armor of heavy armored personnel carriers.

Key words: hetero-modular, structure, high temperature, wetness, wear resistance.

1. INTRODUCTION

Selection of research composite composition and determination of technological parameters

To obtain the research composites, high melting point and wear-resistant components were selected, such as: boron carbide, titanium and silicon carbides, boron nitride, aluminum oxide. {1-3]. Based on them, we made various compositions

to obtain composite materials. We selected magnesium oxide, yttrium oxide as additives.

Magnesium and yttrium oxides are added to determine their effect on the sintering process. Carbon fiber – to increase mechanical strength [4-5]. The effect of their amount on the properties of the composite was studied. The specific surface indicators of the components selected as starting materials for obtaining composites are as follows: aluminum oxide - 6.7 m^2/g., boron carbide - 1.15 m^2/g., boron nitride (a) - 6.5 m^2/g., silicon carbide - 0.72 m^2/g, titanium carbide - 4.0 m^2/g, yttrium oxide - 6.0 m^2/g; Graphite - 20 m^2/g [6-7].

We studied the influence of grinding mode on all cases, grinding and mixing of components was done in mills for 13-30 hours. Grinding was done in the area of alcohol in order to prevent some components, such as titanium carbide, from binding oxygen from water, which deteriorates the properties of titanium carbide. After grinding, the obtained mass was dried in a drying cabinet at a temperature of 60-65 degrees. After grinding the composites, the specific surface of the powders was determined, the size of which after 13 hours of grinding was 2.0-3.0 m^2/g, and after 30 hours it was 4.0-5.0 m^2/g. [8-11].

The specific mass of each composite, which should be obtained after sintering, was theoretically calculated in advance. For this, the law of additivity and the X-ray density of each component were used, taking into account the content of this component in the composite.

The melting temperature limits of the composites were determined theoretically, in which the law of additivity and the relationship between the melting temperature and the sintering temperature of each component were again used. The samples were initially pressed dry at room temperature with a pressure of 10-15 MPa to expel air from the mixture and give the samples some density. Pressing was done in graphite molds, under vacuum. At the next stage, the samples were heated at a speed of 70-80 degrees/minute. When the required temperature was reached, pressure was developed and the material was exposed to both high temperature and high pressure. At this time, the composite undergoes plastic deformation, which increases the intensity of the sintering. The duration of pressing and the delay at the maximum temperature did not exceed 10 minutes, because a long delay contributes to the growth of the grains of the constituent components of the composite, which negatively affects the physical and technical properties of the composite. [12-16].

2. MAIN PART

The compositions and compression parameters of the composites are presented in Table 1.

Dependence between properties of obtained composites and technological parameters

After sintering, test samples were laser cut from the obtained material, which are well-formed solid materials without cracks and deformation. The sintering temperatures in most cases fit within the range that was theoretically calculated.

The water absorption capacity and density of the samples were measured, which gives an idea of the quality of the sintering of the samples. The results are presented in Table 2.

As can be seen from Table 2, the majority of the composites were baked in the selected temperature

interval, and for some compositions this temperature was found to be high. Through these experiments, the sintering interval of each composite was determined, which allowed the optimal baking temperature to be determined. For each case, a theoretical density was calculated, which was compared to the actual density of the hot-pressed composites. According to this, together with other parameters, it was possible to judge the degree of sintering of the obtained composite.

In addition to the parameters of the sintering and the content of the components included in the composite and their nature, the degree of grinding of the components included in the composite, has a certain influence on the quality of sintering. The degree of dispersibility depends on: the strength of the material, the strength of the grinding body, the grinding method, its duration and the dispersion area. A vibrating mill with a high intensity of grinding was used to grind the powders. The duration of grinding has a certain influence on the grinding process, but its influence is more pronounced when testing the mechanical properties of the obtained composites. The mechanical characteristics of the composites milled for 13 hours are significantly inferior to the mechanical indicators of the composites of the same composition, which were milled for 30 hours.

As for the influence of the used additives (magnesium and yttrium oxides, carbon fiber), it contributes to the sintering process, maintaining the initial dimensions of the grains, thus forming a finely dispersed microstructure, which in turn found expression in the mechanical properties of the composites. In the case of composite #3, the positive effect of its action was overshadowed due to the low dispersion quality of the components (grinding duration 13 hours, specific surface index did not exceed 3 m^2/g) [3, 5].

Selection of the optimal composition of composites and their properties

According to the results of the conducted studies, the optimal compositions of the composites obtained on the basis of the research systems B_4C-SiC-BN-TiC-Al_2O_3 were selected, Table 1.

According to the selected optimal compositions, the samples were prepared, ground in a vibrating mill, and the obtained powders were pressed under conditions of high temperature and pressure, namely at 1700-1750^{0}C with a pressure of 30 MPa. Initially, the powders were vibrationally hardened and cold pressed at a pressure of 25 MPa, heated for 30 minutes to 1300^{0}C. At 1300^{0}C, the initial pressing took place for 5 minutes at a pressure of 16 MPa. Then the pressure was stopped and heating of the samples to 1700^{0}C was continued. Pressed at 1700^{0}C for 8 minutes at a pressure of 34 MPa. The obtained samples were visually inspected and cut with a diamond disc, according to the dimensions of the samples required for the parameters to be measured. The water absorption capacity, apparent density [17] and relative density of the obtained composites were measured, according to which indicators the degree of smearing was determined. The obtained results are presented in Table 2.

Table 1

Compositions of composites

Composite Number	Sample composition, mas. %								Theoretical density ρ, g/cm³
	Al_2O_3	TiC	B_4C	BN	SiC	MgO	Y_2O_3	C_{fiber}	
19	38.0	30.0	20.0	-	10.0	1.0	1.0	-	3.68
20	53.4	-	22.2	11.1	11.1	1.1	1.1	-	3.22
22	48.0	25.0	15.0	5.0	5.0	1.0	1.0	-	3.66
K5	27.0…	20.0	20.0	10.0	20.0	1.0	2.0	-	3.30
K6	26.5	-	20.5	20.5	28.5	1.0	2.0	1.0	2.96

Table 2

Technical properties of samples pressed at 1700°C

Composite Number	Theoretical density ρ_t, g/cm³	apparent density ρ_a, g/cm³	relative density ρ_r,	water absorption W, %
19	3.68	3.49	0.95	0.03
20	3.22	3.04	0.95	0.06
22	3.66	3.37	0.92	0.07
K5	3.30	3.14	0.95	0.09
K6	2.96	2.72	0.92	0.25

As can be seen from the table, according to water absorption, almost all composites are baked, but based on the relative density indicators, it is likely that the obtained composites contain closed pores. In order to reduce the closed pores, the composites were sintered at an even higher temperature, namely at 1750^{0}C in the same mode as mentioned above. The water absorption capacity, apparent density and relative density were calculated on the received samples. The results are presented in Table 3.

Table 3

Physical properties of samples pressed at 1750^{0}C

Composite Number	Theoretical density ρ_t, g/cm^3	apparent density ρ_a, g/cm^3	relative density ρ_r,	water absorption W, %
19	3.68	3.59	0.97	0.03
20	3.22	3.13	0.97	0.05
22	3.66	3.55	0.95	0.07
K5	3.30	3.27	0.96	0.08
K6	2.96	2.89	0.94	0.14

The degree of sintering of the samples pressed at 1750^{0}C is higher than that of the samples pressed at 1700^{0}C, which is indicated by a relatively high index of relative density, and as for the water absorption ability, it varies within the error limits.

The phase analysis of the obtained samples was performed on the X-ray structural analysis machine DRON-3. By deciphering the radiographs taken[18-21], it was determined that the components taken in the composites of the B_4C-BN-SiC-Al_2O_3 system do not interact with each other to form any new phase, the baked samples also contain the same phases that were taken in the initial samples (Fig. 1), namely corundum d_{hkl} – 3.493; 2.555; 2.383; 2.086; 1.743 Å, Boron carbide d_{hkl} –4.060; 3.805; 3.350; 2.555 Å; and boron nitride d_{hkl} –3.350; 2.176; 1.817, α-SiC d_{hkl} -2.631; 2,528; 2,383; 2.176 Å;

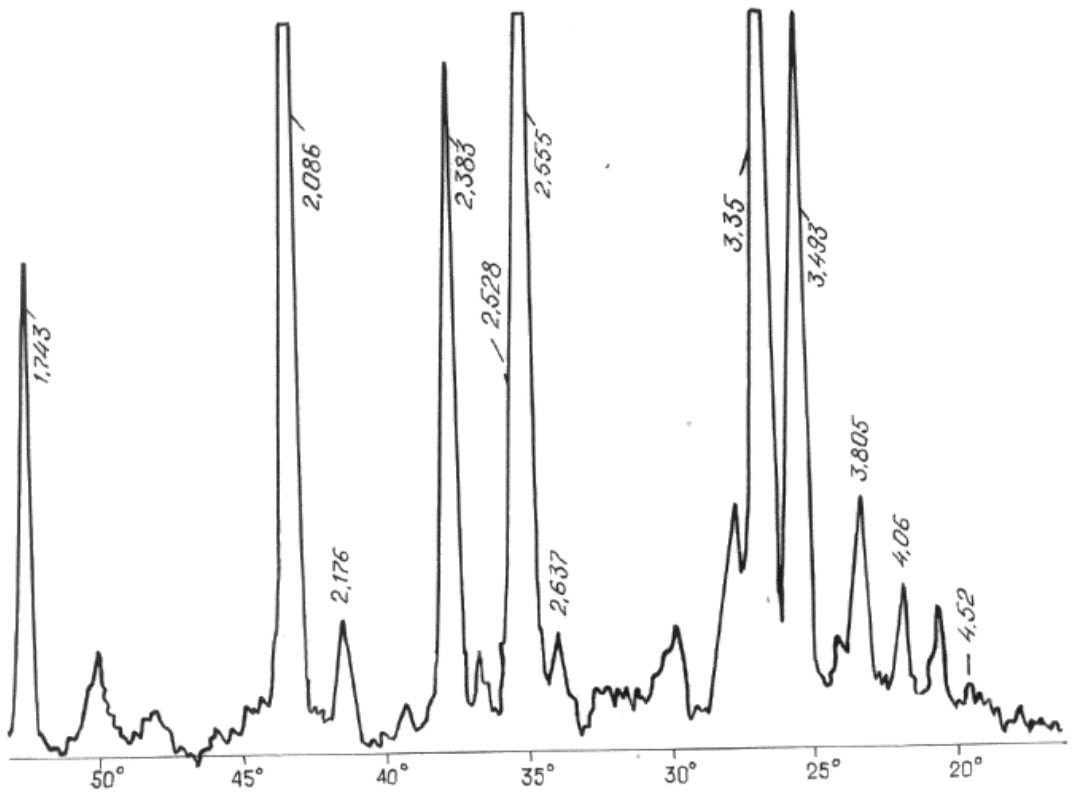

Fig. 1. X-ray of composite #20 sintered at 1750^{0}C

Only their particles were sintered and compacted, as for the systems B_4C-SiC-TiC-Al_2O_3 and B_4C-SiC-BN-TiC-Al_2O_3. Here, under conditions of high temperature and pressure, a reaction between titanium carbide and boron carbide took place, as a result of which a new phase was formed in the material - titanium diboride. Let's consider how this reaction took place on the example of #19 composite:

$B_4C + 2TiC \rightarrow 2TiB_2 + 3C$

As can be seen from the reaction equation, two moles of titanium carbide react with one mole of boron carbide, two moles of titanium diboride and three moles of graphite are formed. Composite #19 contains 30 mass percent titanium carbide, which is 0.5 mol. This amount of titanium carbide will react with 0.25 mol of boron carbide, boron carbide in the composite is 20%, which is equivalent to 0.36 mol, hence titanium carbide should no longer be in the baked sample, and a part of boron carbide still remains, because 0.36-0.25=0.11 mol remained inaccessible to the reaction. As a result of the dissolution of boron carbide, graphite is also formed, as many moles as the moles of boron carbide were dissolved, that is, 0.25 moles, which is fully confirmed by the reflexes recorded on the X-rays: corundum d_{hkl} – 3.470; 2.550; 2.376; 2.086; 1.735; 1.603 Å, boron carbide d_{hkl} –4.020; 3.770; 3.330; 2.550; 2.010 Å, from boron nitride d_{hkl} – 3.330; 2.163; 1.803 Å; α-SiC, d_{hkl} -2.62; 2.51; 2,353; 2.17; 1.538 (100) Å, d_{hkl} of TiB2 – 3.23; 2.62;

2.03(100); 1,612; 1.509 Å, for C-carbon d_{hkl} – 3.37 (100); 2,133; 1682 Å. (Fig. 2).

Figure 3 shows the radiograph of composite #22 based on the B_4C-SiC-BN-TiC-Al_2O_3 system, which shows that titanium diboride is formed by the interaction of titanium carbide and boron carbide, titanium carbide is no longer observed in the material, while part of boron carbide remains, aluminum oxide is observed and boron nitride.

When studying the microstructure of the selected composites, it was observed that their microstructures are characterized by uniformity and relatively fine grain, Fig. 4-6.

In those composites in which a new phase, titanium diboride, was formed, the microstructure is relatively fine-grained, which is probably caused by the diboride phase formed during the sintering period.

A raster-electron microscopic study of the obtained nanocomposites was conducted (Fig. 7 and 8).

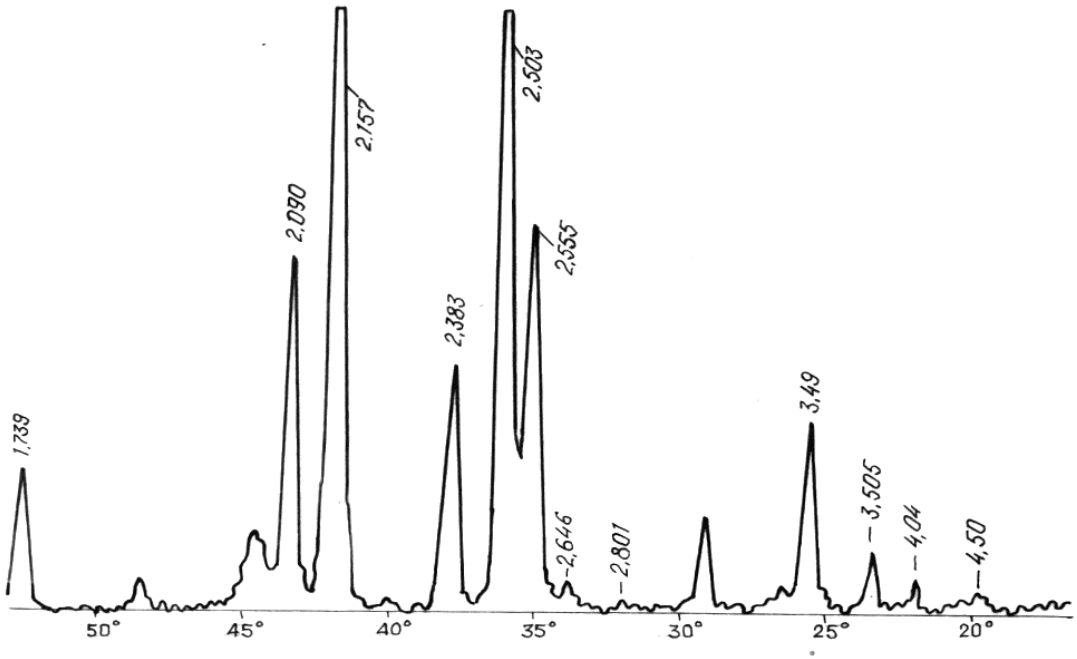

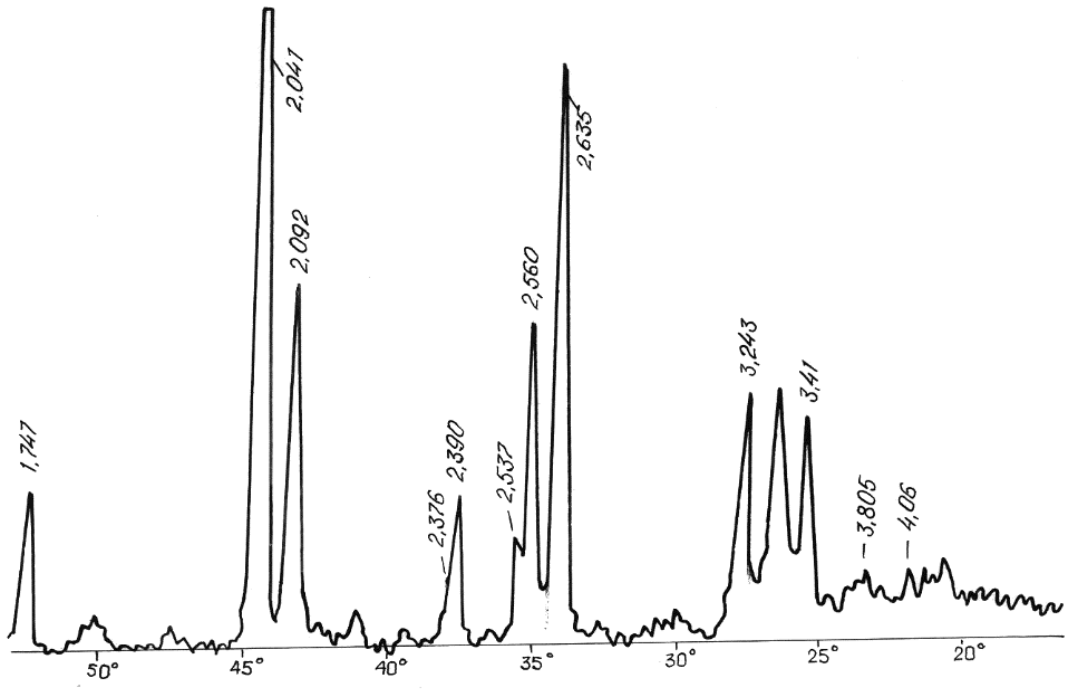

Fig. 2. X-ray of #19 composite, top - raw powder, bottom - baked material at 1750°C

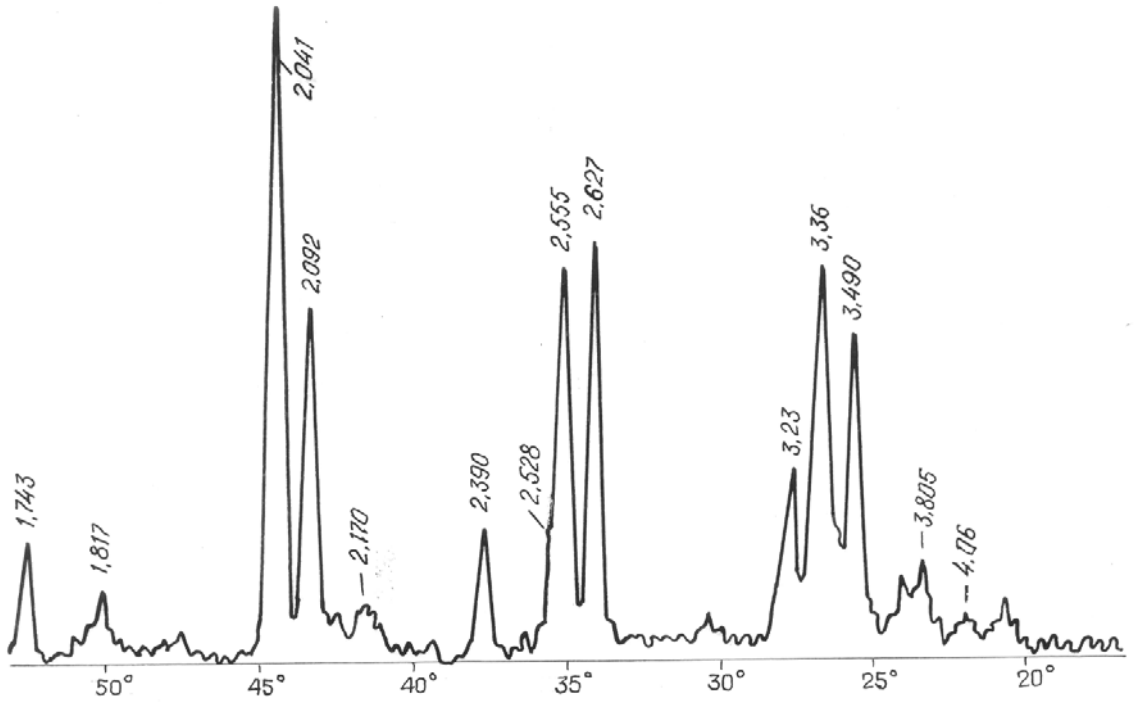

Fig. 3. X-ray image of composite #22 baked at 1750°C

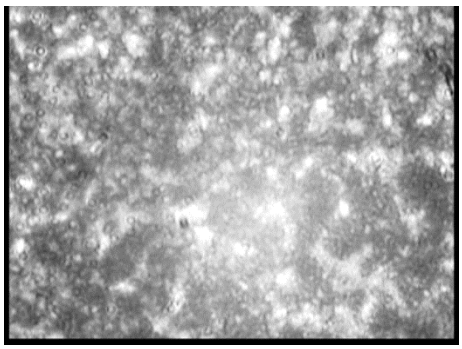

Fig. 4. Microstructure
of #19 composite X 500

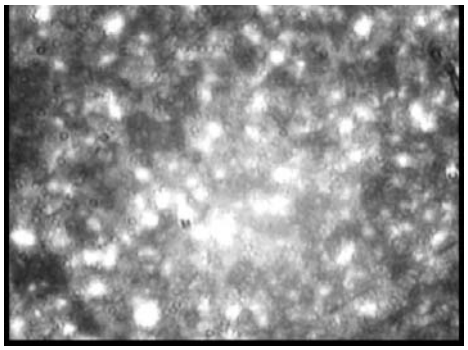

Fig. 5. Microstructure
of #20 composite X 500

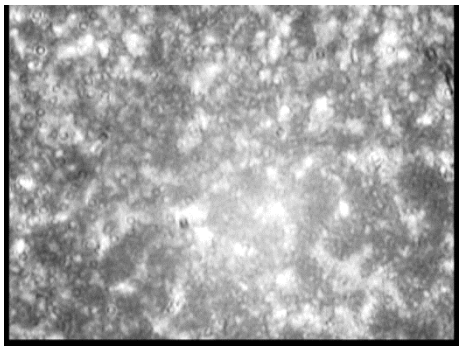

Fig. 6. Microstructure
of #22 composite X 500

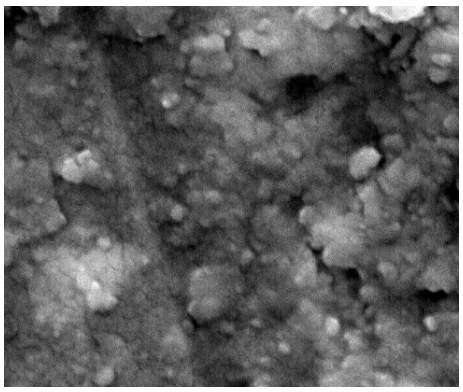

a)

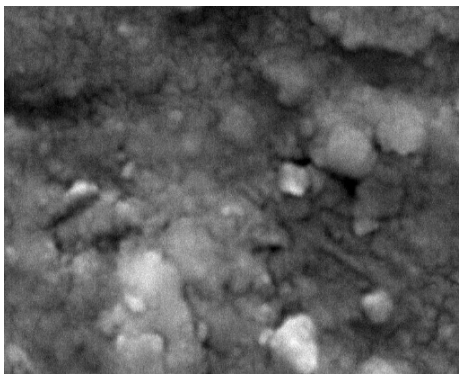

b)

Fig. 7. Electron-microscopic images,
a) TiC 40% - Al_2O_3 60%;
b) TiC 10% - Al_2O_3 90%.
The temperature of hot pressing
is 1450°C. X 2500

As it can be seen from Figure 7, the shape of the grains is almost spherical and the size of the largest grain does not exceed 3 μm, the image shows a sufficiently large number of grains with a size of 400-500 nm.

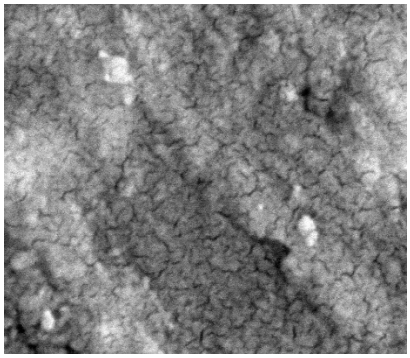

Fig. 8. TiC 10%- Al_2O_3 90% composite matrix structure, hot pressing 1550°C. X4000

When aluminum oxide nano-powder is used, the matrix grains retain their fineness, which can be clearly seen in Fig. 8. The aluminum oxide grains are quite well packed together, the grain size does not exceed 2.0 μm, while it is 10 μm when using technical aluminum oxide.

To measure the mechanical properties, samples of the required size were prepared from the composites of optimal compositions. The coefficient of thermal expansion was measured on a dilatometer in the temperature range of 23-570°C. From the mechanical parameters of the obtained samples, the compressive and bending strength limits were measured, strength with the Vickers method [13] and Rockwell method [14], impact viscosity. The obtained results are presented in Table 4 and Figure 9.

Table 4

Mechanical properties of samples pressed at 1750°C

Composite Number	Tensile strength in compression σ_c, mpa	Bending strength limit, σ_b, mpa	viscosity kj/m²	HV, kg/mm²	HRA
19	1290	360	15	2600	93.5
20	1230	335	14	2300	93.0
22	1195	320	13	2500	93.0
K5	1175	315	13	2550	93.5
K6	1160	255	10	2550	93.5

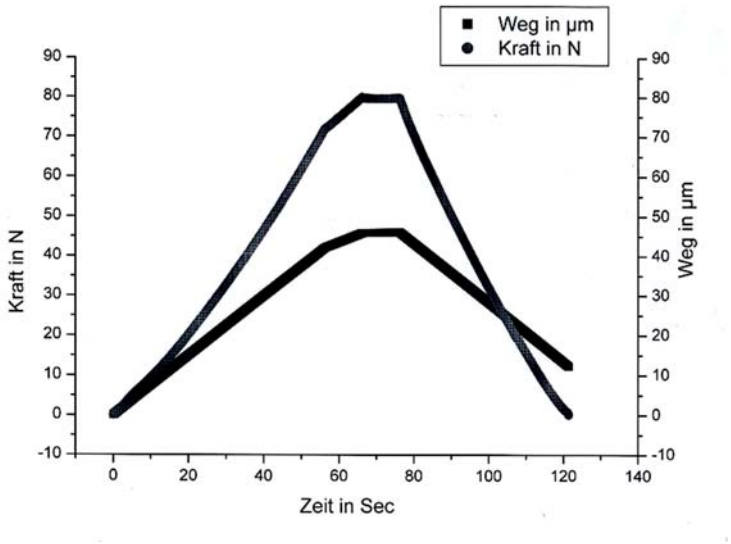

a)

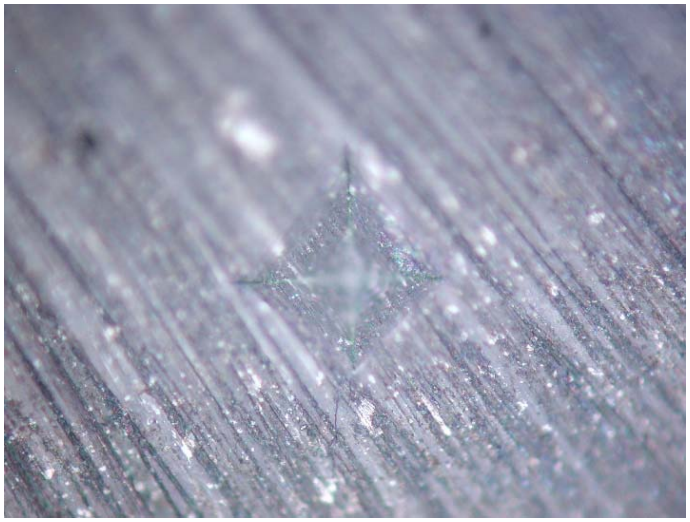

b)

Fig. 9. a); b) HV data of N20-composite.
a) Dependence of the indenter load on the sample and
the distance traveled in time, b) a picture of the indenter print

As the study of the physical-technical properties of the obtained composites showed us, the said composites are characterized by high mechanical properties, particularly high viscosity and microviscosity, according to which we can judge the high wear resistance of these composites. Fig. 9. a) shows the results of composite #19 Vickers test as a diagram,

Microscopic picture of the surface of the same sample in b) after the test. It can be seen from a) that at a load of 80 N, the indenter is inserted into the material with a depth of 42 µM, the shape of the imprint is sharp, with prominent ridges (Fig. 9.b), no crack is observed, therefore there is no place for energy dissipation. The viscous property of the material (Table 4.) is defined here, to withstand the load so that a crack does not appear

and the load energy does not turn into a dissipative event. As for the bending strength index, this parameter is generally low for materials of similar composition, in the case of our composites it is within 255-360 MPa, but the material itself should probably have a higher strength limit. Test specimens are cut from a hot-pressed 6 mm thick disk with a diamond bur, which damages the surface of the specimen. Surface defects are known to have a significant effect on strength performance [22-26]. The physical and technical indicators of the obtained composites allow them to be used in various fields of technology, as a construction material, wearing parts, in hot nodes of flying machines, etc.

Determining the durability of the obtained composites during operation in extreme conditions. Testing samples on thermal resistance

The ability of a material to withstand a sharp change in temperature without breaking is called thermal resistance. This is one of the important properties of brittle materials, which greatly determines their ability to be used in various nodes and constructions. Ceramics are significantly sensitive to thermal loads, and the problem of increasing thermal resistance, as well as mechanical strength, is one of the main factors for the widespread implementation of ceramic materials in processes related to difficult operating conditions.

The main task of the theory of thermal stability is the formulation of any parameter of the material, which can be determined experimentally or calculated from other known mechanical or thermophysical characteristics. One of the main requirements for such a parameter (which is called the "thermos resistance criterion" in the literature) is that it quantitatively characterizes the material's ability to resist the effects of thermal stress and serves the material's ability to work under uneven thermal and force stress conditions. A body will collapse if its strength is less than the thermal stress generated in it.

To determine the response of the samples to sudden temperature fluctuations, they were heated in an oven at 800^0C for 10 minutes and immediately placed in running tap water for 10 minutes to cool. Then the preparations were placed in an optical microscope and after a hundred times magnification, the change in the dimensions of the sample was checked with a micrometer. After 20 cycles, there was no change in the dimensions of the research samples with micrometer accuracy, which indicates the chemical inertness of the mentioned samples to the mentioned conditions. There were also no cases of cracking, while the porcelain samples lasted only 5 cycles and then already cracked.

Dependence of mechanical properties on temperature

Measurement of viscosity is one of the most common methods of mechanical properties of materials, both in research and in production practice. It determines the ability of the surface of the material to resist the penetration of solid particles into it, affects the intensity of abrasive wear. It is even more interesting how the material

maintains its mechanical properties at high temperatures. This property is called heat resistance. The viscosity of the research samples was measured by the Vickers method and the bending strength limit under three-point loading at different temperatures. The measurement results are presented in Tables 5 and 6 and Figures 9 and 10.

Table 5

Dependence of viscosity of composites on temperature

Composite Number	HV, GPa		
	25⁰C	400⁰C	800⁰C
19	18	15	13
20	16	14	11
22	17	15	12
K5	18	15	12,5
K6	18	14,5	13

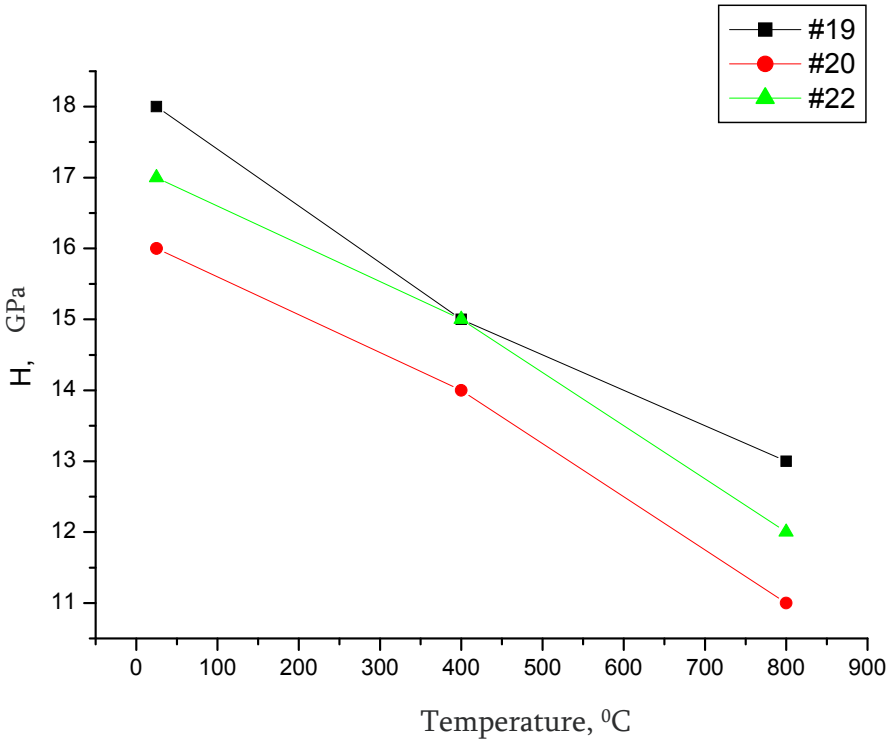

Fig. 9. #19 Dependence of composite viscosity on temperature

Table 6

Dependence of bending strength limit on temperature

Composite Number	bending strength limit σ_b mpa		
	25⁰C	500⁰C	1000⁰C
19	380	400	390
20	350	360	350
22	340	350	340
K5	330	345	340
K6	275	300	280

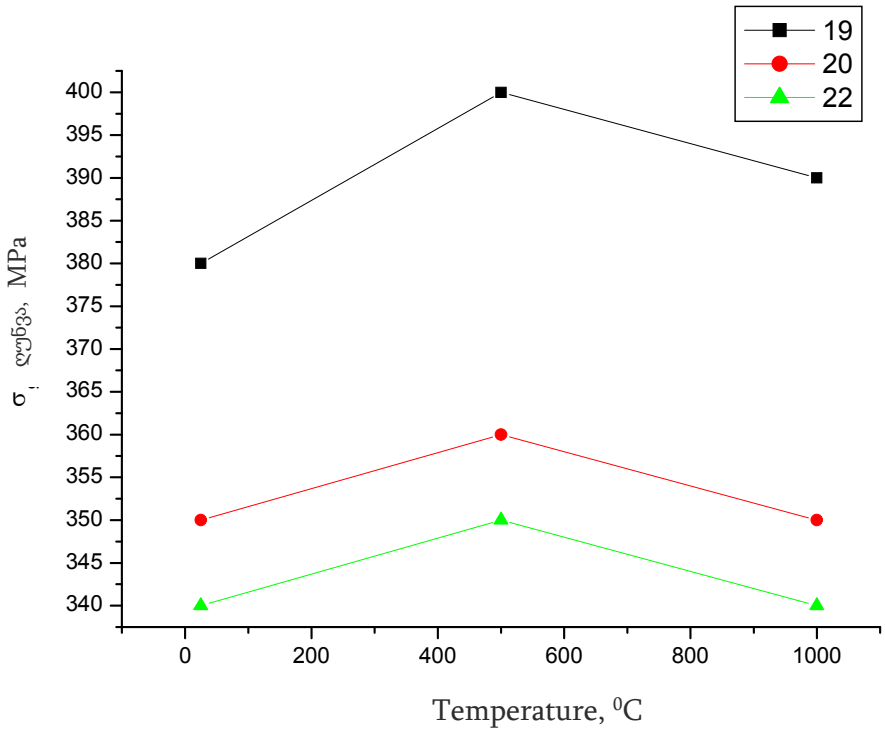

Fig. 10. Dependence of the bending strength limit of #19 composite on temperature

As can be seen from the table and pictures, the viscosity of the composites decreases with the increase in temperature, but it is quite high even at 800⁰, and as for the bending strength limit, with the increase in temperature up to 400⁰, this indicator even increases slightly, which is caused by partial plastic deformation when the temperature is raised to this temperature, and then when the amount of plastic deformation As it increases, the hardness decreases, but at 1000⁰C it still maintains almost its original value. This is probably due to the fact that a small amount of liquid phase is formed in these composites.

3. CONCLUSION

1. Composites with high modular properties were obtained based on B_4C-SiC-TiC-Al_2O_3, B_4C-BN-SiC-Al_2O_3 and B_4C-SiC-BN-TiC-Al_2O_3 systems.

2. Physical and technical properties of composites under high temperature conditions are studied. The viscosity of the obtained composites at 800^0C is 11-13 GPa, the limit of bending strength at 1000^0C is almost the same as at room temperature - 340-390 MPa.

3. It is determined that the obtained composites can withstand thermal shocks without deformation and cracks: 800^0C - water, more than 20 cycles, while technical porcelain can withstand only 5 cycles.

4. Samples were tested under high temperature (≈800-900^0C) and wear conditions. In these conditions, the cutters work when cutting various hard-to-machine materials. The mentioned cutters were tested for processing alloyed cast iron, on a lathe 1K62, under the following cutting conditions: cutting depth t=1.0mm; Supply S=0.21 mm/rev. The wear criterion was taken as h=0.3 mm wear on the back edge of the cutter, which corresponds to the requirements of pure grinding. Durability tests were performed in a certain range of cutting speeds. According to the test results, the performance of the studied composites is not inferior to the standard cutting material "Silinite-P".

5. Analyzing the results of the tests, it was determined that the properties of composites of optimal composition lead to the possibility of their use for operation under high temperature and wear conditions, for example, in dry friction bearings of space vehicles and other similar machines, the so-called Self-lubricating bearings [17-18].

6. In the case of the B11 isotope in boron carbide, these composites can be used as neutron reflectors in nuclear reactors.[22]

7. #20 and K6 composites are recommended due to their low density and relatively high strength for the manufacture of individual and aircraft cabin armor, and composites #19; #22 and K5, for making the armor of heavy armored personnel carriers. [12]

8. The resulting composites can also be used as a cutting material in the technology of hard-to-machine materials: alloyed cast iron, wrought steel, etc. Demand for these materials exists in Georgia and they are imported from abroad.

ACKNOWLEDGMENT

We express our gratitude to Shota Rustaveli Georgian National Science Foundation. The work is done with the grant of the Foundation FR-21-1413 Grant 2022.

REFERENCES

1. Samsonov G.V., Markovsky L.Ya., Zhigach A.F., Valyashko M.G. Boron, its compounds and alloys. Kyiv: Academy of Sciences of the Ukrainian SSR, 1961, pp. 158-194.
2. Lazzari R., Vast N., Besson J. M., Baroni S. and Dal Corso A. Atomic Structure and Vibrational Properties of Icosahedral B4C Boron Carbide. PHYSICAL REVIEW LETTERS, 1999, 83, 16, 3230-3233
3. Z. Kovziridze, G. Tabatadze, N. Kiknadze. Nanoceramic composite in Al_20_3-TiC-TiN system. // 12^{th} Conference of the European Ceramic Society, Stockholm, Sweden, June 19-23, 2011. p.
4. Yulong Wang, Zhoufu Wang, Xitang Wang, Hao Liu, Yan Ma, Pengcheng Jiang, Yunjie

Dong, Jiwei Niu, Effect of short carbon fiber content on strength and toughness of Al_2O_3–C refractories, International Journal of Applied Ceramic Technologies. 17 August 2023.

5. Z. Kovziridze, G. Tabatadze, N. Kiknadze Obtaining of composites based on the Al_2O_3-Thin-Thin system.// Journal of the Association of Ceramicists of Georgia "Ceramics", 2(25), 2011, p. 10-13.
6. Z. Kovziridze, Z. Mestvirishvili, N. Jalabadze, G. Tabatadze. B_4C and Al_2O_3 based composites //2nd International Conference for Students and Young Scientists on Materials Processing Science, Tbilisi, Georgia, 10-13 October 2012.
7. Z. Kovziridze, N.Nizharadze, G.Tabatadze, E.Nikoleishvili, Z.Mestvirishvili, V.Kinkladze. Muitfunctional hetero-modulus composites in the B_4C-BN-TiC-SiC-C system// Journal of the European Ceramic Society, Elsevier, vol.31, issue 10, September 2011, p.1921-1926.
8. Z. Kovziridze, N. Kiknadze, J.G. Hainrich, R. Goerke, G. Tabatadze. STRUCTURAL RESEARCH OF AL_2O_3-TiC SYSTEM NANO-CERAMIC COMPOSITE MATERIAL.// 1st International Conference for Students and Young Scientists on Materials Processing Science,Tbilisi, Georgia 10-13 October 2010, Journal of the Association of Ceramicists of Georgia "Ceramics",, 1(24), 2011, p. 66-72.
9. Jiang T., Jin H., Jin Z., Yang J. and Qiao G. An investigation of the mechanical property and thermal shock behavior of machinable B_4C/BN ceramic composites. Journal of Ceramic Processing Research, 2009, 10, 1, 113-116
10. Mallick P.K. Fiber-reinforced composites materials, manufacturing, and design. Boca Raton: CRC Press, 2008, 619 p.
11. D.Houivet and J.Bernard, Encyclopedia of Materials: Technical Ceramics and Glasses 2021, 112-135 p
12. Karandikar P.G., Evans G., Wong S. and Aghajanian M.K. A REVIEW OF CERAMICS FOR ARMOR APPLICATIONS. Advances in Ceramic Armor IV, Ceramic Engineering and Science Proceedings, 2008, 29, 6, 163-174
13. R.L. Smith & G.E. Sandland, "An Accurate Method of Determining the Hardness of Metals, with Particular Reference to Those of a High Degree of Hardness," Proceedings of the Institution of Mechanical Engineers, Vol. I, 1922, p 623–641.
14. H.M. Rockwell & S.P. Rockwell, "Hardness-Tester," U.S. Patent 1,294,171, Feb 1919.
15. German, R.M.: A-Z of Powder Metallurgy, page 103. Elsevier, 2005.
16. Guillon, O.; et al. (2014). "Field-Assisted Sintering Technology / Spark Plasma Sintering: Mechanisms, Materials, and Technology Developments". Advanced Engineering Materials. 16 (7): 830–849.
17. Mukutadze, M. A.; Khasyanova, D. U. (2019-09-01). "Radial Friction Bearing with a Fusible Coating in the Turbulent Friction Mode". Journal of Machinery Manufacture and Reliability. 48 (5): 421–430.
18. Bearings and Bearing Metals: A Treatise Dealing with Various Types of Plain Bearings, the Compositions and Properties of Bearing Metals, Methods of Insuring Proper Lubrication, and

Important Factors Governing the Design of Plain Bearings Industrial Press, 1921
19. B.D. Cullity, S.R. Stock - Elements of X-Ray Diffraction-Pearson Education Limited (2014)
20. Carmelo Giacovazzo, Hugo Luis Monaco, Gilberto Artioli, Davide Viterbo, Marco Milanesio, Gastone Gilli, Paola Gilli, Giuseppe Zanotti, Giovanni Ferraris, and Michele Catti, Fundamentals of Crystallography, 04 June 2011.
21. Larker, H. T.; Larker, R., Hot isostatic pressing. Materials Science and Technology 1991.
22. Subramanian C., Suri A.K. and Murthy T.S.R.Ch. Development of Boron-basedmaterials for nuclear applications. BARC NEWS LETTER, 2010, 313, 16-22
23. Z. Kovziridze, Z. Mestvirishvili High temperature composites containing boron carbide, Monograph, Technical University of Georgia 2019. 101-104 p
24. S. N. Grigoriev M.A. Volosova, Comprehensive analysis of internal and surface defects of ceramics, MATEC Web of Conferences 65 2016.
25. F. Thevenot, Boron carbide—a comprehensive review, J. Eur. Ceram. Soc., 6 (1990) 205-225
26. Z. Kovziridze, N. Nizharadze, G. Tabatadze, M. Balakhashvili, N. Darakhvelidze, T. Danelia. "OBTAINING NANOCOMPOSITES BASED ON B4C-SIC-BN-TIC-AL2O3 SYSTEM, FOR USE IN DISKS AND WINGS OF TURBINES, HOT NODES OF AIRCRAFT, NUCLEAR REACTORS, FOR BALLISTIC ARMOR" 8th international New York conference on evolving trends in interdisciplinary research and practices, proceedings book, p 816-836.

უაკ 666.946.6

ჰეტერომოდულური ნანოკომპოზიტების მიღება B_4C-SiC-BN-TiC-Al_2O_3 სისტემის ბაზაზე ტურბინების დისკების და ფრთებისთვის, ბალისტიკური ჯავშნებისათვის, მფრინავი აპარატების ცხელ კვანძებში სამუშაოდ

ც. დანელია

ქიმიური და ბიოლოგიური ტექნოლოგიების დეპარტამენტი, ბიონანოკერამიკისა და ნანოკომპოზიტების ტექნოლოგიის ინსტიტუტი. საქართველოს ტექნიკური უნივერსიტეტი. კოსტავას 69. თბილისი. საქართველო.

E-mail: Tsddental@gmail.com

რეზიუმე: მიზანი. ჰეტერომოდულური, მაღალი საექსპლოატაციო თვისებების მქონე ნანოკომპოზიტების მიღება B_4C-SiC-BN-TiC-Al_2O_3 სისტემების ბაზაზე.

მეთოდი. სტრუქტურული კვლევა ჩატარდა რენტგენოსტრუქტურული ანალიზის დანადგარზე DRON 3, ოპტიკურ-მიკროსკოპიული კვლევა განხორციელდა მიკროსკოპზე AC100,

ელექტრონულ-მიკროსკოპიული კვლევა - OPTON დანადგარზე. გაიზომა მიკრო და მაკრომექანიკური თვისებები.

შედეგები. მიღებულია მაღალი მოდულური თვისებების მქონე ნანოკომპოზიტები B_4C-SiC-BN-TiC-Al_2O_3 სისტემის ბაზაზე. სტრუქტურული კვლევით დადგინდა, რომ მარცვლების ფორმა ძირითადად სფერულს უახლოვდება და ყველაზე დიდი მარცვლის ზომა არ აღემატება 3 მკმ-ს, სტრუქტურა ძირითადად ერთგვაროვანია. შესწავლილია კომპოზიტების ფიზიკურ-ტექნიკური თვისებები მაღალი ტემპერატურის პირობებში. მიღებული კომპოზიტების სისალე 800^0C-ზე 11-13 გპა-ს შეადგენს, სიმტკიცის ზღვარი ღუნვაზე 1000^0C ტემპერატურაზე თითქმის იგივეა, რაც ოთახის ტემპერატურაზე - 340-390 მპა.

დასკვნა. მიღებული კომპოზიტები დეფორმაციისა და ბზარების გარეშე უძლებენ თერმულ დარტყმებს: 800^0C–წყალი, 20-ზე მეტ ციკლს. კომპოზიტების თვისებები განაპირობებს მათი გამოყენების შესაძლებლობას მაღალი ტემპერატურისა და ცვეთის პირობებში ექსპლუატაციისათვის, მაგალითად კოსმოსური აპარატებისა და სხვა მსგავსი მანქანების მშრალი ხახუნის საკისარებში, ე.წ. თვით შემზეთი საკისარები. #20 და K6 კომპოზიტები მათი დაბალი სიმკვრივისა და შედარებით მაღალი სიმტკიცის გამო რეკომენდირებულია ინდივიდუალური და თვითმფრინავების კაბინების ჯავშნების დასამზადებლად, ხოლო კომპოზიტები #19; #22 და K5, მძიმე ჯავშან-ტრანსპორტიორების ჯავშნის დასამზადებლად.

საკვანძო სიტყვები: ჰეტერომოდულური, სტრუქტურა, მაღალი ტემპერატურა, სისალე, ცვეთამედეგობა.

UDC 666.946.6

COMPOSITE OF HIGH PHYSICAL AND TECHNICAL PROPERTIES IN THE TiC-Ni-Fe SYSTEM

Z. Kovziridze, N. Nizharadze, G. Tabatadze, M. Mshvildadze

Georgian Technical University. Institute of Bionanoceramics and Nanocomposites Technology. Department of Chemical and Biological Technologies, Georgia, 0175, Tbilisi, Kostava Str. 69

E-mail: kowsiri@gtu.ge

Resume: **Goal:** The goal of the work is to obtain a material with high technical characteristics in the TiC-Ni-Fe system and determine the scope of its application.

Method: Obtaining of the composite by the traditional method of powder metallurgy, hot pressing, phase analysis and microstructure of the resulting material using X-ray diffraction and electron microscopy, mechanical properties: tensile and bending strength were determined using a R-100 tensile testing machine, hardness was determined by the Vickers and Rockwell methods.

Result: The composition of a group of materials with high physical and technical characteristics in the TiC-Ni-Fe system has been developed, the parameters of the technological regime for their implementation have been determined, the physical, mechanical and operational properties have been studied, and the scope of application has been determined.

Conclusion: A group of materials with high physical and technical characteristics in the TiC-Ni-Fe system has been obtained, the hardness of which is 88.0-89.5HRA; bending strength 1300-2000 MPa; Impact strength is 18-38 kJ/m2, maintained up to a fairly high temperature. The area of rational use of a tungsten-free composite can be considered processes of cutting materials that are not associated with the release of a large amount of heat: for the manufacture of punches and die matrices, as well as for the manufacture of various technological equipment, including fillers-for rolling steel pipes, as well as material for cutting non-ferrous metals.

Key words: composite, tungsten-free cutting material, hardness, impact strength.

1. INTRODUCTION

Increasing the level of development of the most important branches of technology includes the need to create new materials, among which metal-ceramic composite materials occupy an important place.

The development of the industry without metalworking materials is unthinkable.

The main part of metalworking materials is produced on the basis of tungsten, the reserves of which are gradually running out, at the same time it is a raw material of strategic importance. In this regard, scientists are faced with the problem of creating new materials from which tungsten will be excluded or its content will be significantly reduced, while it is necessary to preserve the

physical, technical and operational properties of the material characteristics.

A number of important works have been carried out in this direction [1-21], but the main emphasis is still on tungsten-based materials. We also want to try to make a small contribution to solving this problem.

We focused our attention on non-scarce materials and chose the TiC-Ni-Fe system; titanium carbide is not inferior to tungsten carbide in a number of physical and technical properties, and even surpasses it in fire resistance and oxidation resistance, which gives it a significant technical and economic advantage.

One of the important tasks in the field of creating metal-ceramic materials is to determine the optimal ratio between the concentration of the refractory ceramic component and the binder metal when connecting at least two different phases.

The properties of a metal-ceramic material depend on the properties of both the solid and the metal phase; as is known [22-23], the metal binder should be well wetted and distributed over the surface of carbide grains, the interaction between carbide and metal should not exceed a small mutual solubility and new ones should not form brittle intermediate phases, which sharply reduces the strength of the material.

2. MAIN PART

To determine the effect of the content of the metal binder, composites with three different contents of the metal phase (Table 1) were selected and subjected to hot pressing in the temperature range of 1280-1350^0 C. The vacuum was 10^{-3} MPa. Sample forming pressure -25 MPa. Firing duration is 30 minutes. Delay at final temperature - 8 min.

Table 1

Composition of research composites of the TiC-Ni-Fe system, wt.%

Composite name	TiC	Ni	fe	Sintering temperature,^{0}C
TNF-1	90	7	3	1350
TNF-2	85	10	5	1300
TNF-3	80	15	5	1280

As the sintering temperature increases, the shrinkage of the samples increases and the porosity decreases, the higher the content of the binder phase in the composite; based on the data obtained, we determined the optimal tempering temperature for the composite of each composition (Table 2).

Table 2

Sintered samples, open porosity and density

Composite name	Sintering temperature,^{0}C	Shrinkage %	Open porosity, %	Density, g/cm3
TNF-1	1350	19,5	0,1-0,20	5,2
TNF-2	1300	20.5	0,1-0,15	5,3
TNF-3	1280	21,0	0,1-0,15	5,5

The microstructure and phase composition were studied by X-ray phase and electron microscopic analysis, the results of which established that the resulting composites consist of a solid carbide phase and a binder metal phase.

In X-ray diffraction patterns, the reflections of titanium carbide at low temperatures do not have a clearly defined shape, but with increasing temperature they acquire a sharp peak shape. During the process of its activation, stresses and defects accumulate in the titanium carbide powder, which will appear as blurred lines on the ionization curves. During the sintering process, titanium carbide undergoes recrystallization, the crystal grid becomes perfect, and the diffraction lines become sharper. The characteristic diffraction maxima of nickel shift towards small angles when iron is introduced into the binder alloy, which indicates the formation of a Ni-Fe solid solution and an increase in the Messer parameter (Fig. 1).

At sintering temperature, the microstructure is practically non-porous, carbide grains are evenly distributed in the metal phase. (Fig. 2 a); b); c).

Carbide grains have a more or less rounded shape. Once the microstructure is formed, increasing the lubricant temperature has little effect on the growth of carbide grains. When studying the influence of the content of the binder phase, it was found that with a lower content of the metal phase, the microstructure is more fine-grained and uniform, the average size of carbide grains is 1-2 μm, while the liquid phase increases to 15%, the average size of carbide grains also increases to 2-3 μm , metal phase. A further increase to 20% does not have a significant effect on the growth of carbide grains.

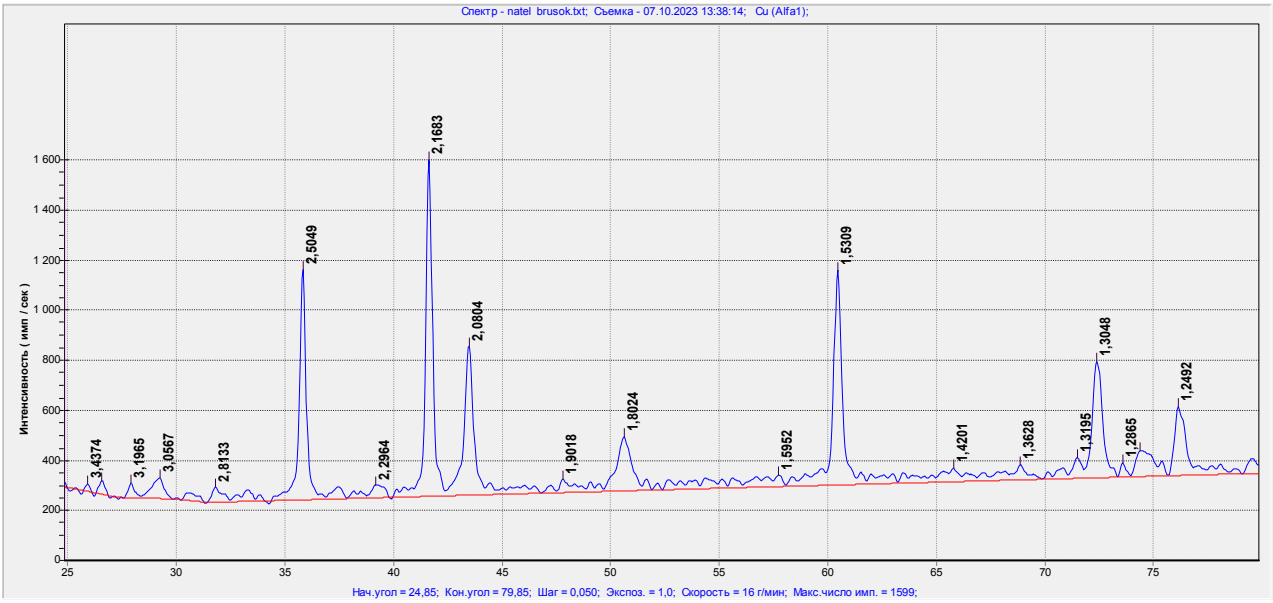

Fig.1 TNF of the composite X-RAY

1.TiC –d_{hkl} 2.50,2.168,1.531,1.305,1.250A^0

2.Fe(Ni)– d_{hkl} 2.080,1.802,1.280 A^0

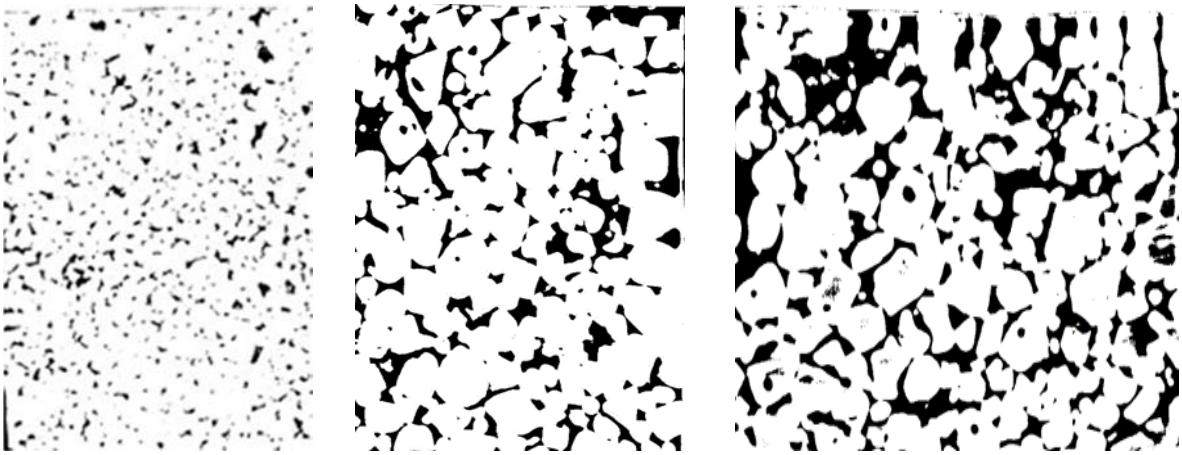

a) X1500 b) X2100 c) X2100

Fig.2. TNF-1 (a), TNF-2 (b) , TNF-3 (c)

Microstructure of composites

From the analysis of the Ti-C-Fe ternary system [24], it follows that the solubility of iron in titanium carbide and iron carbide is insignificantly low, while iron and nickel form a solid solution [25]. A study of a research composite with a 20% binder phase content on a Cameca X-ray spectrometer showed that the grains are pure carbide with a very small concentration of dissolved nickel and iron (Fig. 3 a, b, c, d). Near the boundaries of carbide grains, the radiation intensity of iron atoms sharply decreases compared to the matrix.;

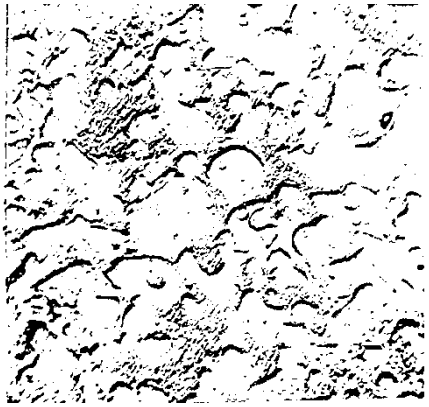

a) Electronic image

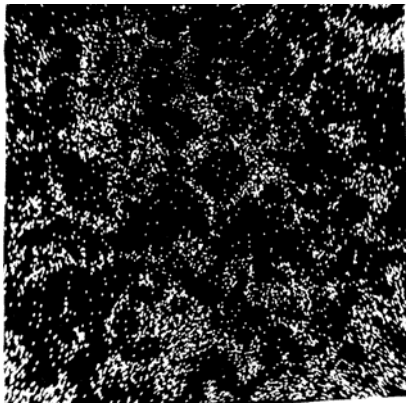

b) Ni-radiation

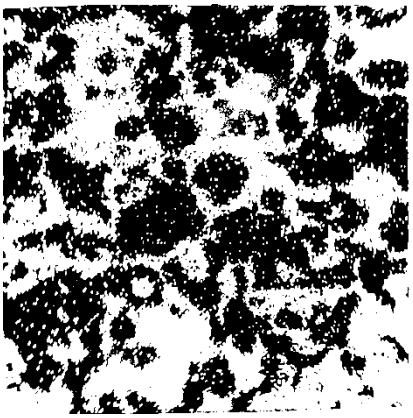

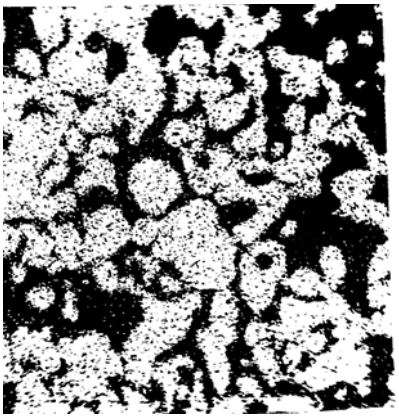

c) Fe-radiation Ti-radiation

Figure 3. Results of micro-X-ray spectroscopic analysis of the TNF composite

Similar behavior is observed in the case of nickel. The distribution of elements in the composite is homogenous, the binder phase contains a very small amount of dissolved titanium and carbon.

Composites with different contents of the binder phase have different optimal sintering temperatures (Table 2); at these temperatures, all composites achieve almost zero porosity. The microstructure is a metal matrix of a Ni-Fe solid solution, in which carbide grains are evenly distributed.

Mechanical properties of cutting materials include hardness, bending strength and toughness.

During the sintering process at relatively low temperatures, when only solid-phase grinding still occurs, the samples slowly gain strength; with the formation of a liquid phase in the material, the grinding process becomes more intense, the bond between solid grains due to the liquid phase acquires greater strength, as evidenced by an increase in hardness and strength. The results of determining the mechanical properties are presented in Table 3.

Table 3

Mechanical properties of TiC-Ni-Fe system composites at room temperature

Composite name	Sintering temperature, ^{0}C	Ultimate bending strength, MPa	Hardness Rockwell, HRA	Impact toughness, kJ/m2
TNF-1	1350	1300-1400	89,0-89,5	18-20
TNF-2	1300	1500-1600	88,0-89,0	25-28
TNF-3	1280	1700-2000	86,0-87,0	32-38
BK8		1400-1500	89,5	42

For comparison, the table presents the mechanical properties of the standard tungsten carbide-based Sal alloy (VK8-composition: WC-92; Co-8 wt.%), from which it can be seen that the studied composites are not much inferior to this.

Determine to what extent composites will retain this property under operating conditions, since high temperatures develop during cutting and the cutting surface undergoes plastic deformation. The mechanical properties of the samples at high temperatures were determined.

Since the metal phase of these composites is ductile, their strength decreases rapidly with increasing temperature, but it is also worth noting that at 1000 ^{0} C it still retains a fairly high strength in the range of 450-550 MPa.

Hardness at high temperature was determined, the test results are presented in Table 4.

Table 4

The mechanical properties of TiC-Ni-Fe system composites at the high temperature

Test temperature, ^{0} C	Hardness		
	TNF-1	TNF-2	BK8
200	16	14	13
400	14	12	10
600	13	7	8
800	5	4	5
1000	4	3	3

Thus, the studied composites in mechanical properties at room temperature are not much inferior to the standard hard alloy containing scarce tungsten and cobalt. It is worth noting the fact that determining hardness at high temperatures is not a long process, but if we are talking about the performance of the material at high temperatures and long-term operation, then the tested samples retains their properties much stronger. We'll talk more about this below.

As for the elongation indices of the studied composites, which have both theoretical and practical significance, at room temperature they are no less than those of tungsten-containing alloys, only at high temperatures their values decrease faster.

The modulus of elasticity of TNF-2 at room temperature is 450 GPa, Poisson's ratio is 0.20, in the range of 800-1100^0 C it decreases from 60 to 30 GPa.

The amount of thermal stress generated during the cutting process of a material significantly depends on the coefficient of thermal expansion of the material. Thermal expansion is also important when comparing bonding inserts or products in general to other materials.

The coefficient of thermal expansion of the studied samples was determined on a quartz dilatometer equipped with a vacuum device, with a residual pressure of 10-3 mm water column of silver and a temperature range of 25-600^{0}C, with automatic registration of sample elongation. For comparison, parallel measurements were carried out on a sample of the standard composition BK8. The results of the analysis are presented in Table 5.

Table 5

Thermal growth coefficient of composites of the TiC-Ni-Fe system (TC)

Name of the composite	Average thermal growth coefficient, TGC α, 10^{-6} C^{-1}		
	25-200	25-400	25-600
TNF-1	5.80	7,65	8,50
TNF-2	5,65	7,44	8,23
TNF-3	5,15	6,54	7,67
BK8	3,57	4,33	4,70

From Table 5 it can be seen that the standard tungsten carbide alloy has the lowest coefficient of thermal expansion, since tungsten carbide has a significantly lower coefficient of thermal expansion than titanium carbide. The studied composites contain an iron-nickel metal binder, the coefficient of thermal expansion of which is zero, therefore, an increase in the content of the metal binder in the studied composites leads to a partial decrease in the value of the coefficient of thermal growth.

It is known that the working surface of a cutting tool intersects with a fairly high temperature during operation. The heated material interacts with atmospheric oxygen and oxidizes, as a result of which the physical, technical and operational properties of the tool change. Therefore, when developing new tool materials, great importance is attached to the ability of the material to resist oxidation. In the literature, information on the degree of oxidation is given mainly for pure substances [26-28], while the data of different authors differ greatly from each other. Pure substances and multicomponent systems undergo oxidation through different mechanisms. This makes it necessary to investigate the resistance to oxidation of each new tool material.

The studies were carried out according to the methodology given in [26]. The samples had a plate shape with dimensions of 15X15X4 mm and a rod shape with dimensions of 5X5X35, surface cleanliness Ra = 1.25, porosity 0.2%.The samples were heated in a muffle furnace in the air zone. The temperature change during the isothermal delay was 5^0°C. The quality of the powder was assessed by the weight gain Δm/S, mg/cm2, depending on the duration of the test and temperature. No change in the thickness of the samples was observed at temperatures of 700-900 degrees, and a change in mass was observed at 750 degrees. Table 6 and Fig. 4

Table 6

Oxidation resistance of TNF composite at different temperatures

Temperatures, ^{0}C	Duration of oxidation, h/weight gain, mg/cm^2				
	1	2	3	4	5
700	0	0,5	0,8	0,9	1,0
750	1,0	1,3	1,5	1,5	1,6
800	1,7	2,1	2,4	2,7	2,9
900	2,0	2,5	3,0	3,4	3,9

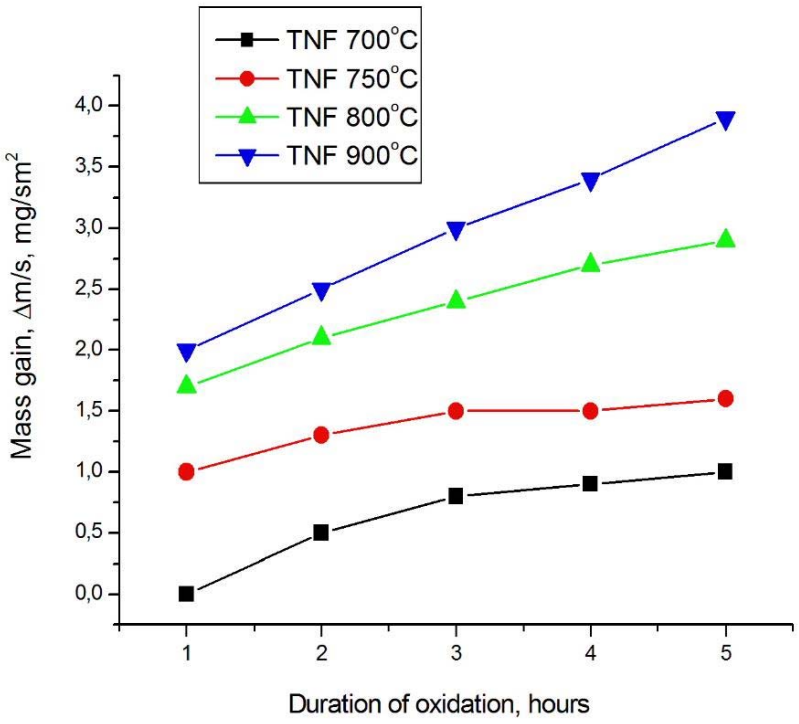

Fig. 4. Oxidation curves of TNF composite samples

As can be seen from the experimental data, with increasing temperature and delay time, the mass gain in the samples increases; it is worth noting that the oxidation rate in the studied composites is very low, the highest rate was recorded in the initial state, the period of the process when oxygen opens on the surface, and then a rusty layer of complex composition is formed, which is a barrier to further diffusion of oxygen deep into the plate, the speed of the process also decreases.

As for the results of the comparative test, in relation to the reference alloy, the oxidation resistance of the alloy under study is significantly higher than the standard, which is presented in Table 7, Fig. at 5 and 6.

Table 7

Oxidation resistance of TNF and BK8 composites at 8000 C

Material name	Duration of oxidation, h/weight gain, Δm/S, mg/cm²				
	1	2	3	4	5
TNF	1,7	2,1	2,4	2,7	2,9
BK8	12	30	43	90	97

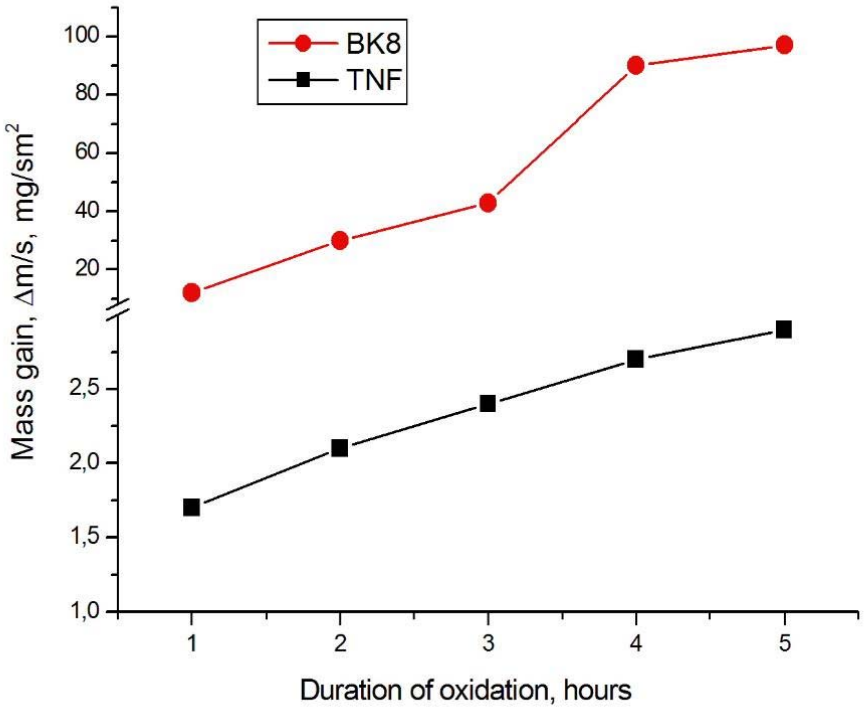

figure 5. Oxidation curves at 800⁰ C for materials TNF-2 and VK8

As shown by layer-by-layer X-ray diffraction analysis, titanium carbide first transforms into oxycarbide, then with a greater delay it is oxidized to TiO_2 and CO_2. On the surface of the TNF-2 plates, where there is more contact with oxygen, iron is oxidized to Fe2O3, and ferrotitanate lines are also observed in the rust layer.

The increase in the thickness of the studied samples at 800^0 C with a five-hour delay for TNF-2 was 0.02-0.10 mm, and for BK8- 1.5-2.8 mm. Thus, the studied composite is significantly more resistant to oxidation than the standard tungsten-based alloy BK8.

a) **b)**

Fig. 6. a) Images of test TNF-2 and b) standard BK8 plates at 700 and 800 degrees after a 5-hour delay

As can be seen from Figure 6, the shape of the composite plates studied did not change, while the standard tungsten-based plates experienced such an increase in corrosion that we ended up with a completely different configuration. From the analysis of electron microscopic images of the surface of the oxidized samples (Fig. 7 a) and b) it is clear that the surface of the sample under study is still dense, while the surface of the standard tungsten-containing alloy sample is loose.

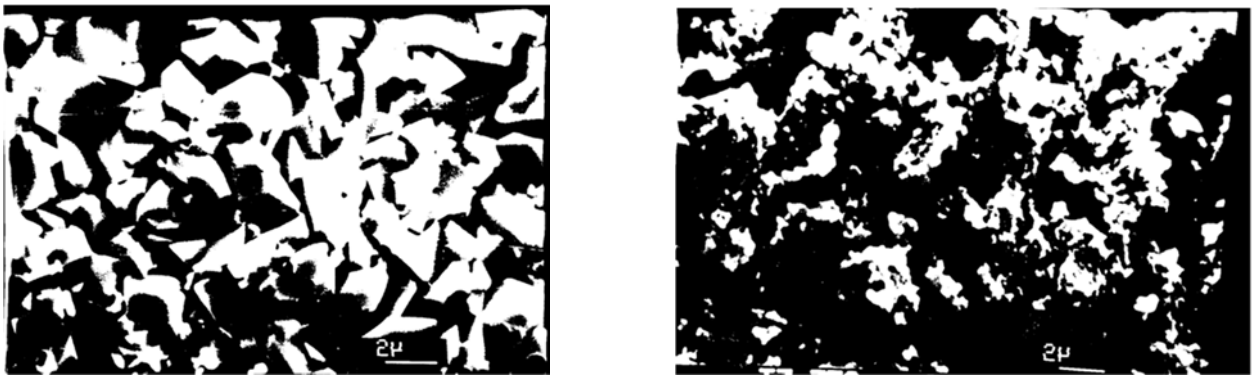

a) **b)**

Fig. 7. Images of the surface of a) TNF composite and b) plates of tungsten-containing alloy VK8 after oxidation at 800^0 C- with a delay of 5 hours

In terms of performance properties at low cutting speeds (0.5 m/s) and a temperature of 600^0 C, the wear resistance of the composite under study is the same as that of standard alloys: titanium carbide and carbonitride based, cobalt binder (Т15К6ж КНТ16). Tests of TNF-2 plates showed good results when cutting non-ferrous metals. It was important here that the so-called hardening is caused by the lack of diffusion of atoms from the processed material into the cutting material.

Tests of eyelets made of research composite for pipes made of steel 20 with a diameter of 25 mm showed much better results than eyes made of BK8.

3. CONCLUSION

in this way a group of materials with high physical and technical characteristics was obtained in the TiC-Ni-Fe system, the HRA of which is 88.0-89.5; bending strength 1300-2000MPa; Impact strength, kJ/m2 – 18-38, is maintained at a fairly high temperature. The area of rational use of a tungsten-free composite can be considered processes of cutting materials that are not associated with the release of a large amount of heat: for the manufacture of punches and die matrices, as well as for the manufacture of various technological equipment, including fillers- for rolling steel pipes, as well as material for cutting non-ferrous metals.

ACKNOWLEDGMENT

We express our gratitude to Shota Rustaveli Georgian National Science Foundation. The work is done with the grant of the Foundation FR-21-1413 Grant 2022.

REFERENCES

1. Panov, V.S., Chuvilin, A.M., and Fal'kovskii, V.A., Tekhnologiya i svoistva spechennykh tverdykh splavov i izdelii iz nikh (Technology and Properties of Sintered Solid Alloys and Their Products), Moscow: Mosk. Inst. Stali Splavov, 2004.
2. Borovinskaya, I., Gromov, A., Levashov, E., Maksimov, Yu., Mukasyan, A., and Rogachev, A., Concise Encyclopedia of Self-Propagating High-Temperature Synthesis: History, Theory, Technology, and Products, Eds., Amsterdam: Elsevier, 2017.
3. Levashov, E.A., Mukasyan, A.S., Rogachev, A.S., and Shtansky, D.V., Self-propagating high-temperature synthesis of advanced materials and coatings, Int. Mater. Rev., 2017, vol. 62, no. 4, pp. 203–239.
4. Levashov, E.A., Pogozhev, Yu.S., et al., in Advances in Ceramics—Synthesis and Characterization, Processing and Specific Applications, Sikalidis, C., Ed., London: IntechOpen, 2011.
5. Amosov, A.P., Borovinskaya, I.P., and Merzhanov, A.G., Poroshkovaya tekhnologiya samorasprostranyayushchegosya vysokotemperaturnogo sinteza materialov (Powder Technology of Self-Propagating High-Temperature Synthesis of Materials), Moscow: Mashinostroenie, 2007.
6. Konyashin, I., The formation of wear-resistant layers, including a stress-relaxing interlayer, during a chromium surface treatment of tic or ticn based cermets, Int. J. Refract. Met. Hard Mater., 1997, vol. 15, pp. 187–195.
7. Konyashin, I., Interaction between the TiC (TiCN)–Ni–Mo hardmetals and chromium

vapours, J. Mater. Sci., 1995, vol. 30, pp. 5723–5731.

8. Prvan Kumar Katiyar,Avala Lavakumar,Rita Maurya &Prince Kumar Singh, . High entropy alloys (HEAs) as a binder material for heavy tungsten alloys, tungsten carbide hardmetals, and titanium carbo-nitride based cermet composites - a comprehensive review ttps://doi.org/10.1080/2374068X.2022.2142397 Accepted 27 Oct 2022, Published online: 04 Nov 2022
9. Y. Fahin Department of Manufacturing Engineering, Faculty of Technology,Gazi University, Besevler, 06500 Ankara,Turkey. Recent Progressin Processing of Tungsten Heavy Alloys. Hindawi Publishing Corporation Journal of Powder Technology Volume 2014, Article ID 764306, 22 pages http://dx.doi.org/10.1155/2014/764306
10. Baharvandi H.R., Hadian A.M., Pressureless Sintering of TiB2- B4C Ceramic Matrix Composite. Journal of Materials Engineering and Performance, 2008, 17,838–841
11. Yamada S., Hirao K., Yamauchi Y., Kanzaki S. Densificationbehaviour and mechanical properties of pressureless-sintered B4C–CrB2 ceramics. J. Eur. Ceram. Soc., 2003, 23, 1123–1130
12. V. A. Pesin, A. S. Osmakov, S. Yu. Boykov. Dependence of the properties of WC–Co hard alloys on their composition and microstructure characteristics; News from universities. Powder metallurgy and functional coatings, Refractory, ceramic and composite materials, No. 3 (2022) 37-44.
13. Nino A., Takahashi K., Sugiyama S., Taimatsu H. Effects of carbon addition on microstructures and mechanical properties of binderless tungsten carbide. Mater. Trans. 2012. Vol. 53. Iss. 8. P. 1475-1480. https://doi.org/10.2320/matertrans.M2012148
14. Nino A., Izu Y., Sekine T., Sugiyama S., Taimatsu H. Effects of TaC and TiC addition on microstructures and mechanical properties of binderless WC. Int. J. Refract. Met. Hard Mater. 2019. Vol. 82. P. 167-173. https://doi.org/10.1016/j.ijrmhm.2019.04.012.
15. Konyashin I., Zaitsev A.A., Sidorenko D., Levashov E.A., Ries B., Konischev S.N., Sorokin M., Mazilkin A.A., Herrmann M., Kaiser A. Wettability of tungsten carbide by liquid binders in WC-Co cemented carbides: Is it complete for all carbon contents? Int. J. Refract. Met. Hard Mater. 2017. Vol. 62. P. 134-148. ttps://doi.org/10.1016/J.IJRMHM.2016.06.006
16. L. E. Agureev, V. I. Kostikov, Zh. V. Eremeeva, B. S. Ivanov, S. V. Savushkina, I. N. Laptev, A. A. Ashmarin, A. V. Ivanov, G. V. Sivtsova. Study of the structure and properties of cermets based on the NiAl–Al2O3 system. News from universities. Powder metallurgy and functional coatings, Refractory, ceramic and composite materials, No. 2 (2021) 31-40
17. Z. Kovziridze, N. Nizharadze, G. Tabatadze. High-strength tungsten-free composite in the TiC-Ni-Fe system. Journal of the Georgian Ceramists Association “Ceramics”, volume 18. 2(36), 2016, pp. 29-39.
18. Z. Kovziridze N. Nijaradze, Z. Mestvirishvili Ceramic Composite in AL2O3-B4C-TiC System 13th Conference of the European Ceramic

Siciety, Limoges-France, June 23-27, 2013 (Thesis)
19. Z. Kovziridze N. Kiknadze, Cutting ceramic composite material on the basis of Al2O3–TiC –WC-TiN system 2nd International Conference for Students and Young Scientists on Materials Processing Science, Tbilisi, Georgia, 10-13 October 2012, pp.136-141
20. Z. Kovziridze N.Kiknadze Nanoceramic composite in Al203-TiC-TiN system 12th Conference of the European Ceramic Society, Stockholm, Sweden, June 19-23, 2011.
21. Z. Kovziridze T. Cheishvili, N. Nizharadze, I. Bairamashvili, E. Nikoleishvili, N. Rekhviashvili, V. Kinkladze, Z. Mestvirishvili MULTIFUNCTIONAL HETERO-MODULE COMPOSITE IN B4C-BN-TiC-SiC-C SYSTEM Journal of Georgian Ceramists Association "Ceramics" N 1(19), Tbilisi, 2009, p.3-9.
22. V.N. Tretyakov. Fundamentals of metallurgy and technology for the production of sintered hard alloys, M., Metallurgy, 1976, 526 p.
23. Ceramic instrumental materials, edited by Dr. Tech. Sciences G.G. Gnesina, Kyiv, "Technology", 1991, p. 390.
24. Eremenko V.N. Multicomponent titanium alloys, Kyiv. From the Academy of Sciences of the Ukrainian SSR, 1962, 209 p.
25. Elliott R.P., Structure of double alloys M., Metallurgy, 1970, 456 p.
26. Voitovich R.F., Pugach E.A., Oxidation of refractory compounds, reference book, "Metallurgy" M., 1978, 106 p.
27. Voytovych R.F., Golovko E.I., High-temperature oxidation of metals and alloys, reference book "Naukova Dumka", Kyiv, 1980, 292 p.
28. Kovsted P., High-temperature oxidation of metals, Ed. Mir, M., 1969, 392 p.

უაკ 666.946.6

მაღალი ფიზიკურ-ტექნიკური თვისებების კომპოზიტი TiC-Ni-Fe სისტემაში

ზ. კოვზირიძე, ნ. ნიჟარაძე, გ. ტაბატაძე, მ. მშვილდაძე

საქართველოს ტექნიკური უნივერსიტეტი. ბიონანოკერამიკისა და ნანოკომპოზიტების ტექნოლოგიის ინსტიტუტი. ქიმიური და ბიოლოგიური ტექნოლოგიების დეპარტამენტი.

E mail: kowsiri@gtu.ge

რეზიუმე. მიზანი: სამუშაოს მიზანს წარმოადგენს მაღალი ტექნიკური მახასიათებლების მასალის მიღება TiC-Ni-Fe, სისტემაში და მისი გამოყენების სფეროს განსაზღვრა.

მეთოდი: კომპოზიტის მიღება ტრადიციული ფხვნილოვანი მეტალურგიის მეთოდით, ცხელი წნეხვით, მიღებული მასალის ფაზური ანალიზი და მიკროსტრუქტურა რენტგენო-სტრუქტურული და ელექტრონული მიკროსკოპიის საშუალებით, მექანიკური თვისებები: სიმტკიცე

კუმსვაზე და ღუნვაზე განისაზღვრა გამგლეჯ მანქანაზე R-100, სისალე განისაზღვრა ვიკერსისა და როკველის მეთოდებით.

შედეგი: შემუშავებულია მაღალი ფიზიკურ-ტექნიკური მახასიათებლების მქონე მასალათა ჯგუფის შედგენილობა TiC-Ni-Fe სისტემაში, დადგენილია მათი მიღების ტექნოლოგიური რეჟიმის პარამეტრები, შესწავლილია ფიზიკურ-მექანიკური და საექსპლუატაციო თვისებები, დადგენილია გამოყენების სფერო.

დასკვნა: მიღებულია მაღალი ფიზიკურ-ტექნიკური მახასიათებლების მქონე მასალათა ჯგუფი TiC-Ni-Fe სისტემაში, რომლის სისალე 88,0-89,5 HRA; სიმტკიცე ღუნვისას 1300-2000 MPa; დარტყმითი სიბლანტე – 18-38კჯ/მ2, რასაც ინარჩუნებს საკმაოდ მაღალ ტემპერატურამდე. უვოლფრამო კომპოზიტის რაციონალური გამოყენების სფეროდ შეიძლება ჩაითვალოს მასალების ჭრით დამუშავების პროცესები, რომლებიც არ არის დაკავშირებული სითბოს დიდი რაოდენობით გამოყოფასთან: შტამპების პუანსონებისა და მატრიცების, ასევე სხვადასხვა ტექნოლოგიური აღჭურვილობის დასამზადებლად, მათ შორის ფილიერებისა - ფოლადის მილების გლინვისთვის, აგრეთვე როგორც მჭრელი მასალა ფერადი ლითონების ჭრით დამუშავებისას.

საკვანძო სიტყვები: კომპოზიტი, უვოლფრამო მჭრელი მასალა, სიმაგრე, დარტყმითი სიმაგრე.

UDC 666.946.6

HIGHLY REFRACTORY MATERIALS BASED ON ZIRCONIUM DIOXIDE

Z. Kovziridze, N. Nizharadze, M. Balakhashvili, G. Tabatadze, M. Mshvildadze,

R. Gaprindashvili

Department of Chemical and Biological Technologies, Center for Materials Science of Nanotechnologies and Nanocomposites, Institute of Bionanoceramics and Nanocomposites Technology, Georgian Technical University, Kostava street 69,Tbilisi, Georgia, 0175

E-mail: kowsiri@gtu.ge

Resume: Goal: development of technology for the manufacture of refractory products based on zirconium dioxide.

Method: the study was conducted using thermographic, X-ray diffraction and electron microscopy methods.

Result: a refractory material based on zirconium dioxide with high physical and technical properties was obtained.

Conclusion: Refractories based on zirconium dioxide are characterized by high fire resistance (2500^{0}C). High thermal resistance, chemical resistance to both acidic and alkaline slags. They are mainly used for the manufacture of melting crucibles for non-ferrous metals.

Key words: high fire resistance, zirconium dioxide, monoclinic zirconium dioxide, plasticizer, binder.

1. INTRODUCTION

The appearance of new technological processes in the production of ferrous metallurgy has led to increased requirements for zirconium oxide refractories. High strength, slag and metallurgical resistance at high temperatures, and the stability of ZrO_2 products in oxidizing and reducing environments dramatically improve the properties of the liquid metal and ensure an increase in the service life of equipment.

Refractories containing zirconium mainly consist of zirconium dioxide, which is obtained from natural raw materials - the mineral Baddeleyite or zirconium ore. It contains 80-99% zirconium dioxide and about 20% impurities of various metal oxides.

Pure zirconium dioxide can be obtained artificially by chemical processing of zircon concentrate from natural raw materials.

For the production of refractories based on zirconium dioxide, charge is composed of well-crushed, pre-fired briquettes of zirconium mass and raw zirconium dioxide added as a binder mass, about 10%.

The second method of producing refractories is natural rocks containing 56-67% ZrO_2, zirconium silicate and 33-35% SiO2.

Zirconium refractories are characterized by high fire resistance (2500^{0}C), high thermal resistance, chemical resistance to both acidic and alkaline slags. They are mainly used for the

manufacture of melting crucibles for non-ferrous metals.

ZrO_2 exists in two modifications: monoclinic, stable up to 1000^{0}°C, and denser pseudocubic (tetragonal) ZrO_2, formed at this temperature. The transition from monoclinic to tetragonal modification is a reversible process and is accompanied by a decrease in the volume of ZrO_2 by approximately 7%. Since this transformation occurs so quickly, the product contracts when heated and expands when cooled. Therefore, ZrO_2 products crack during this process. The pseudocubic modification of ZrO_2 can be stabilized at 2000 ^{0}C and above and the decomposition of related products can be stopped by adding some oxides structurally close to ZrO_2 (CaO, MgO, SrO,V_2O_3,, CeO_2, Sc_2O_3), the cation radius of which is close to the Zr^{4}+ ion radius.It is completely stabilized by practically adding 3-8% or more CaO and heating the mixture to 1700 ^{0}C. The addition of 8-15% MgO only increases the transformation temperature, but does not completely stabilize it.

ZrO_2 can be used to make products if it is first stabilized, regardless of whether it is obtained by chemical methods or by melting.Stabilization of zirconium dioxide consists of mixing it (co-fine grinding) with a stabilizing additive and further firing the mixture (briquettes) at 1700-1750 ^{0}C.

Plasticization of crushed stabilized zirconium dioxide allows:

1) Adding $ZnCl_2$, $MgCl_2 \cdot 2H_2O$ or other easily hydrolyzed salts;

2) ZrO_2, calcined and grind at high temperature and treated with dilute acids or alkalis;

3) With the addition of finely ground zirconium hydroxide;

Phosphoric and boric acids, starch, resins and others can be used as binding additives.

2. MAIN PART

For the manufacture of samples, the following starting materials were used: stabilized zirconium dioxide, monoclinic zirconium dioxide, kaolin, pitch, complex plasticizer and 25% magnesium sulfate solution as a binder. The density of the solution used was 1.12 g/cm^{3}.

Kaolin is a rock made up of clay minerals. The main clay mineral is kaolinite, which is a hydrosilicate of aluminum. Its formula is: Al2O3•2SiO2•2H2O.

The chemical composition of kaolin is given in Table 1.

Table 1

Chemical composition of kaolin, mass %.

SiO_2	Al_2O_3	Fe_2O_3	TiO_2	CaO	MgO	SO_3	hl	Sum
44.52	39.58	0.43	0.21	0.51	0.04	0.08	13.88	99.25

The addition of kaolin is due to the fact that it facilitates the annealing process of zirconium dioxide products at a relatively lower temperature, since its annealing temperature is 1450-1500^{0}C. Simultaneously improve the molding properties of products.

The only crystalline phase in calcined kaolin that is sufficiently stable at high temperatures (1910^{0}C) is mullite, the formation process of which is expressed by the reaction:

$$3(Al_2O_3 \cdot 2SiO_2 \cdot 2H_2O) =$$
$$= 3(Al_2O_3 \cdot 2SiO_2) + 4SiO_2 + 6\ H_2O$$

In Fig. 1 shows a thermogram of kaolin. The endoeffect is associated with the loss of water at 500-600^{0}C. This corresponds to the endo-peak on the thermogram with a maximum of 610^{0}C.

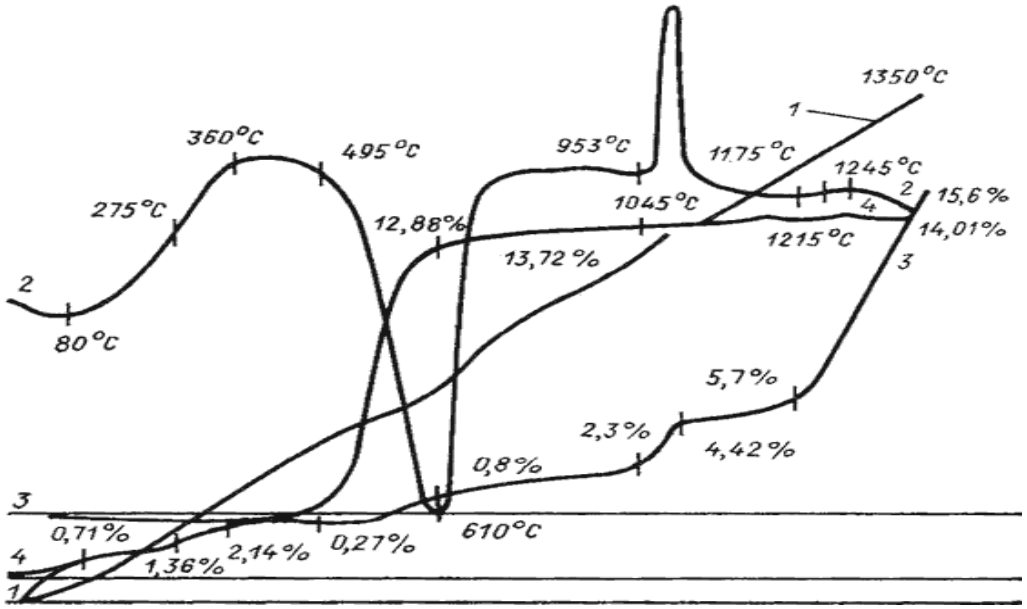

Fig. 1. Kaolin thermogram

Carbon-containing materials are used as additives in the production of refractory products, especially products based on refractory oxides. They play the role of a binding agent not only in shaping, drying and baking, but also in baking. During heat treatment, carbon particles form aggregates in contact with each other and form continuous chains throughout the entire volume of the product. Individual carbon groups can be present both in the space between the grains and in contact with each other on the surface of the grains of the material. They increase the chemical resistance of the product. In particular, the resistance to slags.

Soot was used as a carbon additive. Soot – carbon black is a dispersed carbonaceous product of incomplete combustion, the thermal decomposition of hydrocarbons. Consists of black spherical particles. The average size of soot particles is 100-350 Å. Particles are formed from layers of carbon atoms. Each layer consists of carbon atoms located at the vertices of a hexagon with a distance of 1.42 Å between them.

Natural gas, acetylene, liquid hydrocarbons and petroleum distillation residues are used as raw materials for the production of soot.

Plasticizers are organic substances that are introduced into masses to give them plasticity (the ability to undergo irreversible deformations) and prolong the highly plastic state of the material. Plasticizers facilitate the processing of materials and increase the strength of samples during molding, drying and firing.

Such substances are used as plasticizers, which are characterized by low volatility and high heat resistance. The most commonly used types of plasticizers are: esters of phthalic acid and phosphoric acid. Dibutyl phthalate, tributyl phosphate, epoxy vegetable oils, low molecular weight polyesters, petroleum products containing aromatic hydrocarbons. We used a plasticizer with plastic properties.

Currently, a large number of binders for refractory materials are known, but regardless of what class of compounds this or that binder belongs to, what its composition is and what physical and chemical processes occur when it is introduced into the ceramic mass, their main purpose is always the same - to impart mass smoothing properties during the preparation of the product and such mechanical strength that will be sufficient for further operation of the molded product. Technological binders, by their chemical nature and properties, can be soluble in water and soluble in organic liquids. It may be organic and inorganic. Inorganic binders include magnesium sulphate solution. We chose a 25% magnesium sulfate solution.

Zirconium dioxide was crushed in a jaw crusher into pieces measuring 3-5 mm. It was then ground in a metal ball mill and sieved through a No. 05 sieve. Monoclinic zirconia, pitch and kaolin were used without processing, in the form of fine powders.

Dense products made from stabilized zirconium dioxide are characterized by a high thermal expansion coefficient, which is the reason for the low thermal resistance of these products. Their thermal stability is significantly increased by the addition of 10-15% monoclinic ZrO2 by mass.It has a low thermal expansion coefficient. At this time, $ZrO_2$with a different coefficient of thermal expansion creates microcracks in the product, which helps the grains move more freely when the temperature changes and increases heat resistance.

To obtain samples, mixtures were prepared with the ratio of components given in Table No. 2. To the mass of all compositions above 100%, 0.8% of a complex plasticizer was added.The weighed components were mixed manually. After homo-genization, the mixtures were moistened by adding a 10-12% magnesium sulfate solution to form samples. To distribute moisture evenly, the well-mixed mass was passed through a N2 sieve.After this, mix again and the mass is ready for molding. The samples were molded in a cylindrical metal mold measuring 20x20 mm under hydraulic pressure of 20, 30, 40 MPa.After drying in air for two days, drying was continued in a thermostat at a temperature of 110^0C. Firing was carried out in a silit kiln at a temperature of 1500^0C. The samples were placed on a fireclay support coated with monoclinic zirconium dioxide. The average rate of temperature increase was 250°C/h. The delay time at the final temperature was 2 hours.

Table 2

Material composition of mixtures,

wt. %

Sample index	Components					Amount of $MgSO_4$ solution, %
	ZrO_2 Stabiliz.	ZrO_2 monocl.	Soot	Kaolin	Complex plasticizer, over 100%,%	
1	88	6	-	6	0.8	10
2	88	6	6	-	0.8	10
3	88	6	3	3	0.8	10
4	88	-	-	12	0.8	10
5	100	-	-	-	0.8	10

The fired samples are externally characterized by a smooth surface, dense structure, well baked, and no cracks are observed on any of the samples. The compressive strength was determined based on physical and technical parameters. The obtained results are presented in table 3.

From the data presented in the table, it can be seen that this indicator is quite high for all samples of the composition. N5 and N2 stand out among them. As the molding pressure of the samples increased from 20 to 40 MPa, the strength of the samples increased (Table 3). To form the product, mass composition N2 was chosen with the following composition of components: zirconium dioxide 88.22%, monoclinic zirconium dioxide 6.22 wt.%, carbon black 6 wt.%, a complex plasticizer was added over 100% - in the amount of %0.8.Having mixed the components well, it was moistened with a 25% solution of magnesium sulfate, which was added to 10-12%. Mix well again to equalize the humidity, then pass through a No. 2 sieve and mix again. It should be formed under a pressure of 20-40 MPa.During molding, pressure should be released twice and held to release air trapped in the powder and prevent further cracking. Drying was carried out in air for several days. Then into the drying cabinet.

The properties of zirconium-carbon material are presented in table 4.

The X-ray diffraction pattern obtained as a result of X-ray phase analysis is presented in Figure 2, from which it can be seen that the main phases are cubic and monoclinic zirconia, carbon and mullite.

Table 3

Compression strength of samples

Sample index	Molding pressure, MPa	Sample area, cm^2	Manometer indication, kgs	Compression strength, MPa	Note
1	20	1.4	2720	194.3	
1/1	30	1.4	2500	178.6	
				186.1	
1/1	30	1.41	2920	193.6	
1/2	40	1.5	2980	198.7	
				203.1	
1/2	40	1.45	3010	207.6	
2	20	1.28	3100	242.1	
				234.8	
2	20	1.30	2960	227.6	
2/1	30	1.35	2759	204.4	
2/2	40	1.35	3200	237.0	
				242.5	
2/2	40	1.35	3350	248.0	
3	20	1.38	2300	1666	
3/1	30	1.36	2300	169.1	
				182.35	
3/1	30	1.36	2660	195.6	
3/2	40	1.35	2730	202.2	
4	20	1.5	2420	172.8	
4/1	30	1.5	2600	173.3	
4/2	40	1.5	2740	182.6	
5	20	1.28	3860	307.5	
5/1	30	1.30	3930	302.3	
5/2	40	1.30	4420	340.0	

Table 4

The properties of zirconium-carbon material

Properties	Results
Molding pressure, MPa	52
Density, g/cm^3	3,98
Porosity, %	11,4
Fire resistance,^{0}C	➢ 1800

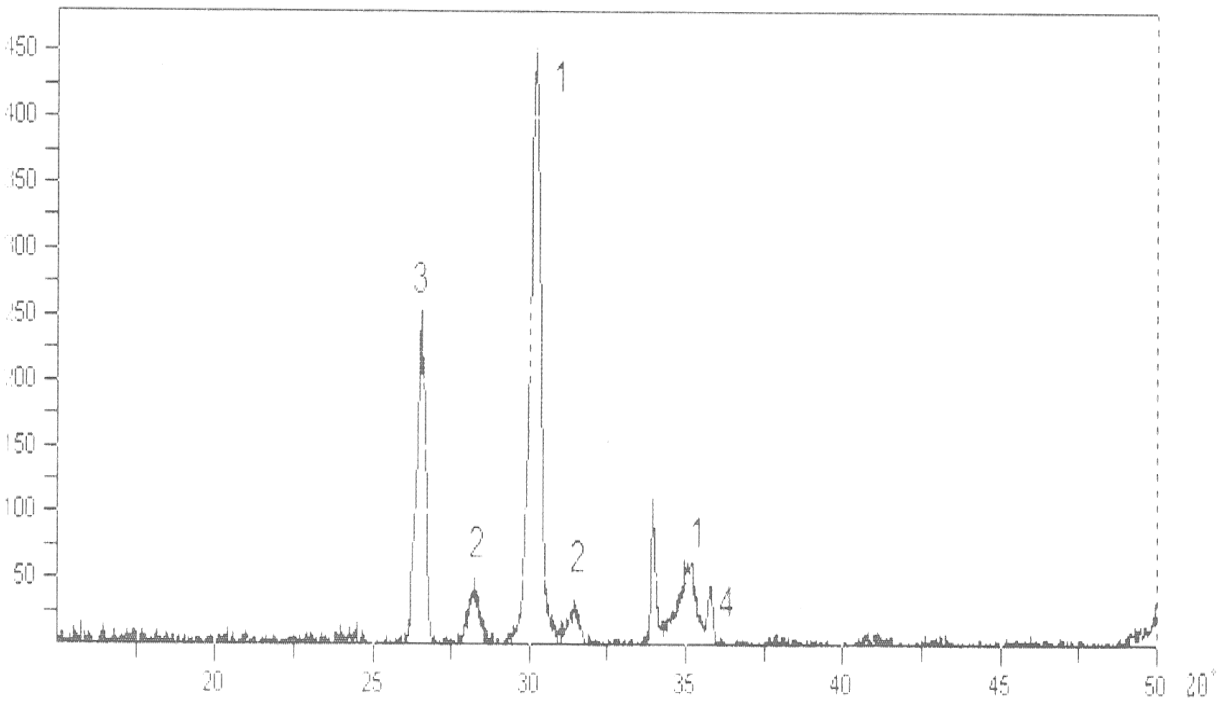

Fig. 2. X-ray diffraction pattern of zirconium-carbon material

1. Cubic zirconium dioxide, 2. Carbon, 3. Monoclinic zirconium dioxide, 4. Mullite

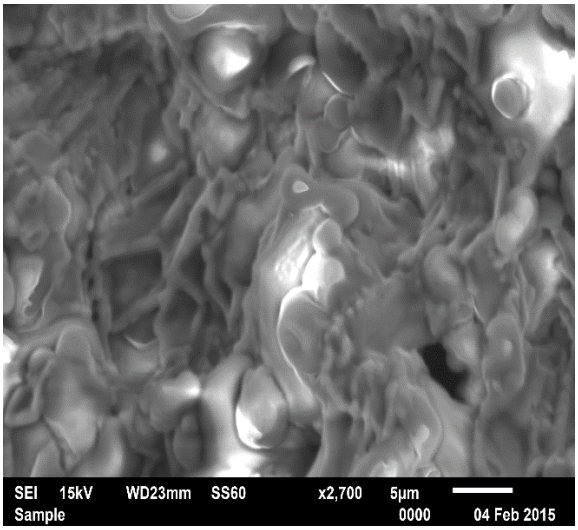

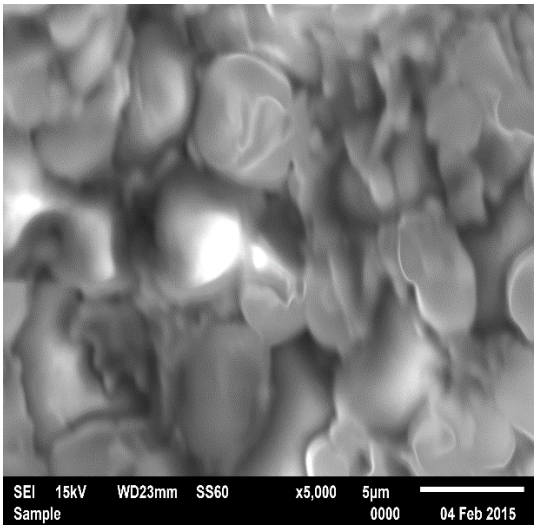

a) b)

Fig. 3. Electron microscopic images of zirconium-carbon material at different magnifications.
a) X1900 b) X2700

Electron microscopic images of composite 3 show the surface of a well-baked sample, on which formed crystals of the main phases contained in the sample, namely cubic and monoclinic zirconium dioxide, are visible.

The micromechanics of the composite obtained on the basis of zirconium dioxide was determined by the Vickers method. Identer Diamond Pyramid. Different loads were used. In Fig. Figure 7 graphically shows the movement of the indenter through the material for 60 seconds, as well as the time dependence of the indenter load on the sample and the changes it makes. From the figure we can conclude that the optimal load for the resulting composite is 50-55 N, at which the material exhibits its maximum micromechanics.

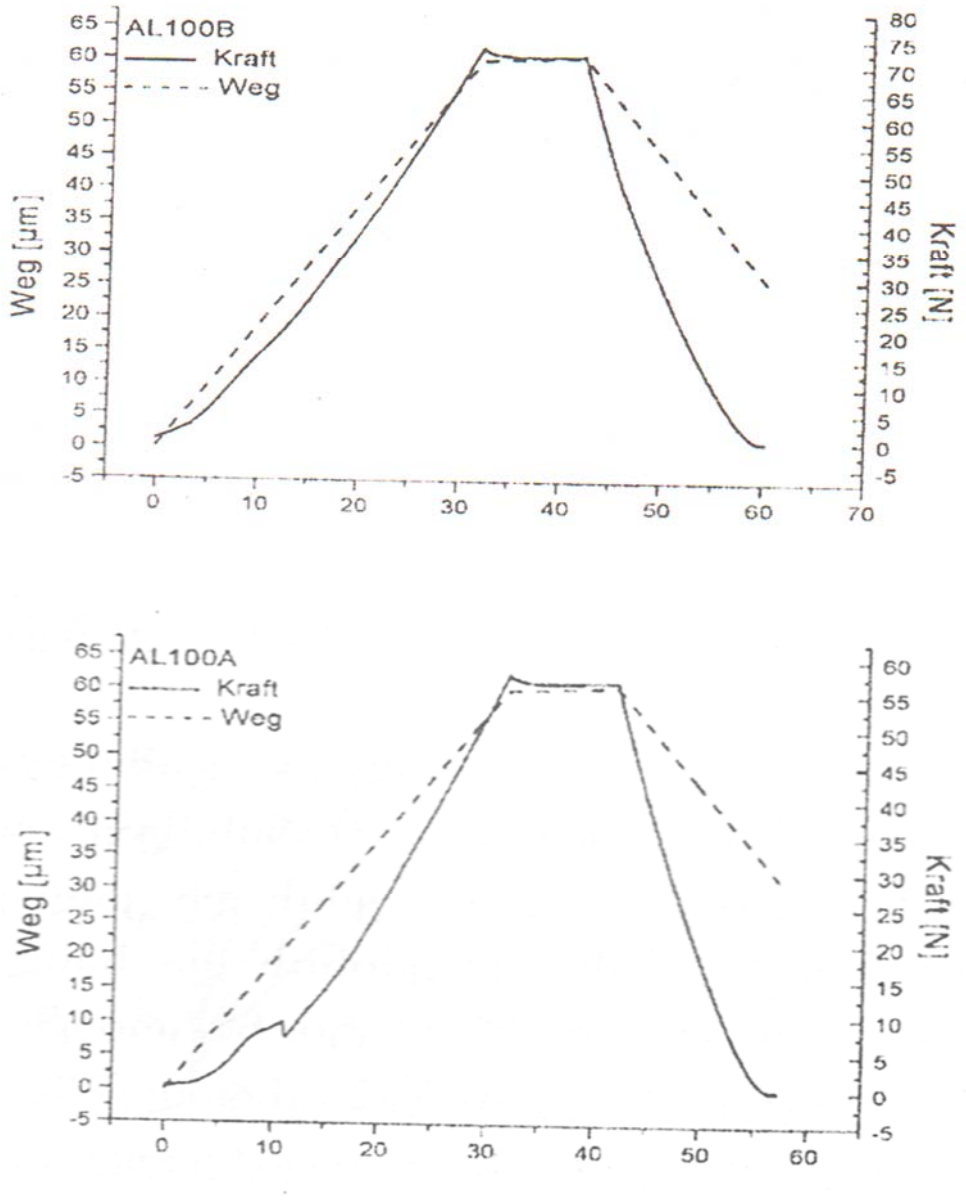

Fig. 4.Dependence of the indenter load on the sample and its change over time. Veg – road; Zeit – time; Kraft –power

3. CONCLUSION

Based on the data obtained as a result of the experiment, we can conclude that refractories based on zirconium dioxide are highly fire resistant, have high electrical conductivity among refractory oxides, therefore they are used for heating in furnaces, as reflectors in nuclear reactors.The products are resistant to thermal shocks. The crucibles can melt potassium, sodium, aluminum and iron. It is resistant to fluorides and feldspars. The crucibles can withstand 30 melts of platinum. Palladium, ruthenium and rhodium can be smelted. They do not get wet in steel and do not dissolve.

ACKNOWLEDGMENT

We express our gratitude to Shota Rustaveli Georgian National Science Foundation. The work is done with the grant of the Foundation FR-21-1413 Grant 2022.

REFERENCES

1. Shveikin G.P. Ceramics: Development forecasts for 2000-2005. Refractories and technical ceramics. 2000. No. 7.S.5-9. Containing zirconium dioxide. Refractories. 1991, no. 9.P.5-7.
2. Colin, S. Ceria-doped zirconia-graphite as possible refractory for tundish nozzles in steclmaking / S. Colin, F. Jeannot, B. Dupre [et al.] // Journal of the European Ceramic Society. - 1993. -№6. -C.515-521.
3. Lin, W. Decarbonization Behavior of Graphite-Containing Refractories by Molten Steel / W. Lin, O. Nomura. R. Nakamura [et al.] // Taikabutsu Overseas. -1999. -№4. - C. 15-24.
4. Uchida, K. Influence of Zirconia Grain Size on Corrosion Resistance of Zirconia-Graphite Refractories / K. Uchida, M. Ando, S. Takahashi [et al.] // Taikabutsu Overseas. - 2000. - №3. - C.229.
5. Kashcheev, I.D. Oxide-carbon refractories / I.D. Kashcheev. - M.: Intermet-engineering, 2000. – 265 p.
6. Shevchenko A.B., Ruban A.K., Dudnik E.B. High-tech ceramics based on zirconium dioxide. Refractories and technical ceramics. 2000. No. 9.P.2-8.
7. L. Hongxia, Y. Bin, Y. Jinshong, and L. Guoqi, "Improvement on Corrosion Resistance of Zirconia-Graphite Material for Powder Line of SEN", UNITECR 2003, Osaka, Japan, 2003, C.588-591.
8. Golak, II. Zirconium dioxide is an indispensable material for the production of special-purpose refractories / P. Golak, O.G. Oganov // New refractories. - 2006. - No. 4. P. 33-34.
9. Refractory Slag Band. Заявка 20130045856. США. МПК6 C04B 35/482; N.E. Rogers, D. Kennedy - 12/735762. Заявлено 12.02.2009 Опубл. 21.02.2013
10. Yoshitsugu, D. Effect of Apparent Porosity on the Corrosion Index of Zirconia-Graphite, with Higher Zr02 Content / D. Yoshitsugu, K. Morikawa, J. Yoshitomi, K. Asano // Taikabutsu Overseas. - 2007. - №2. - C. 116.
11. Ochagova, I.G. Properties of refractory with a high Zr02 content for the slag belt of immersed glasses / I.G. Ochagova // News of ferrous metallurgy abroad. - 2007. - No. 4. - P. 83-86.
12. Ochagova, I.G. Mechanisms of corrosion of zirconium oxide-carbon refractory materials by slag in the presence of steel / I.G. Ochagova // News of ferrous metallurgy abroad. - 2010. - No. 1. - P.90-93.
13. Yagovtsev, A.V. Study of the influence of the composition of zirconist-graphite material on one hundred properties / A.V. Yagovtsev, N.V. Obabkov, I.D. Kashcheev // New refractories. - 2013. -№10 - pp. 17-20.
14. Yagovtsev, A.V. Interaction of zirconium circide. –L.: Nauka, 1991. –P.13
15. Song Y. L., Tsai S. C., Chen C. Y., Tseng T. K., Tsai C. S., Chen J. W., Yao Y. D. Ultrasonic Spray Pyrolysis for Synthesis of Spherical Zirconia Particles // J. Amer. Ceram. Soc. –2004. –87, –№10. –P.1864-1871.

16. Wang S., Zhai Y., Li X., Li Y., Wang K. Coprecipitation Synthesis of MgO Doped ZrO_2 Nano Powder // J. Amer. Ceram. Soc. –2006. – 89, –№11. –P.3577-3581.
17. Xin M. Wang, Lorimer G., Ping Xiao. Solvothermal Synthesis and Processing of Yttria-Stabilized Zirconia Nanopowder // J. Amer. Ceram. Soc. –2005. – 88, –№4. – P. 809.
18. Yagovtsev, A.V. Study of slag resistance of zirconistographite refractory materials /A.V. Yagovtsev, V.A. Perepelitsyn, II.V. Obabkov [et al.] // Refractories and technical ceramics. - 2014. - No. 6. - P.39-44.
19. Stubican V. S. Phase equilibria and metastabilities in the systems ZrO_2–MgO, ZrO_2–CaO, and ZrO_2–Y_2O_3 // Advancesinceramics. – 1980. –Vol.24. –P.71-82.
20. Yin Y., Argent B. B. Phase diagrams and thermodynamics of the systems ZrO2–CaO and ZrO_2–MgO // J. Phase Equilibria. –1993. –14. – №4. –P.439-450.
21. Wu J., Wei X., Padture N. P., Klemens P. G., Gell M., Garcia E., Miranzo P., Osendi M. I. Low-thermal-conductivity rare-earth zirconates for potential thermal-barrier-coating applications. Journal of the American Ceramic Society. 2002; 85(12): 30313035. https://doi.org/10.1111/j.1151-2916.2002.tb00574.x
22. Okovity V. A., Panteleenko F. I., Okovity V. V., Astashinsky V. M., Uglov V. V., Shimansky V. I., Cherenda N. N. Formation and study of plasma powder coatings made of oxide ceramics modified by high-energy influences. Sciencean-dtechnology. 2018; 17(5): 378-389. https://doi.org/10.21122/2227-1031-2018-17-5-378-389
23. Almyasheva O. V., Vlasov E. A., Khabensky V. B., Gusarov V. V. Thermal stability and catalytic activity of the amorphous Al_2O_3-ZrO_2 nanocrystals composite. Journal of Applied Chemistry. 2009; 82(2): 224-229. Access mode: https:// www.elibrary.ru/item.asp?id=44517142
24. Artemov S.A., Borik M.A., Volkova T.V., Gerasimov M.V., Kulebyakin A.V., Lomonova E.E., Mi-lovich F.O., Myzina V.A., Ryabochkina P.A., Tabach-kova N.Y. Influence of growth and heat treatment conditions on lasing properties of ZrO_2-Y_2O_3-Ho_2O_3
25. Ivanov Yu. F., Tumanov Yu. M., Dedov N. V., Khasanov O. L. Structure and phase composition of nano-structured powder based on zirconium dioxide, produced by plasma-chemical synthesis methods. Physics and chemistry of materials processing. 2012; 5: 3. Access mode: https://www.elibrary.ru/item.asp?id=18053701.
26. Geodakyan D.A., Kostanyan A.K., Geokchyan O.K., Geodakyan K.D. Zirconium dioxide heat-resistant compositions. Refractories and technical ceramics. 2010; 6: 11-15. Access mode: https://www.elibrary. ru/item.asp?id=15483557.
27. Shukla S., Seal S. Mechanisms of room temperature metastable tetragonal phase stabilisation in zirconia //International materials reviews. - 2005. - V. 50. - №. 1.
28. Ohtaka, O., Yamanaka, T., Kume, S., Ito, E., Navrotsky, A. Stability of Monoclinic and Orthorhombic Zirconia: Studies by High- Pressure Phase Equilibria and Calorimetry // Journal of

the American Ceramic Society. - 1991. - V. 74. - №. 3. - pp. 505-509.
29. Smith D. K., Cline C. F. Verification of existence of cubic zirconia at high temperature //Journal of the American Ceramic Society. - 1962. - V. 45. - №. 5. - pp. 249-250
30. Kucza W., Oblakowski J., Gajerski R., Labus S., Danielewski M., Malecki A., Morgiel J., Michalski A. Synthesis and characterization of alumina– and zirconia based powders obtained by the ultrasonic spray pyrolysis // J. Thermal Analysis and Calorimetry. –2007. –Vol.88. –№1. – P. 65-69.

უაკ 666.946.6

მაღალცეცხლგამძლე მასალები ცირკონიუმის დიოქსიდის ბაზაზე

ზ.კოვზირიძე, ნ.ნიჟარაძე, მ. ბალახაშვილი, გ. ტაბატაძე, მ. მშვილდაძე, რ. გაფრინდაშვილი.

ქიმიური და ბიოლოგიური ტექნოლოგიების დეპარტამენტი, ნანოტექნოლოგიის და ნანოკომპოზიტების მასალათმცოდნეობის ცენტრი, ბიონანოკერამიკისა და ნანოკომპოზიტების ტექნოლოგიის ინსტიტუტი, საქართველოს ტექნიკური უნივერსიტეტი, საქართველო, 0175, თბილისი, კოსტავას 69.

E-mail: kowsiri@gtu.ge

რეზიუმე: მიზანი: ცირკონიუმის დიოქსიდის ბაზაზე ცეცხლგამძლე ნაკეთობების მიღების ტექნოლოგიის დამუშავება. **მეთოდი:** ჩატარებულია კვლევა თერმოგრაფიული, რენტგენოსტრუქტურული და ელექტრონული მიკროსკოპიის მეთოდებით.

შედეგი: მიღებულია ცეცხლგამძლე მასალა ცირკონიუმის დიოქსიდის ბაზაზე მაღალი ფიზიკურ-ტექნიკური თვისებებით.

დასკვნა: ცირკონიუმის დიოქსიდის ბაზაზე მიღებული ცეცხლგამძლეები ხასიათდებიან მაღალი ცეცხლგამძლეობით (2500^{0}C). მაღალი თერმომედეგობით, ქიმიური მედეგობით, როგორც მჟავა, ასევე ფუძე წიდების მიმართ. ძირითადად იყენებენ ფერადი ლითონების სალღობი ტიგელების დასამზადებლად.

საკვანძო სიტყვები: მაღალცეცხლგამძლე, ცირკონიუმის დიოქსიდი, მონოკლინური ცირკონიუმის დიოქსიდი, პლასტიფიკატორი, შემკვრელი.

UDC 661.971.2

PURIFICATION OF FLUE GASES GENERATED DURING CEMENT PRODUCTION FROM CO_2, SO_x, NO_x USING A TWO-STAGE PROCESS

G. Loladze, T. Cheishvili, R. Skhvitaridze, N. Kutsiava, E. Uchaneishvili, N. Mukhadgverdeli, M. Kekelidze

Georgian Technical University, Faculty of Chemical Technology and Metallurgy. M Kostava Str 69, Tbilisi, Georgia, 0175

E-mail: g.loladze@gtu.ge

Resume: **Goal.** Development of a highly efficient method for capturing and recycling CO_2 and associated gases SOx, NOx released from clinker production kilns at cement plants. The proposed approach includes (based on) the use of clinophtholite as an adsorbent and passing flue gases into it: determining the optimal variant of the technological process for gas capture by experimenting on hybrid adsorption-drying equipment in laboratory conditions.

Method. Production of briquettes from an acceptable carbon-containing mixture of clinker, firing it in an experimental furnace at a temperature not lower than 1450^{0}C and supplying the resulting gases to a combined hybrid drying-adsorption unit specially created by the testing laboratory. Thus, harmful gases (mainly CO_2) released during the combustion of acceptable clinker briquettes are absorbed by the zeolite tuff used as an adsorbent. At the same time, a purposeful transformation of the structural design of the laboratory adsorption apparatus was carried out from a single-node unit to a two-node unit to ensure effective absorption.

Result. The dependence of the absorption capacity of the adsorbent on the physical characteristics of the zeolite (granulometry and mass of the adsorbent, the degree of filling of the adsorbent block), as well as the contact of gases passing through the drying-adsorption units of the hybrid adsorber and on the surface of the contact mechanism of the adsorbent (through the adsorbate in the mobile-immobile layers of the adsorbent), etc.

Conclusion. A laboratory experiment established the possibility of capturing harmful gases (mainly CO_2) from flue gases generated during the production of cement clinker using zeolite tuff as an adsorbent. In order to increase the efficiency of this process, a two-stage technological mode is recommended, the implementation of which is recommended to be carried out in two node blocks of different designs, in which the adsorber - zeolite tuff - is located. The first unit provides drying-activation of the adsorber (t>150^{0}C), and the second - intensive implementation of the required adsorption process (t<70^{0}C). The prospect of using a predominantly CO_2-saturated adsorbent (grain size 3-8 mm) is its grinding along with clinker and the expected improvement in the quality of cement.

Key words: briquette, firing, gases, zeolite, drying, adsorption, adsorbent, adsorption unit.

1. INTRODUCTION

Climate change leading to global warming is the greatest challenge of humanity in the 21st century, and finding ways to prevent it is also a great challenge and a practical task that needs to be addressed as a priority.

The creation and existence of the problem is facilitated by an excess of CO_2 irreversibly emitted into the atmosphere from various production processes, the scale of which reached 421 ppm in 2022 [1, 14]. Cement production accounts for 6-8% of CO_2 emissions into the atmosphere worldwide [2, 4, 16, 17, 18]. It is known that out of 1.6-1.8 tons of raw materials spent on the production of 1 ton of cement, at least 0.64 tons of CO_2 are irretrievably released into the atmosphere with hot flue gases of 50-400^{0}C from the clinker kiln, which is a technological loss. This worsens the material balance of the enterprise and increases costs SOx (1.15-9.18 kg/kg.cem.) and NOx (0.285-1.14 kg/kg.cem.) are emitted into the atmosphere with flue gases, which contributes to the formation of "acid rain" [5, 19, 20, 21]. Currently, there is no global problem of preventing their emissions, but they are necessary compounds for modifying cement and concrete.

It should be noted that CO_2 is "useful" when 0.05-0.35 t/t $CaCO_3$ is added to cement for carbonate modification/carbonization. However, SOx is "useful" when added to cement at levels up to 5 wt.% as CaSO4 to provide the 1-4 wt.% SO3 content needed to control the setting/hardening rate. At the same time, the use of both additives requires the extraction of minerals and increased material costs. NOx is also introduced into cement concrete as a hardening accelerator - in the form of special additives [6-8].

Nowadays, in order to prevent the problem of climate change, enterprises have created up to 20 technologies for capturing and recycling CO_2 from exhaust gases, which cannot reduce CO_2 emissions into the atmosphere and losses of material production [9, 10].

The approach we propose is comprehensive, as it combines the prevention of irreversible emissions of CO_2, SOx, NOx into the atmosphere from flue gases of industrial enterprises, the use of a natural adsorbent - zeolite tuff and also the "zeolite - harmful gases (CO_2, SOx, NOx)" obtained in this way in the cement-concrete composition of the target recycling complex. For this purpose, studies were carried out taking into account the known thermal and molecular sieve sorption properties of zeolite tuff containing the mineral clinoftilolite (Tedzami deposit, Georgia) [11].

2. MAIN PART

As already mentioned, for the purposes of the study - the capture and utilization of gases (CO_2, SOx, NOx) emitted by enterprises into the atmosphere, Tedzami zeolite tuff (Kaspi municipality) was chosen. The chemical composition of the sample of the material used in the study in wt.% is given in Table 1.

Table 1

Chemical composition of zeolite (Tedzami deposit), wt.%

Composition, mass %									Sum
SiO_2	Al_2O_3	Fe_2O_3	CaO	MgO	MnO	R_2O	SO_3	ბ.ც.	
73,55	11,43	0,65	2,12	0,95	0,24	3,99	0,02	7,05	100,0

The prerequisite for including zeolite tuff as a sorbent in the research was the following circumstance: when heated in the temperature range 300+/-50^{0}C, dehydration/activation of the zeolite tuff occurs, and therefore the effectiveness of contact with flue gases (CO_2, SOx, NOx) is determined by the critical diameters molecules (corresponding to 0.31; 0.36; 0.33) nm, as well as a dynamic capacity ranging from (3-4.5; 2.5-3.8; 2.7-4.2) cm3/ g respectively. Gases at different temperatures (CO_2=20-230^{0}C, SOx=20-150^{0}C, NOx= 20-50^{0}C) are adsorbed in zeolite tuff (dry/activated form) with pores of 0.2-1.5 nm, separated from water using van der Waals. forces characteristic of the adsorption process by filling channels and cavities - until saturation [11].

At the same time, zeolite is known for its high sorption, but selective ability to absorb steam, CO_2 and other compounds at the same temperature [11]. Thus, a two-stage, but technologically sequential technological process for absorbing production emissions gases was compiled. At the first stage, flue gases containing (CO_2, SOx, NOx) at a temperature of 150-350 ^{0}C are supplied to the 1st dryer unit of the adsorption unit. A cylindrical rotating cylinder is a dryer that dries zeolite tuff of a 3-8 mm fraction containing the mineral clinoftilolite in a direct-flow method - in contact with hot gases and moving parallel to them. The flue gas is "cooled" while the zeolite tuff is dehydrated/activated and, in the presence of voids free of water, successively captures as a result of flue gas sorption: (230 ^{0}C-ზე CO_2; 150 ^{0}C-ზე SOx; 70 ^{o}C-ზე NOx); while it is modified, but not completely/partially at the 2nd stage, "cooled" and partially purified to 70-150 ^{0}C flue gases are fed into a sorber installed in front of the chimney, where zeolite tuff, modified at the first stage, acts as a sorbent. In the second unit, the flue gases are "cooled" to 20-60^{0}C, and final sorption capture (CO_2, SOx, NOx) by zeolite tuff occurs. This type of zeolite tuff, saturated and completely modified by harmful gases that determine the technological development of cement in the future, enters the cement mill.

Validation of this two-stage technological process was carried out by upgrading LPPA type equipment. The specified basic device was created on the basis of the Department of Chemical and Biological Technologies of the Georgian Technical University, and its design diagram is described in detail in [12,13, 15]. A laboratory experiment to modify the basic configuration, a laboratory prototype close to the production process - device (LPPA) was carried out with one flue gas emission unit according to the transport-adsorption scheme

with the addition of a technological adsorption process unit - a vertical tubular adsorber one more in a row (Scheme 1).

And high-temperature (t>150^{0}C) drying-activation processes of the adsorbent in the rotating cartridge block of the new LPPA unit and combining it with a vertical zeolite adsorber (low-temperature adsorbent) made it possible to effectively capture harmful gases that make up the exhaust gases.

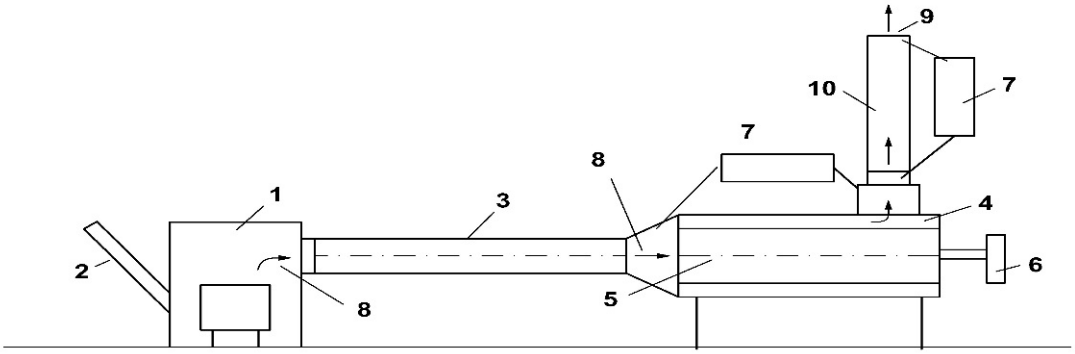

Fig. 1. Laboratory prototype of a production apparatus LPPA
1. Shaft futnace; 2. Briquette loader; 3. Smoke pipe; 4. Drying absorption node; 5. Rotating cartridge; 6. Engine; 7. Gas analyzer "VARIOluxx"; 8. Flue gases with CO_2; 9. Purified flue gas; 10. Sorber

Additional studies have established that increasing the overall efficiency of absorption of harmful gases to 15-20% is modified and is actually possible by adjusting the filling factor of the adsorption space and the speed of movement of the adsorber in the two included adsorption units in an LPPA-type unit (taking into account the structural location of the first and second units).

3. CONCLUSION

Based on the studies conducted, it was established that with the perfect design of the laboratory unit, the LPPA was able to effectively absorb a large amount of gases (CO2, SOx, NOx) released as a result of clinker grinding with zeolite tuff. Therefore, it is recommended to carry out the adsorption process with a developed two-stage technological process: activation of zeolite tuff grains in dynamic rotational modes, dehydration (processes occur at t>1500C) and saturation of zeolite grains with harmful gases in a vertical sorber - due to the ideal adsorption process (t<700C)

Pilot studies carried out on a modified laboratory installation of the LPPA type established the general conditions for an effective adsorption process, which can become the basis for further research - by establishing the possibility of further utilization of an adsorbent saturated with CO2 (plus SOx, NOx) - zeolite tuff,

by introducing it into technological process for the production of cement.

ACKNOWLEDGMENT:

We express our gratitude to Shota Rustaveli Georgian National Science Foundation. The research was carried out with the financial support of SHOTA RUSTAVELI NATIONAL SCIENCE FOUNDATION OF GEORGIA, grant AR-22-1730. “A method for the production of cement for purifying flue gases from (CO2, SOx, NOx), passing them through a clinoftilolite sorber before being released into the atmosphere, determining the applicability through experiments in laboratory conditions, with approval of the concept.”

REFERENCES

1. https://www.vesti.ru/nauka/article 2785376;
2. European Commission. Integrated Pollution Prevention and Control. Reference Document on Best Available Techniques in the Cement and Magnesium Oxide Manufacturing Industries. May 2010”.
http://eippecb.jrc. ec.europa.eu;
3. Global Environment Division Greenhouse Gas Assessment Hand-book –A Practical Guidance Document for the Assessment of Project-level Grenhouse Gas Emissions. World Bank Archived from the original on 3 June 2016. Retrieved 10 November 2007;
4. CARBON DIOXIDE CAPTURE AND STORAGE //Cambridge University, International Panel on Climate Change 2005. ISBN 0 – 521 – 86643 – x;
5. European Commission. Integrated Pollution Prevention and Control. Reference Document on Best Available Technoques on the Cement /Lime/Magnesium Oxide. Manufacturing Industries. May 2010;
6. Harold F.W.Taylor. Cement Chemistry. Academic Press. London, 1990;
7. Council Directive 96/61/EC of 24 September 1996 concerning integrated pollution prevention and control. http://www.ifc.org;
8. EN 197-1:2011. EUROPEAN STANDARD. CEMENT-PART 1. www.Cembureau.be.;
9. Cuéllar-Franca, Rosa M.; Azapagic, Adisa (March 2015). "Carbon capture, storage and utilisation technologies: A critical analysis and comparison of their life cycle environmental impacts". Journal of CO2 Utilizat-ion. 9: 82–102. doi:10.1016/j.jcou. 2014.12.001;
10. "Carbon Capture". Center for Climate and Energy Solutions. Retrieved 2020-04-22;
11. G.V. Tsitsishvili, N.S. Skhirtladze, T.G. Andronikasvili, V.G.Tsitsishvili, A.V.Dolidze. “Natural zeolites of Georgia: occurrences, propertie, and application. Studies in Surface Science and Catalysis. Volume 125.1999..Pages 715-722. https://doi.org/10.1016/50167 - 2991(99)80278-x.
12. CARYS – 19 – 674. Creation of laboratory prototype of continuous-action drying-adsorbing apparatus, and development of (CO_2, SOx,NOx) catching-utilization technology from burnt gases using zeolites. Shota Rustaveli National Science Foundation of Georgia (SRNSFG) https://rustaveli.org.ge/;
13. R. Skhvitaridze, T. Cheishvili, T. Kordzakhia, I. Giorgadze, A. Skhvitaridze, G. Loladze. “CO_2ZEOCEM technology for capturing/ utilization of CO_2,(SOx,NOx) from the flue

gases". J. "CEMENT INTERNATIONAL". № 5.2021, vol. 19, p. 38 – 41; https://digital.verlagbt.de/CI/CI-2021-5-258/;

14. Global Carbon Projeqt: http://www.globalcarbonproeqt.org;
15. Patent of Georgia: "Method of cement production" P 2022 7452 B (AP 2021 15578/1). 03.03.21. Pub.: off. Bull. N 24.2022.12.26. Authors: R. Skhvitaridze, T. Cheishvili, G. Loladze, I. Giorgadze, T. Tsintskaladze, T. Kordzakhia, Sh. Verulava. A. Skhvitaridze, G. KavtiaSvili
16. Kordzakhia T.N., R. Skhvitaridze, T. Tsintskaladze, I.Giorgadze, Sh. Verulava. ,,ADSORBCIA OKIDOV AZOTA PRIRODNIM KLINOPTILOLITOM". XVI Vserossiiskai Simpozium s mejdunarodnim uchastie: AKTUALNIE PROBLEMI TEORII ADSORBCIi, PORISTOSTI I ADSORBCIONNOI SELEKTIVNOSTI. MOSKVA KLIAZMA, 22-26 MAIA y 2017. p. 156-157
17. T. Kordzakhia, R. Skhvitaridze, T. Tsintskaladze. "Scientific foundation and practice of using zeolite in cement production". Proceeding of The IV International Scientific and Practical Conference, Topical Problrms of Modern Science and Possible Solutions". (September 30, 2017, Dubai, UAE). "World Science" № 10 (26), vol. 1. October 2017, p. 15-19. http://ws-conference.com/.
18. Kordzakhia T.N., Tsintskaladze G.P. Skhvitaridze R.E, Eprikishvili L.G., Zautashvili M.G., Giorgadze I.M, Verulava Sh. I. ,,Prirodni Klinoptilolit Gryzinskogo Mestopojdenia kak Adsorbent Oksidov Azota. Proceeding of the International Scientific Conference ,,International Trends in Scientific and Technology". October 17, 2017, Warsaw, Poland. Vol.5., p. 7-8
19. Kordzakhia T.N., Tsintskaladze G.P. Skhvitaridze R.E, Giorgadze I.M, Verulava Sh. I. ,,Ochistka objigovogo gaza cementnogo proizvodstva prirodnimi ceolitami. WEB of SCHOLAR Multidisciplinari Scientific Journal. #5(23), Vol. I, May 2018. P. 28-30. [http:// ws-conference. Com/webofscolar.
20. Kordzakhia T., Tsintskaladze G., Skhvitaridze R., Giorgadze I., Verulava Sh. ,,NATURAL ZEOLITES SATURATED WITH TECNOGENIC GASSES< ADDITIVES OF BULDING MATERIALS". Proceeding of the VII International Scientific and Practical Conference. "International Trends in Scientific and Technology". Vol.I, November 30, 2018, Warsaw, Poland. p. 55-58
21. Kordzakhia T.N., Skhvitaridze R.E, Tsintskaladze G.P., Cheishvili T.Sh., Sharashenidze T.M., Antia G.R., Kutsiava N. A. ,,Adsorbcia Oksidov Azota Klinoptilolitom". THE INTERNATIONAL SCIENTIFIC CONFERENCE "ENVIRONMENTAL PROTECTION AND SUSTANEBEL DWVELOPMENT" DEDICATED TO PROFESSOR VICTOR ERISTAVIS MEMORY. BOOK of ABSTRACT. TBILISI, GTU, November 11-12, 2019, p.60-61

უაკ 661.971.2

ცემენტის წარმოებაში წარმოქმნილი საკვამლე აირების CO_2,SOx,NOx-გან გასუფთავება ორსაფეხურიანი პროცესით

გ. ლოლაძე, თ. ჭეიშვილი, რ. სხვიტარიძე, ნ.კუცნავა, ე. უჩანეიშვილი,
ნ. მუხადგვერდელი, მ. კეკელიძე

საქართველოს ტექნიკური უნივერსიტეტი, ქიმიური ტექნოლოგიის და მეტალურგიის ფაკულტეტი. საქართველო, 0175, თბილისი, მ. კოსტავას 69.

E-mail: g.loladze@gtu.ge

რეზიუმე: მიზანი. ცემენტის ქარხნების კლინკერმწარმოებელი ღუმელებიდან ემისირებული საკვამლე აირების შემადგენლობაში მყოფი CO_2 და მისი თანმხლები SOx, NOx აირების დაჭერა-უტილიზაციის მაღალეფექტური ხერხის დამუშავება. შემოთავაზებეული მიდგომა მოიცავს (ემყარება) ადსორბენტად კლინოფთოლითის გამოყენებას და მასში საკვამლე აირების გატარებას: ლაბორატორიულ გარემოში საადსორბციო-საშრობ ჰიბრიდულ აპარატურაზე ექსპერიმენტაციით აირების დაჭერის ტექნოლოგიური პროცესის ოპტიმალური ვარიანტის დადგენას.

მეთოდი. გამოსაწვავი კლინკერის მისაღები ნახშირშემცველი ნარევიდან ბრიკეტების დამზადება, ექსპერიმენტულ ღუმელში მისი გამოწვა არანაკლებ 1450^0C ტემპერატურაზე და ამ დროს წარმოქმნილი აირების სპეციალურად შექმნილ საცდელ ლაბორატორიულ კომბინირებულ ჰიბრიდულ საშრობ-საადსორბციო ბლოკში გატარება. ამ გზით ხდება კლინკერის მისაღები ბრიკეტის შეცხობისას გამოყოფილი მავნე აირების (ძირითადად CO_2) ადსორბენტად გამოყენებული ცეოლითური ტუფით შთანთქმა. ამავე დროს, ეფექტური შთანთქმის უზრუნველმყოფად - ლაბორატორიული საადსორბციო აპარატის დანადგარის კონსტრუქციული მოწყობის მიზნობრივი ტრანსფორმირება ერთკვანძიანიდან ორკვანძიან ბლოკში.

შედეგი. ლაბორატორიული დანადგარის კონსტრუქციული მოწყობის და საექსპლოატაციო პარამეტრების ცვლათა განხორციელების ხარჯზე დაზუსტდა ადსორბენტის შთანთქმის უნარიანობის დამოკიდებულება როგორც ცეოლითის ფიზიკური მახასიათებლების (ადსორბენტის გრანულომეტრია და მასა, საადსორბციო ბლოკის შევსების ხარისხი), ასევე ჰიბრიდული ადსორბერის საშრობ-საადსორბციო კვანძებში გამავალი აირების და ადსორბენტის საკონტაქტო მექანიზმის სახეზე (ადსორბენტის მოძრავ-უძრავ ფენებში ადსორბატის გავლით) და ა.შ.

დასკვნა. ლაბორატორიული ექსპერიმენტით დადგინდა, რომ ცემენტის კლინკერის წარმოებისას წარმოქმნილი საემისიო საკვამლე აირებიდან შესაძლებელია ცეოლითური ტუფით -

როგორც ადსორბენტით, მავნე აირების (ძირითადად CO_2-ის შემცველი) დაჭერა. აღნიშნული პროცესის ეფექტურობის ზრდის მიზნით რეკომენდირებულია ორსაფეხურიანი ტექნოლოგიური რეჟიმი, რომლის განხორციელება მიზანშეწონილია ჩატარდეს განსხვავებული კონსტრუქციული მოწყობის ორ კვანძიან ბლოკში, რომლებშიც განთავსებულია ადსორბერი - ცეოლითური ტუფი. პირველ კვანძი უზრუნველყოფს ადსორბერის შრობა-გააქტიურებას ($t>150^0C$), ხოლო მეორე - სასურველი ადსორბციის პროცესის ინტენსიურად ჩატარებას ($t<70^0C$). ძირითადად CO_2-ით გაჯერებული ადსორბენტის (მარცვლები 3-8 მმ ზომით) გამოყენების პერსპექტიულობას წარმოადგენს მისი კლინკერთან ერთად დაფქვა და ცემენტის ხარისხის მოსალოდნელი გაუმჯობესება.

საკვანძო სიტყვები: ბრიკეტი, გამოწვა, აირები, ცეოლითი, შრობა, ადსორბცია, ადსორბენტი, საადსორბციო კვანძი.

UDC 666.3

IMPACT OF BORON NITRIDE ADDITION ON THERMOELECTRIC PERFORMANCE OF $Bi_2Sr_2Co_{1.8}O_y$ CERAMICS

I. Kvartskhava

Vladimer Chavchanidze Institute of Cybernetics of the Georgian Technical University. Z. Anjaparidze St. 5, Tbilisi 0186, Georgia

E-mail: iakvartskhava@gmail.com

Resume: **Goal**. The present study aims to enhance the thermoelectric performance of $Bi_2Sr_2Co_{1.8}O_y$ ceramics by the addition of boron nitride (BN).

Method. Reference and BN-added $Bi_2Sr_2Co_{1.8}O_y$ ceramic materials were synthesized by a solid-state reaction method. Electrical and thermal transport measurements were carried out.

Results. Based on the obtained experimental results, the values of power factor (PF) and figure of merit (ZT) were calculated to evaluate the thermoelectric performance of prepared composites.

Conclusions. The incorporation of BN additives into the $Bi_2Sr_2Co_{1.8}O_y$ host matrix leads to an increased density of samples. Electrical conductivity is significantly enhanced by a reduction in porosity. The BN-added sample's Seebeck coefficient reveals an almost identical temperature dependence as compared to the reference sample. Thermal conductivity of prepared samples rises with increasing BN content. At 973 K, the PF values obtained for compositions with 0.60-0.75 wt% BN are 80–84% higher than the reference value. The ZT value increases slightly with the addition of 0.45-0.60 wt% BN. These results confirm that suitable additives can optimize the performance of the $Bi_2Sr_2Co_{1.8}O_y$ thermoelectrics.

Key words: $Bi_2Sr_2Co_{1.8}O_y$ ceramics, BN addition, transport properties, thermoelectric performance.

1. INTRODUCTION

Due to their ability to directly transform waste heat into electricity, thermoelectric (TE) materials have attracted a lot of interest as a source of sustainable, environmentally friendly energy to address the energy crisis and environmental problems. The development of highly efficient TE materials is expected to promote the broad application of thermoelectric generators (TEGs) for electrical power generation from waste heat discharged from various industrial systems and heat arising from renewable energy sources [1]. Conventional intermetallic thermoelectrics often contain toxic as well as rare elements such as Te, Se, Sb, and Pb [2, 3]. Furthermore, because intermetallic compounds have poor structural and chemical stability at high temperatures, they exhibit the evaporation and oxidation of constituent elements at high temperatures [4-6]. Layered thermoelectric Na_xCoO_2, $Bi_2Sr_2Co_{1.8}O_y$, and $Ca_3Co_4O_9$ cobaltites [7-10] are free of these

drawbacks. However, the real-world application of cobaltites remains a challenge due to their relatively low heat-to electricity conversion efficiency to the conventional ones [11]. Doping with various elements and compounds has been widely used as a successful approach to increasing thermoelectric performance of cobaltite materials [3, 11-18]. Thermoelectric performance is governed by the dimensionless figure of merit [19]: $ZT=\sigma S^2T/k$, where σ, S, T, and k are electrical conductivity, Seebeck coefficient, absolute temperature, and total thermal conductivity, respectively. Therefore, the thermoelectric conversion efficiency rises with increasing ZT, implying that a high-performance thermoelectric material is characterized by a high σ, large S and low k. The electrical component of the ZT expression, called power factor ($PF=S^2\sigma$), is also used to evaluate the output electrical power [20-21]. The present study aims to investigate the impact of BN additives on the thermoelectric properties of the $Bi_2Sr_2Co_{1.8}O_y$ ceramics.

2. MAIN PART

Reference (undoped) and BN-added samples with the nominal composition of $Bi_2Sr_2Co_{1.8}O_y(BN)_x$, x=0, 0.10, 0.15, 0.20, and 0.25 (0, 0.30, 0.45, 0.60, and 0.75 wt %, respectively) were prepared by the conventional solid-state reaction route from the reagent grade Bi_2O_3, $SrCO_3$, Co_3O_4, and BN commercial powders. The mixtures of these raw powders were homogenized in a planetary mill (Fritsch Pulverisette 7 Premium line) for 20 min at a rotating speed of 150 rpm. Homogenized powders were calcined at 1040÷1080 K for 20 hours with an intermediate manual grindings in an agate mortar. Then the powders were pressed into pellets at a hydrostatic pressure of 200 MPa. Finally, the pellets were sintered at 1100 K in air for 25 h. Electrical resistivity values of prepared samples are given in Fig. 1.

The addition of boron nitride leads to a marked decrease in electrical resistivity in the temperature range of 293 K to 973 K. Densities of prepared samples are shown in Table 1.

Density values rise with the increasing content of BN additive, which is favorable for lowering resistivity. The temperature dependence of the Seebeck coefficient is displayed in Fig. 2. A positive S value is observed in all of them, indicating p-type conduction.

The Seebeck coefficient of prepared materials increases as the temperature rises, and its value is not significantly influenced by the BN concentration. The temperature dependence of the power factor (PF) is shown in Fig. 3.

Due to the reduced resistivity, the BN-added samples possessed significantly higher PF compared to the reference sample. At 973 K, maximum of PF values reach 0.047-0.048 $mW/m\cdot K^2$ for 0.60-0.75 wt. % BN-added samples. Fig. 4 shows the temperature dependence of thermal conductivity in the temperature range from 300 K to 570 K.

Thermal conductivity of BN-added $Bi_2Sr_2Co_{1.8}O_y$ thermoelectrics increases markedly with increasing BN content. Based on obtained results, the values of thermoelectric figure of merit (ZT) were calculated (Fig. 5).

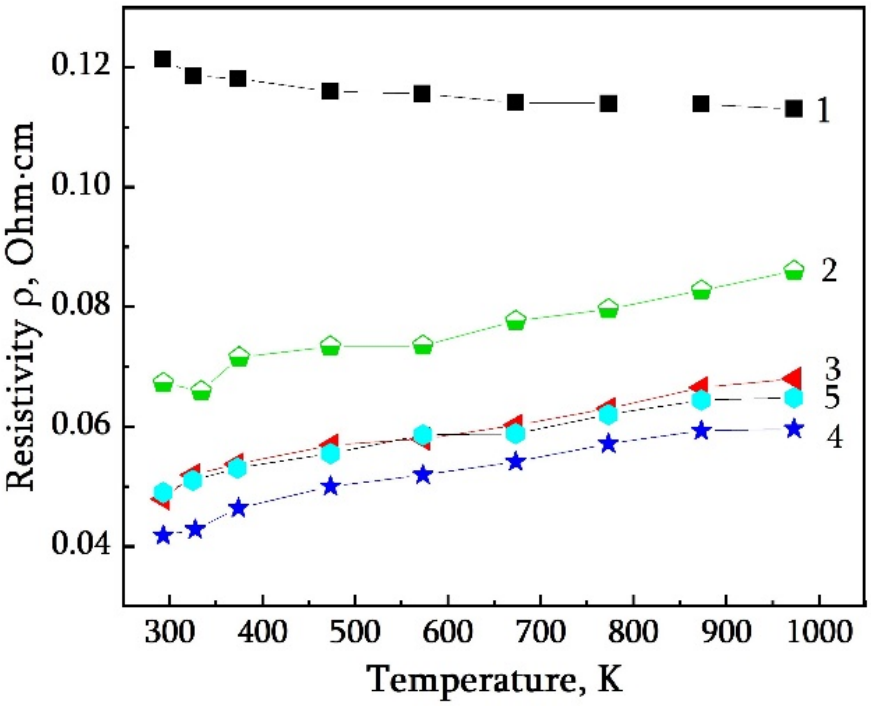

Fig. 1. Temperature dependences of electrical resistivity.
(1)-Reference $Bi_2Sr_2Co_{1.8}O_y$, (2)-$Bi_2Sr_2Co_{1.8}O_y$ +0.30 wt % BN,
(3)-$Bi_2Sr_2Co_{1.8}O_y$ +0.45 wt % BN, (4)-$Bi_2Sr_2Co_{1.8}O_y$ +0.60 wt % BN,
(5)-$Bi_2Sr_2Co_{1.8}O_y$ +0.75 wt % BN

Table 1

N	(1) Reference $Bi_2Sr_2Co_{1.8}O_y$	(2) $Bi_2Sr_2Co_{1.8}O_y$ +0.30 wt % BN	(3) $Bi_2Sr_2Co_{1.8}O_y$ +0.45 wt % BN	(4) $Bi_2Sr_2Co_{1.8}O_y$ +0.60 wt % BN	(5) $Bi_2Sr_2Co_{1.8}O_y$ +0.75 wt % BN
Density, g/cm^3	3.7	4.3	4.8	5.2	5.4
% of theoretical	54.4	63.2	70.6	76.5	79.4

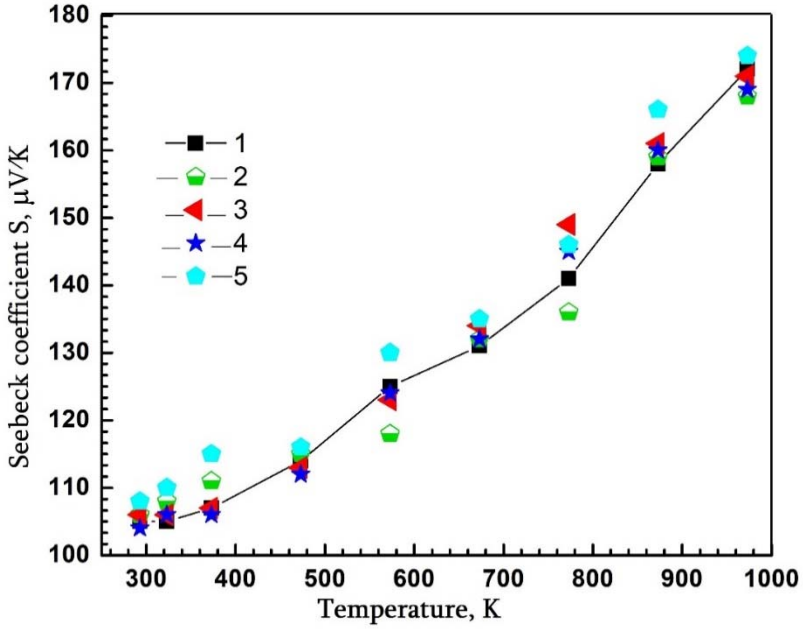

Fig. 2. Temperature dependences of Seebeck coefficient.
(1)-Reference $Bi_2Sr_2Co_{1.8}O_y$, (2)-$Bi_2Sr_2Co_{1.8}O_y$ +0.30 wt % BN,
(3)-$Bi_2Sr_2Co_{1.8}O_y$ +0.45 wt % BN, (4)-$Bi_2Sr_2Co_{1.8}O_y$ +0.60 wt % BN,
(5)-$Bi_2Sr_2Co_{1.8}O_y$ +0.75 wt % BN.

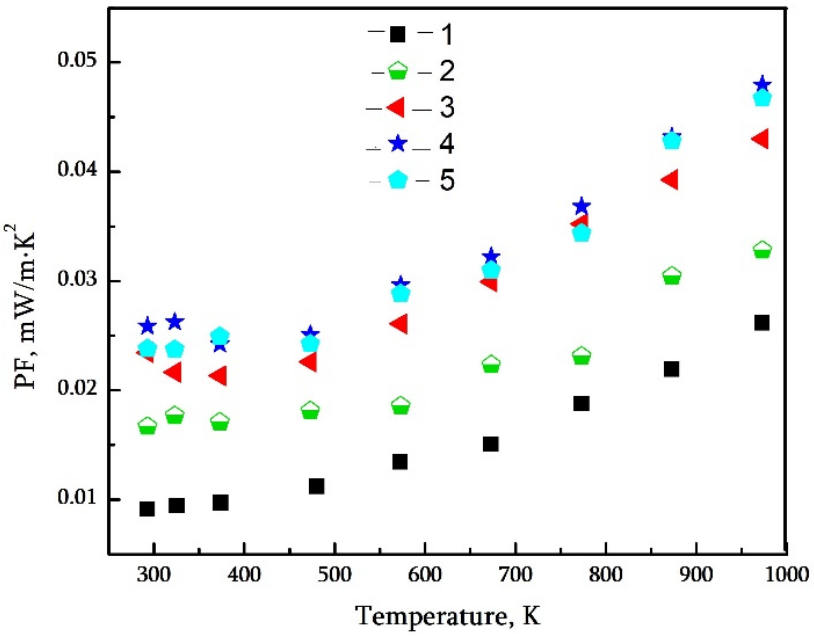

Fig. 3. Temperature dependences of Power Factor.
(1)-Reference $Bi_2Sr_2Co_{1.8}O_y$, (2)-$Bi_2Sr_2Co_{1.8}O_y$ +0.30 wt % BN,
(3)-$Bi_2Sr_2Co_{1.8}O_y$ +0.45 wt % BN, (4)-$Bi_2Sr_2Co_{1.8}O_y$ +0.60 wt % BN,
(5)-$Bi_2Sr_2Co_{1.8}O_y$ +0.75 wt % BN.

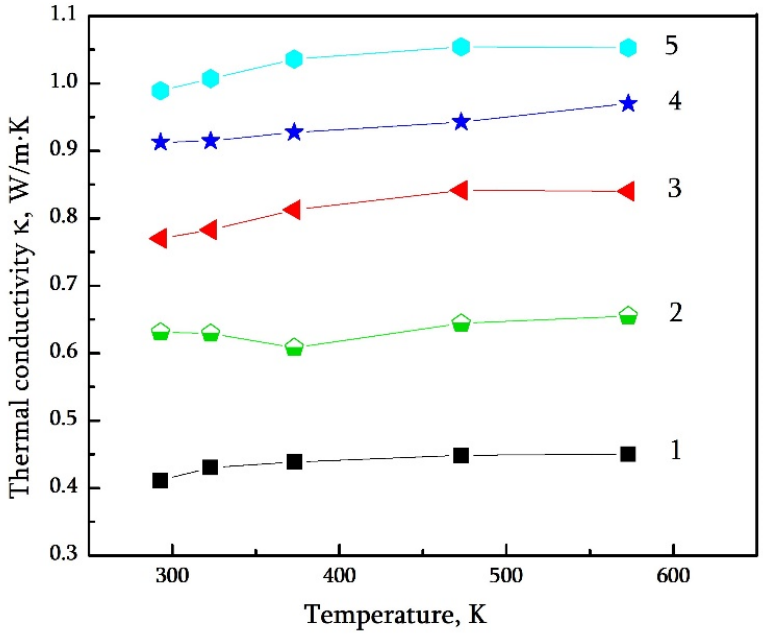

Fig. 4. Temperature dependences of thermal conductivity.
(1)-Reference $Bi_2Sr_2Co_{1.8}O_y$, (2)-$Bi_2Sr_2Co_{1.8}O_y$ +0.30 wt % BN,
(3)-$Bi_2Sr_2Co_{1.8}O_y$ +0.45 wt % BN, (4)-$Bi_2Sr_2Co_{1.8}O_y$ +0.60 wt % BN,
(5)-$Bi_2Sr_2Co_{1.8}O_y$ +0.75 wt % BN.

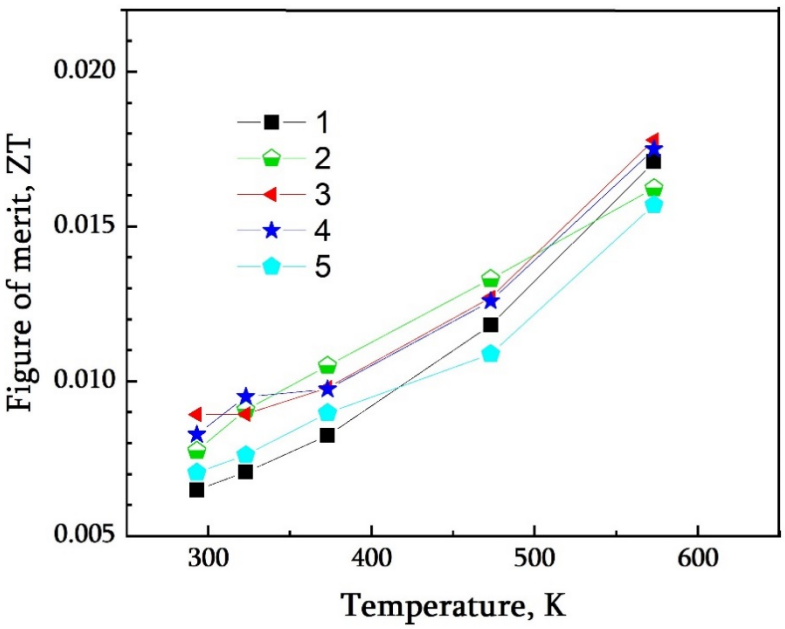

Fig. 5. Temperature dependences of figure of merit.
(1)-Reference $Bi_2Sr_2Co_{1.8}O_y$, (2)-$Bi_2Sr_2Co_{1.8}O_y$ +0.30 wt % BN,
(3)-$Bi_2Sr_2Co_{1.8}O_y$ +0.45 wt % BN, (4)-$Bi_2Sr_2Co_{1.8}O_y$ +0.60 wt % BN,
(5)-$Bi_2Sr_2Co_{1.8}O_y$ +0.75 wt % BN

The figure of merit ZT for $Bi_2Sr_2Co_{1.8}O_y$ thermoelectrics increases slightly with the addition of 0.45-0.60 wt % BN.

3. CONCLUSION

In summary, reference and BN-added $Bi_2Sr_2Co_{1.8}O_y$ ceramic materials have been prepared by a solid-state reaction method. Electrical resistivity, Seebeck coefficient, and thermal conductivity have been measured and analyzed. Based on the obtained data, the power factor and figure of merit have been calculated. Overall, the obtained results show that incorporating BN additives into $Bi_2Sr_2Co_{1.8}O_y$ host matrix provides a denser materials, enhanced electrical conductivity, and therefore higher PF values than the reference material.

ACKNOWLEDGMENT:

This research [PHDF-22-442/Influence of borax doping on the thermoelectric performance of layered cobaltites] has been supported by Shota Rustaveli National Science Foundation of Georgia (SRNSFG).

The author would like to thank laboratory member V.V. Zhghamadze for providing assistance with the physical measurements.

REFERENCES

1. He J., Liu Y., Funahashi R. Oxide thermoelectrics: the challenges, progress, and outlook, Journal of Materials Research, 2011, vol. 26: pp.1762–1772.
2. Koumoto, Kunihito, Funahashi, Ryoji, Miyazaki, Yuzuru, Weidenkaff, Anke, Wang, Yifeng, and Wan, Chunlei. Thermoelectric Ceramics for Energy Harvesting. Journal of the American Ceramic Society. 2013, vol. 96, # 1, pp. 1–23.
3. I.V. Matsukevich, A.I. Klyndyuk, E.A. Tugova, A.N. Kovalenko, A.A. Marova, N.S. Krasutskaya. Thermoelectric properties of $Ca_{3-x}Bi_xCo_4O_{9+\delta}$ ($0.0 \le x \le 1.5$) ceramics. Inorganic Materials, 2016, vol. 52, No. 6, pp. 593–599.
4. Ho Young Hong, Soyeon Gwon, Donghoon Kim, Kyeongsoon Park. Influence of sintering temperature and Li^+/Mg^{2+} doping on the thermoelectric properties of $Bi_{2-2x}Li_xMg_xSr_2Co_2O_y$, Advances in Applied Ceramics, 2022, vol. 121, No. 4, pp. 124-131.
5. S. Bresch, B. Mieller, C. Selleng, T. Stöcker, R. Moos, T. Rabe. Influence of the calcination procedure on the thermoelectric properties of calcium cobaltite $Ca_3Co_4O_9$. J. Electroceram., 2018, vol. 40, pp. 225–234.
6. E. Combe, R. Funahashi, F. Azough, and R. Freer. Relationship between microstructure and thermoelectric properties of $Bi_2Sr_2Co_2O_x$ bulk material, Journal of Materials Research, 2014, vol. 29, pp. 1376–1382.
7. Y. Terasaki, Y. Sasago, and K. Uchinokura. Large thermoelectric power in $NaCo_2O_4$ single crystals, Phys. Rev. B, 1997, vol. 56, # 20, pp. R12685–7.
8. R. Funahashi, I. Matsubara, H. Ikuta, T. Takeuchi, U. Mizutani, and S.Sodeoka. An oxide single crystal with high thermoelectric performance in air, Jpn. J. Appl. Phys., 2000, # 39, L1127–9.
9. C. Masset, C. Michel, A. Maignan, M. Hervieu, O. Toulemonde, F.Studer, B. Raveau, and J. Hejtmanek. Misfit-layered cobaltite

with an anisotropic giant magnetoresistance: $Ca_3Co_4O_9$, Phys. Rev. B, 2000, vol. 62, pp. 166–75.

10. R. Funahashi, I. Matsubara, and S. Sodeoka. Thermoelectric Properties of $Bi_2Sr_2Co_{1.8}O_y$ Polycrystalline Materials, Appl. Phys. Lett., 2000, # 76, pp. 2385–7.
11. G. Çetin Karakaya, B. Özçelik, M. A. Torres M. A. Madre, A. Sotelo. Effects of K substitution on thermoelectric and magnetic properties of $Bi_2Sr_2Co_{1.8}O_y$ ceramic, J. Mater Sci: Mater. Electron. 2017, vol. 28, Issue 17, pp. 12652–12659.
12. S. Saini, H. Yaddanapudi, K.Tian, Y. Yin, D. Magginetti, A.Tiwari. Terbium Ion Doping in Ca3Co4O9: A Step towards High-Performance Thermoelectric Materials, Sci. Rep, 2017, vol. 7, No. 1, article #44621.
13. Xin Liu, Mengmeng Fan, Xuguang Zhu, Zengguo Tian, Xin-Jian Li, Hongzhang Song. Optimising the thermoelectric properties of $Bi_2Sr_2Co_2O_y$ using Ag substitution and Nano-SiC doping, Ceramics International, 2021, vol. 47, Issue 21, pp. 30657-30664.
14. Shufang Wang, Zilong Bai, Haifeng Wang, Qing Lü, Jianglong Wang, Guangsheng Fu. High temperature thermoelectric properties of $Bi_2Sr_2Co_2O_y$/Ag composites, Journal of Alloys and Compounds. 2013, Vol. 554, pp. 254-257.
15. Hira, U., Pryds, N., Sher, F. Thermoelectric Properties of Dual Doped $Bi_2Sr_2Co_2O_y$-Based Ceramics. J. Electron. Mater, 2019, vol. 48, pp. 4618–4626.
16. G.A. Mumladze, I.G. Kvartskhava, A.I. Klyndyuk, V.V. Zhghamadze, N.G. Margiani, and A.S. Kuzanyan. Effect of $Pb(BO_2)_2$ Doping on Power Factor of $Bi_2Sr_2Co_{1.8}O_y$ Thermoelectric Ceramics, Acta physica polonica A, 2022, vol. 141, No. 4, pp. 319-322.
17. N. Margiani, V. Zhghamadze, G. Mumladze, I. Kvartskhava, Z. Adamia, A. Klyndyuk, A. Kuzanyan. Impact of Graphene Addition on the Microstructure and Thermoelectric Properties of $Bi_2Sr_2Co_{1.8}O_y$ Ceramics, Bulletin of the Georgian National Academy of Sciences, 2022, vol. 16, No. 1, pp. 17-24.
18. A.S. Kuzanyan, N.G. Margiani, V.V. Zhghamadze, I.G. Kvartskhava, G.A. Mumladze, and G.R. Badalyan. Impact of $Sr(BO_2)_2$ Dopant on Power Factor of $Bi_2Sr_2Co_{1.8}O_y$ Thermoelectric, Journal of Contemporary Physics (Armenian Academy of Sciences), 2021, vol. 56, No. 2, pp. 146-149.
19. Mohamed Amine Zoui, Saïd Bentouba, John G. Stocholm and Mahmoud Bourouis. A Review on Thermoelectric Generators: Progress and Applications. Energies, 2020, vol. 13, issue 14, article #3606.
20. Y.C. Zhou, C.L. Wang, W.B. Su, J. Liu, H.C. Wang, J.C. Li, Y. Li, J.Z. Zhai, Y.C. Zhang, L.M. Mei. Electrical properties of Dy^{3+}/Na^+ Co-doped oxide thermoelectric [$Ca_{1-x}(Na_{1/2}Dy_{1/2})_{(x)}$]MnO3 ceramics. Journal of Alloys and Compounds, 2016, vol. 680, pp. 129-132.
21. Weishu Liu, Hee Seok Kim, Qing Jie, Zhifeng Ren. Importance of high power factor in thermoelectric materials for power generation application: A perspective, Scripta Materialia, 2016, vol. 111, pp. 3-9.

უაკ 666.3

ბორის ნიტრიდის დანამატის ზეგავლენა $Bi_2Sr_2Co_{1.8}O_y$ კერამიკის თერმოელექტრულ მახასიათებლებზე

ი. ქვარცხავა

საქართველოს ტექნიკური უნივერსიტეტი ვლადიმერ ჭავჭანიძის სახელობის კიბერნეტიკის ინსტიტუტი, ზ. ანჯაფარიძის ქ. 5, თბილისი 0186, საქართველო

E-mail: iakvartskhava@gmail.com

რეზიუმე: მიზანი. წარმოდგენილი ნაშრომი მიზნად ისახავს $Bi_2Sr_2Co_{1.8}O_y$ კერამიკის თერმოელექტრული მახასიათებლების გაუმჯობესებას ბორის ნიტრიდის (BN) დამატებით.

მეთოდი. მყარფაზური რეაქციის მეთოდით სინთეზირებულ იქნა საყრდენი და BN–ის დანამატიანი $Bi_2Sr_2Co_{1.8}O_y$ კერამიკული მასალა. ჩატარდა ელექტრული და თერმული სატრანსპორტო გაზომვები.

შედეგები. მიღებულ ექსპერიმენტულ შედეგებზე დაყრდნობით გამოითვალა სიმძლავრის ფაქტორის (PF) და ვარგისობის მაჩვენებლის (ZT) რიცხვითი მნიშვნელობები სინთეზირებული კომპოზიტების თერმოელექტრული ეფექტურობის შესაფასებლად.

დასკვნები. $Bi_2Sr_2Co_{1.8}O_y$ საყრდენ მასალაში BN დანამატის შეტანა განაპირობებს ნიმუშთა გაზრდილ სიმკვრივეს. ფოროვნების შემცირება მნიშვნელოვნად ზრდის ელექტრულ გამტარობას. BN დანამატიანი ნიმუშების ზეებეკის კოეფიციენტი ავლენს საყრდენი ნიმუშის თითქმის იდენტურ ტემპერატურულ დამოკიდებულებას. მომზადებული ნიმუშების თბოგამტარობა იზრდება BN–ის შემცველობის ზრდასთან ერთად. 973 K–ზე PF–ის მნიშვნელობები, მიღებული BN –ის 0.60-0.75 წონითი %–ის პირობებში, 80–84 %–ით მაღალია საყრდენ ნიმუშთან შედარებით. ZT–ის მნიშვნელობა ოდნავ იზრდება 0.45–0.60 წონითი % BN–ის შემთხვევაში. ეს შედეგები მოწმობს, რომ შესაბამისად შერჩეულ დანამატებს ძალუძს $Bi_2Sr_2Co_{1.8}O_y$ თერმოელექტრიკების ეფექტურობის ოპტიმიზირება.

საკვანძო სიტყვები: $Bi_2Sr_2Co_{1.8}O_y$ კერამიკა, BN დანამატი, ტრანსპორტული თვისებები, თერმოელექტრული ეფექტურობა.

UDC 615.11

STUDY OF PHYSICAL-CHEMICAL PARAMETERS OF CLAYS OBTAINED ON THE TERRITORY OF GEORGIA

M. Tsivadze, T. Tsintsadze, M. Gabelaia, P. Iavichi

Department of pharmacy. Georgian Technical University. 0075 Tbilisi. Kosstava Str. 69. Georgia

E-mail: mtsivadze05@mail.ru

Resume: **Goal:** The aim of the study is to investigate the granulometric composition, elemental composition, sorption properties, absorption coefficient and a comparative study of colloidity of the clay samples obtained on the territory of Georgia - blue clay - Lentekhi district, Chukuli village, Fishkor river (sample 1) and red clay - Ozurgeti district, Gomi mountain (sample 2). Clay minerals are characterized by fundamental structural properties, although they also have characteristically different properties that determine their interaction with other chemical substances. It is the variation of the structure that leads to the diversity of their use.

Method: gravimetric, photometric, volumetric and atomic-absorption methods;

Result: Fractionation of clay particles was carried out by granulometric analysis of two types of clay - blue clay - Lentekhi district, Chukuli village, Fishkor river and red clay - Ozurgeti district, Gomi mountain. According to the comparative study of the elemental composition, the red clay of Gomi Mountain is characterized by a high content of such elements as Zn, Ti, Fe, Cu and others, which allows this clay to be used as a mineral filter in photoprotective cosmetics.

Conclusion. As a result of the study of two types of clay - blue clay, Lentekhi district, Chukuli village, Fishkor river and red clay - Ozurgeti district, Gomi mountain by physical and chemical methods, it was established that the red clay of Gomi Mountain (Ca bentonite clay) is a good adsorbent with its physico-chemical properties, has a high value of the coefficient of competition and is characterized by the ability to create a hydrogel. It can be used in cosmetics both in its native form and in the form of hydrogels with different concentrations. 50% of Lentekhi blue clay is quartz, so its use in cosmetics is complicated.

Keywords: clay, adsorbent, coefficient of competition, cosmetics, fractionation of particles.

1. INTRODUCTION

Clay is widely used in pharmaceuticals, it is one of the excellent auxiliary substances, it is used in many medicinal forms - suspension, emulsion, ointments, gels, tablets and others.Clays are characterized by pharmacological action as antacid, antibacterial, antiemetic, antidiarrheal, as skin protective agents, etc. Their unique structure determines their ability to be absorbed, allowing for a wide range of applications in drug delivery.

The study of the surface and granulometric composition of clay minerals led to many directions and future perspectives of the pharmaceutical field [1-4].

2. MAIN PART

Two samples of clay were investigated:

1. The native form of blue clay of the Lashkheti River in the village of Chukuli, Lentekhi district,

2. Native form of red clay of Gomi mountain, Ozurgeti region.

Clay samples were dried, cleaned, ground, suspended and decanted under the same conditions, according to the same technological scheme. Clay samples were dried at 90^{0}C; large, foreign, solid particles were removed and ground mechanically. The clay was suspended in water in a ratio of 1:5, left for 2 days and nights. We obtained purified fractions of native clay samples by decantation.

1. Organoleptic examination of purified fractions 1 and 2 of native samples of various clays was conducted [5-6];

2. Granulometric composition of particles of cleaned samples according to international standard GOST 28177-89 Molding bentonite clays. In accordance with the General specifications, it was determined by the sieve analysis method. According to norms, sieves with 5 mm, 2.5 mm and 0.16 mm holes were used during the analysis [9-10];

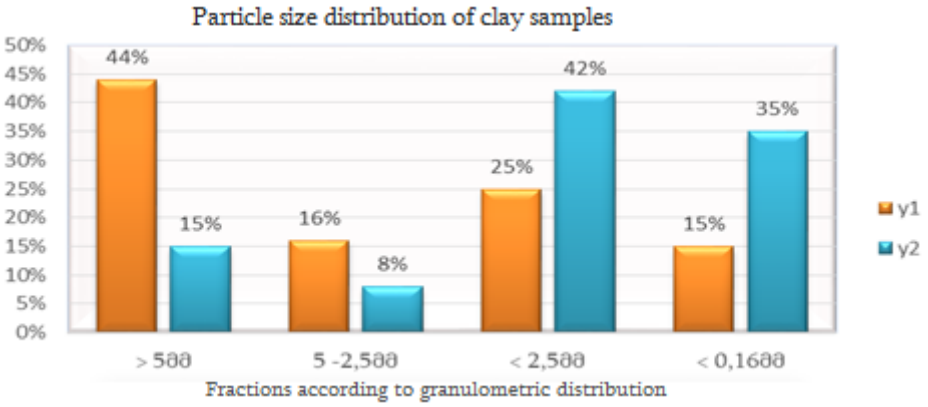

Figure 1. Granulometric composition of particles of clay samples:
Y1-blue clay of the Lashkheti River of Chukuli village of Lentekhi district;
Y2-Red clay of Gomi Mountain, Ozurgeti district

Medical and cosmetic clay forms a very finely dispersed powder. Therefore, for the next study of clay samples, fraction №4 of both samples with particle size < 0.16 mm was selected.The granulometric composition of the particles is presented in the form of diagrams (Figure 1). As can be seen from the diagram, the percentage of the 4th fraction (particle size < 0.16 mm) of the red clay of Gomi Mountain is almost 2.5 times higher

than the percentage of the same fraction of the blue clay of Lentekhi district.

3. Elemental analysis of clay samples 1 and 2 was carried out - through gravimetric, photometric, volumetric and atomic-absorption methods. The results of the analysis are given in Table1.

The results of a comparative study of different clay samples showed that they are almost identical in their qualitative elemental composition, while the quantitative content of some elements differs.

Table 1

Elemental composition of clay samples

N	parameter (mass fraction)	unit of definition	Obtained Results		Identified Test Method
			Sample 1	Sample 2	
1	moisture	%	0,28	6,03	gravimetric
2	closing loss	%	6.00	10,4	gravimetric
3	SiO_2	%	61,8	42,2	gravimetric
4	CaO	%	1,7	2,4	gravimetric
5	MgO	%	2,2	5,9	gravimetric
6	Fe_2O_3	%	7,05	10,3	gravimetric
7	Al_2O_3	%	16,5	18,3	gravimetric
8	TiO_2	%	0,13	0,83	gravimetric
9	Na_2O	%	1,40	0,60	gravimetric
10	K_2O	%	2,05	1,70	gravimetric
11	SO_3	%	0,14	0,12	gravimetric
12	MnO	%	0,12	0,12	photometric
13	P_2O_5	%	0,91	0,28	photometric
14	Cl^-	%	0,004	0,004	voluminous
15	Cu	mg/kg	105,0	121	Atomic absorption
16	Pb	mg/kg	not found	26	Atomic absorption
17	Zn	mg/kg	1470	280	Atomic absorption
18	Co	mg/kg	22,6	43	Atomic absorption
19	Ni	mg/kg	64,1	212	Atomic absorption

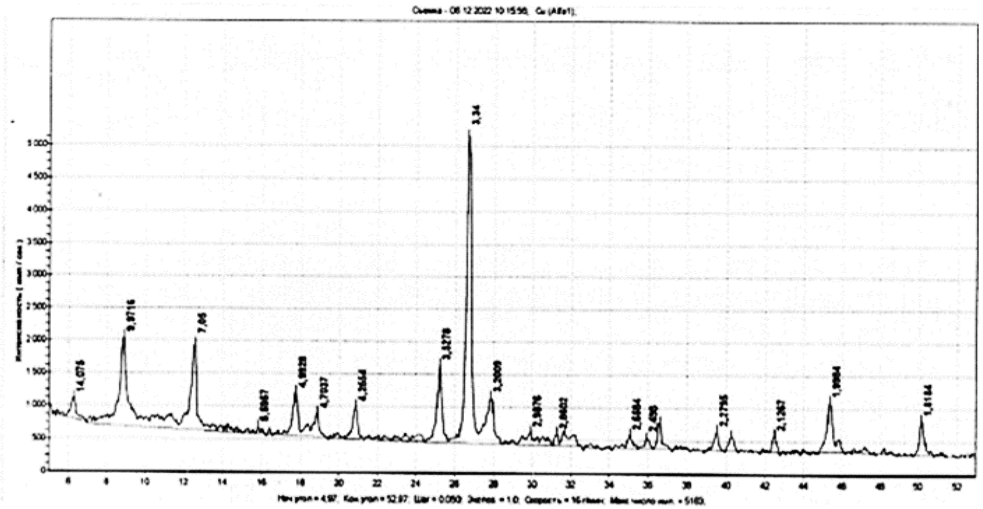

1. Quartz – 4.255,3.34,2.279,2.127,1.818 Å (500 : 12000) x 100% = 40-50 %·
2. Fe – Mg chloride – 14.08,7.05,4.704,3.54Å
3. The wind – 9.97,4.99,3.34,1.998Å
4. Field spat – 3.20 Å

\

Figure 2. Mineral composition of clay sample #1

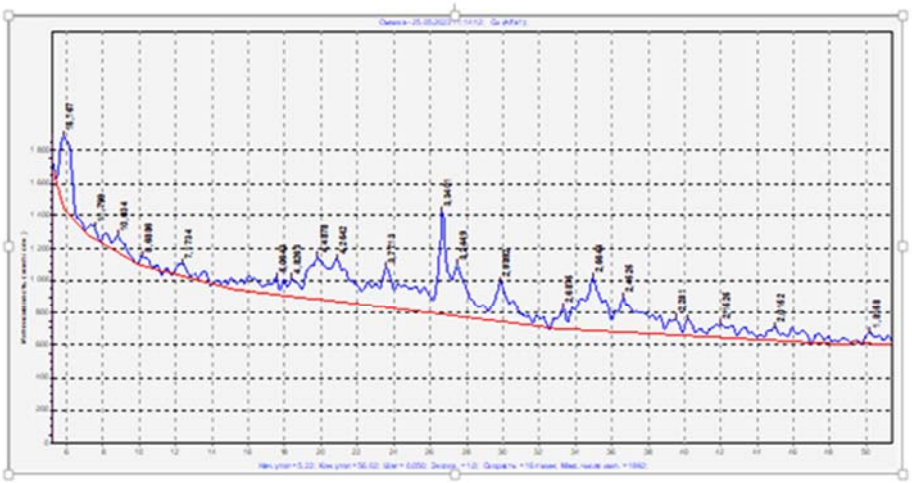

1. Montmorillonite – 15.17,4.448,3.77,2.99,2.564 Å
2. The wind – 4.254,3.34,2.455,1.816 Å (signs)
3. Field spat – 3.77,3.24 Å(signs)

Figure 3. Mineral composition of clay sample #2

As can be seen from the figure, 50% of the research sample is quartz, that is, 50% of the research sample is sand particles

A study of the mineral composition of the clay samples was conducted, 50% of the research sample 1 is quartz, that is, 50% of the research sample is sand particles (Figure 2, 3), and the clay of the sample 2 is a calcium form of bentonite. The amount of quartz is insignificant, so this clay can be used in cosmetics [11-12].

4. The adsorption capacity of sample 1 and 2 clays for dyeing was determined using methylene blue according to the international standard GOST 28177-89 Molding bentonite clays. in accordance with General specifications.

The analysis technique: we placed a clay weight (weight - 0.30 g) in a 100 ml conical flask and added 25 ml of the coloring solution. Optical density was measured using a photoelectrocolorimeter. Mode of operation - blue light filter, wavelength in the cuvette 400 nm, distance between working tips - 10 mm. We used distilled water as a control solution. The residual concentration of the dye was determined by the obtained optical density values. Adsorption activity was calculated by the formula:

$$X = \frac{(C_1 - C_2 K) \cdot 0.025}{m},$$

where, C_1 - the concentration of the initial dye solution, mg/ml;

C_2 - concentration of dye solution after contact with clay, mg/l;

K - dilution factor;

m - weight of clay, g;

25 - volume of coloring solution, ml.

The results are presented in Table No. 2. As can be seen from the table, the adsorption capacity of bentonite clay is higher than that of blue clay, which means that bentonite clay has stronger adsorption properties [14-16].

Table 2

Experimental data for determining the concentration of methylene blue in solution

N	Clay sample	initial concentration, g/ml	Weight of clay, g	residual concentration, mg/l	adsorption capacity, mg/g
1	№1	1,5	0,3	2,4	82
2	№2	1,5	0,3	0,6	125

5. The resistance index of the clay test samples in water was determined according to the ASTMD 5890-95 method.

The analysis technique: we obtained 2±0.1 g of powder of the fourth fraction of clays. We poured 90 ml of distilled water into a 100 ml measuring cylinder. We took 0.1 g of a weighed 2 gram clay sample, placed it in a cylinder without a funnel and left it for 10 minutes until complete hydration and sedimentation. In the same way, we placed the rest of the weighed clay in the cylinder at 10-minute intervals. Cover the measuring cylinder with parchment paper and leave it for 16 hours. Then we carefully measured the height of the gel formed at the bottom of the cylinder.

6. The colloidal index of the clay research samples was determined according to the inter-

national standard GOST 3594.10-93 Molding refractory clays. Method for determination of colloidal state according to the guidelines [17-18].

We placed a 1 gram weight of clay sample in a measuring cylinder, added water to the total volume of 30 milliliters. We shook until a homogeneous suspension was obtained. We added 0.2g of Mg oxide to the suspension and shook it again, leaving it for 24 hours. We measured the volume of formed sediment. Colloidity (in K%) was calculated by the formula:

We placed 1 g weight of the clay sample in a measuring cylinder, added water to the total volume of 30 ml. We shook until a homogeneous suspension was obtained. We added 0.2 g of MgO to the suspension and shook it again, leaving it for 24 h. We measured the volume of formed sediment. Colloidity (in K%) was calculated by the formula:

$$K=Vx\cdot 100/30$$

K -colloidy, %;

V - volume of sediment produced, ml;

30 - Clay and water area, ml.

Standardization of clay samples was practically carried out [19-10]. The obtained results are presented in Table 3.

Table 3

Summary table of results of standardization of research clay samples

N	Clay quality indicator	unit of definition	Clay samples	
			sample 1	sample 2
1	moisture	%	0,28	6,03
2	closing loss	%	6,00	10,4
3	The winning ratio	%	3,20	5,10
4	colloidal	%	7,60	12,7
5	adsorption capacity	mg/g	82	125

The following equipment was used during the analysis:

- Atomic absorption spectrophotometer Analyst – 200 U = 0.054mg/dm³;
- Photocolorimeter КФК -2;
- General purpose X-ray diffractometer ДРОН-2 with copper anode;

Electronic scale # 5034/120 max 120g d = 0.1mg.

3. CONCLUSION

If we summarize the results of the calculations, we can conclude that the the percentage of the 4th fraction (particle size < 0.16 mm) of the red clay of Gomi Mountain is almost 2.5 times higher than the percentage of the same fraction of the blue clay of Lentekhi district. As can be seen from the data in the table, the sample of bentonite clay of Caform (red clay of Ozurgeti district, Gomi mou-

ntain) is higher than the blue clay sample of Lashkheti river of Chukuli village of Lentekhi district.

The red clay of Gomi mountain is a good adsorbent with its physico-chemical properties, it is characterized by a high absorption coefficient and the ability to create hydrogels. It can be used in cosmetics both in native, powdery form and in the form of hydrogel of various concentrations.

Lentekhi blue clay contains up to 50% silt, so its use in cosmetics is complicated.

REFERENCES

1. Novelli G. Applicazionimedicali e igienichedellebentoniti. In: Veniale F, editor. AttiConvegno "Argille Curative", SaliceTerme/PV. Gruppo Italy. AIPEA; 1996. pp. 25-43
2. Robertson RHS. Cadavers, choleras and clays. Mineralogical Society of Great Britain & Ireland. 1996;113:3-7
3. Carretero MI. Clay minerals and their beneficial effects upon human health. A review. Applied Clay Science. 2002;21:155-163
4. Gomes CSF, Pereira Silva JB. Minerals and Human Health. Benefits and Risks. Centro de Investigação "MineraisIndustriais e Argilas". Fudação para a Ciência e a Tecnologia do Ministério da Ciência, Tecnologia e Ensino Superior. Aveiro (Portugal); 2006
5. Carretero MI, Gomes C, Tateo F. Clays and human health. In: Bergaya F, Theng BKG, Lagaly G, editors. Handbook of Clay Science. Amsterdam: Elsevier; 2006. pp. 717-741
6. Porubcan LS, Born GS, White JL, Hem SL. Interaction of digoxin and montmorillonite: Mechanism of adsorption and degradation. Journal of Pharmaceutical Sciences. 1979;68:358-361
7. Forteza M, Galan E, Cornejo J. Interaction of dexamethasone and montmorillonite. Adsorption – degradation process. Applied Clay Science. 1989;4:437-448
8. Cornejo J, Hermosin MC, White JL, Barnes JR, Hem SL. Role of ferric iron in the oxidation of hydrocortisone by sepiolite and palygorskite. Clays and Clay Minerals. 1983;31:109-112
9. Forteza M, Cornejo J, Galan E. Effects of fibrous clay minerals on dexamethasone stability. In: Konta J, editor. Proceedings of the Tenth Conference on Clay Minerals and Petrol, Ostrava. Prague: Universitas Carolina; 1988. pp. 281-286
10. McGinity JW, Lach JL. Sustainedrelease applications of montmorillonite interaction with amphetamine sulfate. Journal of Pharmaceutical Sciences. 1977;66:63-66
11. Gabriel DM. Vanishing and foundation creams. In: Harry RG, editor. Harry's Cosmeticology. The Principles and Practice of Modern Cosmetics. Vol. I. 6th ed. London: Leonard Hill Books; 1973. p. 83
12. Russel WB, Saville DA, Schowalter WR. Colloidal Dispersions. Cambridge: Cambridge University Press; 1995. p. 525
13. Vanderbilt Report. Technical Information: "VEEGUM-The Versatile Ingredient for Pharmaceutical Formulations". R.T. Vanderbilt Company Bulletin No. 91R. 1984. Available from: www.rtvanderbilt.com
14. Clarke MT. Rheological additives. In: Laba D, editor. Rheological Properties of Cosmetics

and Toiletries. New York: Marcel Dekker; 1994. pp. 55-152
15. Dechow HJ, Von Dölcher D, Hübner G, Kim S, Lämmerhirt K, Pich CH, et al. Zurentwicklung von oralesdareichungsformen der kombination sulfamoxol/ trimethoprim (CN3123). Arzneimittel-Forschung. 1976; 26:596-613
16. Vanderbilt. Technical Information. 2006. Available from: www. rtvanderbilt.com
17. Kovacs P. Useful incompatibility of xanthan gum with galactomannans. Food Technology. 1973;27(3):26-30
18. McDonald C, Richardson C. The effect of added salts on solubilization Clay Science and Technology 20 by a nonionic surfactant. The Journal of Pharmacy and Pharmacology. 1981;33:38-39
19. Kpogbemabou D, LecomteNana G, Aimable A, Bienia M, Niknam V, Carrion C. Oil-in-water Pickering emulsions stabilized by phyllosilicates at high solid content. Colloids and Surfaces A: Physicochemical and Engineering Aspects. 2014;463:85-92
20. Kpogbemabou D, LecomteNana G, Aimable A, Bienia M, Niknam V, Carrion C. Oil-in-water Pickering emulsions stabilized by phyllosilicates at high solid content. Colloids and Surfaces A: Physicochemical and Engineering Aspects. 2014; 463:85-92.

უაკ 615.11

საქართველოს ტერიტორიაზე მოპოვებული თიხების ფიზიკურ-ქიმიური პარამეტრების შესწავლა

მ. ცივაძე, თ. ცინცაძე, მ. გაბელაია, პ. იავიჩი

საქრთველოს ტექნიკური უნივერსიტეტი, ქიმიური ტექნოლოგიისა და მეტალურგის ფაკულტეტი, ფარმაციის დეპარტამენტი

E-mail: mtsivadze05@mail.ru

რეზიუმე: მიზანი. კვლევის მიზანია ჩატარებულ იქნას საქართველოს ტერიტორიაზე მოპოვებული თიხის ნიმუშების - ცისფერითიხა - ლენტეხისრაიონი, სოფელიჩუქული, მდინარეფიშყორი (ნიმუში 1) და წითელი თიხა - ოზურგეთის რაიონი, გომის მთა (ნიმუში 2), ნაწილაკების გრანულომეტრული შედგენილობის, ელემენტური შედგენილობის, სორბციული თვისებების, გაჯირჯვების კოეფიციენტის და კოლოიდურობის შედარებითი კვლევა. თიხის მინერალები ხასიათდებიან ფუნდამენტალური სტრუქტურული თვისებებით, თუმცა კიდევ მათ გააჩნიათ დამახასიათებელი განსხვავებული თვისებები, რომელიც განსაზღვრავს მათ

ურთიერთქმედებას სხვა ქიმიურ ნივთიერებებთან. სწორედ სტრუქტურის ცვალებადობა იწვევს მათი გამოყენების მრავალფეროვანებას

რეზიუმე. ორი სახის თიხის - ცისფერი თიხა, ლენტეხის რაიონი, სოფელი ჩუქული, მდინარე ფიშყორი და წითელი თიხა - ოზურგეთის რაიონი, გომის მთა ნაწილაკების ზომების გრანულომეტრული ანალიზით ჩატარდა თიხის ნაწილაკების ფრაქციონირება. ელემენტური შედგენილობის შედარებითი შესწავლით გომის მთის წითელი თიხისთვის დამახასიათებელია ისეთი ელემენტების მაღალი შემცველობა, როგორიცაა Zn, Ti, Fe, Cu და სხვა, რაც საშუალებას იძლევა ეს თიხა გამოყენებულ იქნას როგორც მინერალური ფილტრი ფოტოპროტექტორულ კოსმეტიკურ საშუალებებში.

მეთოდი. გრავიმეტრული, ფოტომეტრული, მოცულობითი და ატომურ-აბსორბციული მეთოდების მეშვეობით;

დასკვნა. ორი სახის თიხის - ცისფერი თიხა, ლენტეხის რაიონი, სოფელი ჩუქული, მდინარე ფიშყორი და წითელი თიხა - ოზურგეთის რაიონი, გომის მთა ნაწილაკების ფიზიკურ ქიმიური მეთოდებით კვლევის შედეგად დადგინდა, რომ გომის მთის წითელი თიხა (Ca ფორმის ბენტონიტის თიხა) თავისი ფიზიკურ-ქიმიური თვისებებით წარმოადგენს კარგ ადსორბენტს, გააჩნია გაჯირჯვების კოეფიციენტის მაღალი მნიშვნელობა და ხასიათდება ჰიდროგელის შექმნის უნარით. მისი გამოყენება შესაძლებელია კოსმეტიკურ საშუალებებში როგორც ნატიური ფორმით, ისე სხვადასხვა კონცენტრაციის მქონე ჰიდროგელების სახიტ. ლენტეხის ცისფერი თიხის 50%-ს წარმოადგენს კვარცი, ამიტომ მისი გამოყენება კოსმეტიკურ საშუალებებში გართულებულია.

საკვანძო სიტყვები: თიხა, ადსორბენტი, გაჯირჯვების კოეფიციენტი, კოსმეტიკურ საშუალებები, ნაწილაკების ფრაქციონირება.

UDC 543.4:546.72

COMPLEX FORMATION OF COOPER (II) WITH AZO PRODUCTS OF ACETYL ACETONE

M. Tsintsadze, M. Kochiashvili, I. Ugrekhelidze, N. Imnadze

Georgian Technical University, Department of Chemistry, Georgia, 0075, Tbilisi, Kosstava Str. 69.

E-mail: m.koridze@yahoo.com

Resume: Goal: For the photometric determination of cooper, a new class of reagents is used - ethyl acetate azone products, which generate different functional groups at the expense of the tautomeric weight shift, and as a result, complexation reactions proceed selectively. Dissociation and stability constants for analytical evaluation of organic reagents of this class are also determined.

The aim of this work is to study the complex formation of cooper (II) with azone products of acetyl-acetone, which contain different functional groups.

Method: The mentioned ligands were obtained by azo-conjugation reactions in a weak alkaline environment. The purity of the reagents was controlled spectrophotometric ally by the absorption spectra of the solutions and by the method of thin layer chromatography. Their composition and structure are established by different physic-chemical methods of analysis.

Result: At the expense of shifting the tautomeric equilibrium, the following compounds were obtained: - 3-(2-hydroxy-3-sulfo-5-nitrophenylazo) pentane-2,4-dione(L^1),

3-(2-hydroxy-3,5-disulfophenylazo) pentane-2,4-dione(L^2), 3-(2-hydroxy-3-sulfo-5-chlorophenylazo) pentane-2,4-dione(L^3), 3-(2-hydroxy-4-nitro-phenylazo) Pentane-2,4-dione(L^4), 3-(2-hydroxyphenylazo) pentane-2,4-dione(L^5). The result is also the possibility of their use for the photometric determination of cooper in zinc alloys.

Conclusion. The effect of free ions, masking substances and functional groups on binary and multi-ligand complexes of copper (II) has been studied by photometric method. Optimum conditions and a new class of reagent have been found, the effect of which significantly increases its selectivity.

Keywords: functional groups, influence of tautomeric equilibrium shifts.

1. INTRODUCTION

Photometric methods of analysis are currently widely used for the determination of metals.

Azone compounds are one of the best for the determination of cooper (II).

Complex formation of cooper (II) with azo derivatives of acetyl acetone - 3-(2-hydroxy-3-sulfo-5-nitrophenylazo) pentane-2,4-dione (L^1), 3-(2-hydroxy-3,5-disulfophenylazo) has been studied) pentane-2,4-dione(L^2), 3-(2-hydroxy-3-sulfo-5-chlorophenylazo) pentane-2,4-dione(L^3), 3-(2-hydroxy-4-nitrophenylazo)pentan-2,4-dione (L^4), 3-(2-hydroxy¬xyphenylazo)pentane-2,4-dione(L^5).

2. MAIN PART

experimental part. solutions and reagents.

The reagent is synthesized according to the method [2], its composition and structure are determined by analysis by various physico-chemical methods and are given in figure1(1).

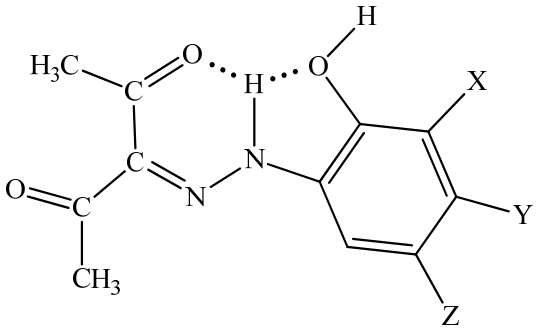

L¹ X = SO_3H; Y = H; Z = NO_2
L² X = Z = SO_3H; Y = H
L³ X = SO_3H; Y = H; Z = Cl
L⁴ X = Z = H; Y = NO_2
L⁵ X = Y = Z = H

Figure 1. of reagents 3-2-hydroxy-3-sulfo-5-nitrophenylazo-Structure of pentanedione

We prepared M solutions of azone compounds ((L^1, L^2, L^3, L^4, L^5) $1\cdot10^{-3}$ by dissolving them in ethanol, and dissolving the reagent in acetone. Fixanol HCl (pH 1-2) and ammonia-acetate solutions (pH 3-11) were used to create the required acidity. We controlled the pH of the solutions using a glass electrode ionometer H-130.

The synthesis was carried out in aqueous and mixed ethanolic solutions. The dissociation constant of the reagents was determined according to the Schwarzenbach equation. The following values of the dissociation constants of the reagents were calculated L^{1-5}:

$$pK_1 = 5{,}71 \pm 0{,}01 \;\; pK_2 = 8{,}84 \pm 0{,}01 \;\; (L^1)$$
$$pK_1 = 6{,}03 \pm 0{,}03 \;\; pK_2 = 9{,}78 \pm 0{,}06 \;\; (L^2)$$
$$pK_1 = 6{,}28 \pm 0{,}01 \;\; pK_2 = 10{,}14 \pm 0{,}01 \;\; (L^3)$$
$$pK_1 = 6{,}35 \pm 0{,}04 \;\; pK_2 = 10{,}22 \pm 0{,}04 \;\; (L^4)$$
$$pK_1 = 6{,}50 \pm 0{,}01 \;\; pK_2 = 10{,}41 \pm 0{,}01 \;\; (L^5)$$

We measured the optical density of the solution on a spectrophotometer "Lambada-40" (PerkinElmer company) with computer support and on a photoelectric colorimeter KFK-2 1 cm. layer thickness in the cuvette. We controlled the pH of the solutions with a pH-121 glass electrode pH meter.

The study of the proteolytic properties of the reagents showed that when the negative inductive effect of the functional groups introduced into the aromatic part of the molecule increases, their acidic properties increase. Based on the quantum-chemical data, it can be assumed that pK_1 characterizes the deprotonation of the –OH group,

which is in the ortho state in the aromatic part of the molecule, and pK 2 - the deprotonation of the hydrazone form (=N–NH–).

Bieru's method is used to determine stability step constants:

$$[\mathrm{L}] = \frac{(2-m)\cdot c_{\mathrm{L}} - [\mathrm{H}^+] + [\mathrm{OH}^-]}{[\mathrm{H}^+]\cdot K_1 + 2[\mathrm{H}^+]^2 \cdot K_1 K_2},$$

$$\alpha_{\mathrm{L(H)}} = 1 + [\mathrm{H}^+]\cdot K_1 + [\mathrm{H}^+]^2 \cdot K_1 K_2,\ \bar{n} = \frac{c_{\mathrm{L}} - [\mathrm{L}]\cdot \alpha_{\mathrm{L(H)}}}{c_{\mathrm{Fe}}}$$

Where $c_{\mathrm{L}} = 2\times 10^{-3}$ mole/l,

$Ccu = 1\times 10^{-3}$ mole/l, Cu : L = 1 : 2, K1 and K2 are reagent protonation constants; m-point of neutralization.

Table 1 shows the logarithms of stability constants of $L^{1\text{-}5}$ complexes.

Table 1

Logarithms of stability constants of $L^{1\text{-}5}$ complexes

L	L^1 [11]	L^2	L^3[11]	L^4	L^5[12]	acetylacetone
lgK_1	10.43±0.02	11.53±0.03	11.68±0.02	11.93±0.05	12.24±0.03	9.8
lgβ_2	20.54±0.04	22.11±0.04	22.63±0.03	22.85±0.04	23.14±0.07	18.8
lgβ_3	–	–	–	–	–	26.4

The results of potentiometric titration showed that the stability constants of FeIII complexes with L1-5 change in the following order: $L^5 > L^4 > L^3 > L^2 > L^1$. The comparison of the stability constants showed that the functional groups introduced into the aromatic part of the molecule affect the change in the order of stability of the complexes, and L^5 complexes are characterized by the highest stability. This is related to the less negative value of the induction effect –H.

The calculation of complex formation functions ($\bar{n}$) showed that they change in the limits of 0 < 2, which in Fe(III) acetylacetonates change as follows: 0 < 3. This shows that when introducing functional groups into the acetylacetone molecule Reaction centers change. It seems that the ratio of components in the complexes during transition from Cu(II) acetylacetonates to acetyl-a-cetonate azo product complexes is related to steric factors and reactivity of tautomeric forms of reagents. Comparison of stability constants shows that complexes with $L^{1\text{-}5}$ are characterized by higher stability. Thus, the high analytical capability of $L^{1\text{-}5}$ ligands can be predicted.

Azone products of acetylacetone react with cooper (II) ions in a weak acidic environment to form yellow soluble compounds. The maximum color of the solutions will be revealed under the following conditions pH 2.0 (λ_{max} = 443 nm) L^1, pH 3.5 (λ_{max} = 414 nm) L^2, pH 4.5 (λ_{max} = 432 nm) L^3, pH 4.5 (λ_{max}= 413 nm) L^4, pH 5.5 (λ_{max} = 395 nm) L^5

The result of the experiment shows that upon introduction of electron-accepting groups into the aromatic part of the molecule, the speed of the complex formation reaction increases, i.e. complexes L^1, L^2, L^3, L^4 და L^5 and are formed within 5, 15, 25, 40 and 55 minutes, respectively, and are stable for a long time. The ratio of reactive components in the complexes is determined by the approximate yield method of Starik-Barbanel, by the methods of equilibrium shift and iso-molar series. The molar absorption coefficients of the complexes were calculated by the saturation method.

The degree of polymerization of the complexes was also calculated according to the following equation [24]

$$\gamma = (\lg A_i / A_k)/[(q+1)\lg\{(c_i\varepsilon l - A_i)/(c_k\varepsilon l - A_k)\}]$$

where A_i, A_R are the optical densities of the complex solutions in tests I and k;ε-complex absorption molar coefficient;l - the thickness of the solution layer in the cuvette, cm; c_i, c_k - copper concentration I and k;q - the number of reagent molecules in the complex.

The polymerization coefficients of the complexes were calculated. It is established that these compounds do not polymerize, they are in monomeric form.

Table 2

Main photometric characteristics of the reaction of cooper (II) with azo products of acetylacetone

reagents	pH	λ_{max}, nm	$\Delta\lambda$, nm	$\varepsilon_{max}\cdot10^{-4}$	Bar interval under Berry's law, μg/ml
1,10-phenanthroline	2-9	512		1.11	
2,2'-dipyridyl	3.5-8.5	522		8.60	
L_1	1.0-4.0	443	50	1.45±0.01	0.11-2.24
L_2	2.5-5.5	414	31	1.34±0.01	0.22-2.24
L_3	2.0-6.0	432	39	1.38±0.01	0.18-2.24
L_4	3.5-6.0	413	67	1.01±0.01	0.22-1.79
L_5	3.5-7.0	395	35	0.83±0.01	0.45-4.03

It can be seen from the table that when a functional group is introduced into the aromatic part of the molecule, the stoichiometry of the components in the complexes does not change, but the molar absorption coefficients increase and significant bathochromic effects were observed during complex formation in the following order: $L^2 < L^5 < L^3 < L^1 < L^4$. It can be seen that there is a correlation between the stability of the complexes and the molar absorption coefficient. The relative sensitivity of the reaction of cooper (II) with L1-5, 1,10-phenan-throline and 2,2-dipyridyl shows that it is the most sensitive using the equation and based on the calculated mole fractions of L1-5 and for ionic forms, construct distribution diagrams of reactants in solutions. under conditions of complex formation [$CuH(L)_2$ pH $_{opt}$ = 2.5-6] The most reactive form of reagents is H_2L, whose content at pH_{opt} is 100%.

The influence of free ions and masking substances on the complex formation process has been studied.

In terms of selectivity, L^1 is superior to 1,10-phenanthroline and 2,2-dipyridyl.

3. CONCLUSION

There were 5 reagents obtained due to the shift of the tautomeric equilibrium. Their dissociation constants were determined according to the Schwarzenbach equation, proteolytic properties were studied and it was shown that when the negative inductive effect of the functional groups introduced into the aromatic part of the molecule increases, their acidic properties increase. Based on the quantum-chemical data, deprotonation of the OH- and hydrazone form (=N–NH–) group in the aromatic part is assumed. Stability step constants are also determined by Bierum's method. By comparing the results of potentiometric titration, a change in the stability constants of Cu(II) complexes with L^{1-5} is shown, and a high analytical capability of L^{1-5} ligands is assumed. The ratio of reactive components in the complexes is determined by the Starik-Barbanel approximate yield method, equilibrium shift and isomolar series methods.

The influence of free ions and masking substances on the complex formation process has been studied. Possibilities of their use for photometric determination of copper in alloys are proposed.

References

1. Bandel S., Prodhan A, / N,N`-bissalisiden-2,3-diamino-benzofuran as an analytical reagent for copper // Bunsekikadaku= J. Jap. Soc Anal. Chem.-1999-48, №4- p. 429-433. (RJXim00.24-19Г.242)10.
2. Chaisuksant R, Palkawong-na-ayuthaya W, Crupan K. / Spectrophotometricdetermination of copper (II) in alloys using napthazarin / Talanta. 2000. 53, №3. - p. 579-585 (РЖХим 01.22-19Г.99)12.
3. ChandakPrite, ShinghalSummet, MathurS.P./ Photometric determination of copper (II) by adsorption on its 1-phenyl-3-(2-thiazolyl) thi-ourea complex on pholyurethane foam // Indian. J. Chem. A.-1997.-36, №5 - p. 453-454. (РЖХим 00.02-19Г.152)4.
4. Desai J.J, Desai P.G., Mehta A.G., /2`-Hyd-roxy-4`-exhoxychalconeoxime as an analytical reagent for copper // Oriental J/Chem.-1999-

15, № 1- p.169-171(RJXIM 00.17-19Г.114)5, 7 page.

5. Gandhe S., Prodhan A., Dave, Gautam M. / 5-(2-methyl-4-N-cyanoethyl-N-benzensulphonylaminobenzylidine)-rhodamine as a selective reagent for rapid spectrophotometric determination of copper, silver and nickel // Oriental J. Chem./-1999-15, №1--p.189-190 (RJXIM 00.12-19Г.135)6.
6. Gao Hong-Wen / Investigation of Al and Cu comlex solutions with calcon and selective competition coordination determination of trace amounts of copper. // J. Chem.anal. 2001.46, №2 – p. 249-259 (RJXim 02.15 19Г.132)15.
7. Gao N.-W., Zhans P.-F / Investigation of copper comlex solutions with new ligand 0-chlorobenzenediazoaminobenzene-p-azobenzene and determination of trace copper in wastewater // J. Indian Chem. Soc-2000-77, № 5. - p..249-251(РЖХим 00.23-19Г.395) 9.
8. IssaV.M., Omar M.M., Rizk M.S., Mohaned S/ Spectrophotometricdetermination of Co (II), Cu (II) and Cd (II) using benzoylformazons // Indian J. Chem. Anal.-1996,-35, №8 - p.718-720 (РЖХим 00.14-19Г.182)6.
9. Işildak İbrahim, AsanAdem, AndaçMüherra /Spectrophotometricdetermination of Cu (II) at low-ug 1-1 levels using cation-exchange microcolumn in flow injection // Talanta – 1999-48, №1. - p. 219-224 (РЖХим 00.17-19Г.117)8.
10. Krishna Reddy V., Mutta Reddy S., Raweendra Reddy P., SreenivasuluReddy T.J. / Individual simultaneous first derivative spectrophotometricdetermination of Cu (II) and V(V) in alloy steels and complex materials with 2-hydroxy-1-napthaldehiydebenzoyl hydrazone // J. Indian Chem. Soc-2002,-79, № 1. - p.71-74 (РЖХим 00.17-19Г.146)15.
11. LongChaoyang, YuYing / (Department of Chemistry, South China Normal University, Guangzhou 510631. China) Huanan Shifandaxuexuebao. Zirankexueban = J.S. China. Norm. Univ. Natur. Sci 2000. №4. - p. 63-66 (01.09-19Г.153)12.
12. Ma Donglan, Xia Dongsheng, Cui Fengling,LiJianping ,Wang Yulu / A new sensitive reagent for identifying and determining Cu (II). // Talanta- 1999-48, №1-p. 9-13 (RJXIM 00.17-19Г.116)8.
13. Nazareth Ronald Aquin, Narayana B, SreekumarN.V./Spectrophotometric determination of copper (II) using 4-vanillideneamino-3-methyl-5-mercapto-1,2,4-triazole// Indian J. Chem. A. 2001. 40.№9. -p.1016-1018 (RJXIM 02.14-19Г.94)15.
14. PawarR.B., Padgaonkar S.B., Sawant A.D. /Piclinoldehydenicotinoylhydrazone for trace level separation and spectrophotometric determination of copper (II)// Indian J.Chem.A. 2001. 40.№12. -p.1359-1361 (RJXIM 02.14-19Г.93)14.
15. PurachatBoonlom, LiawruangrathSaisunee, SooksamitiPonlayuth, Pathanaphani Sauwanee, Buddhassukh Duang / Univariate and simple optimization for the flowinjection spectrophotometric determination of copper (II) using nitroso-R salt as a complexing agent // Anal. Sce. 2001. 17.№3. -p.443-447 (RJXIM 02.12-19Г.118) 14.
16. Sharma K, Marao U, ChaanR.S., Goswaunu A.K., PurohitD.N. /Spectrophoto metric determination of Cu (II) with 3-hydroxy-3-m-

tolyl-l-p-sulphonato (Na-salt) phenyltriazene // Oriental J.Chem.-1999-15, №1. -p.177-178 (RJXIM 00.17-19Г.113)7.
17. Singh Ishwar, Sushma / Spectrophotometric determination of Zn (II), Cd (II), Hg (II), Fe(II), Co(II), Ni(II) and Cu (II) with 2-(4,6-dimethyl-2-pyrlmdylazo)-1-napthol-4-sulphonate, sodium salt. (Department of Chem. M.B. Univ. Rohtak 124001, India). Indian J.Chem.A.: (Inorganic, Bio-inorganic, Theoretical and Analytical Chemistry) 2000. 39, №5. -p.545-547 (RJXIM 01.13-19Г.117)12.
18. Singh Ishwar, YodawSanjiv K. / Spectrophotometric determination of copper (II), silver (I) and palladium (II) with 4-(2,6-diamino-2-pyrlmdylazophenol. (Department of Chem. M.B. Univ. Rohtak 124001, India). Indian J.Chem.A.: (Inorganic, Bio-inorganic, Theoretical and Analytical Chemistry) 2000. 39, №7. -p.784-785 (RJXIM 01.13-19Г.119)12 .
19. TandelS.P.,JadhavS.B., MalveS.P. / Extraction and spectrophotometric determination of Cu(II) with 3-izonitroso-5-methyl-2-hexanone and 5-methyl-2,3-hexanedione dioxime // ISEC 2002: Proceedings of the International Solvent Extraction Conference, Cape Town, 17-21 March, 2002. VI. Marshalltown: S.Afr.Iht. Mining and Met. 2002, p.570-575 (RJXIM 01.20-19Г.156)16, 7.

УДК 543.4:546.72

სპილენძი(II)-ის კომპლექსწარმოქმნა აცეტილაცეტონის აზონაწარმებთან

მ. ცინცაძე, მ. ქოჩიაშვილი, ი. უგრეხელიძე, ნ. იმნაძე

საქართველოს ტექნიკური უნივერსიტეტი, ქიმიური ტექნოლოგიისა და მეტალურგის ფაკულტეტი, ქიმიის დეპარტამენტი

E-mail: m.koridze@yahoo.com

მიზანი. კვლევის მიზანია გამოყენებულ იქნას სპილენძის ფოტომეტრული განსაზღვრისათვის რეაგენტების ახალი კლასი - ეთილაცეტატის აზონაწარმები, რომლებიც ტაუტომერული წონასწორობის გადანაცვლების ხარჯზე წარმოქმნიან სხვადასხვა ფუნქციონალურ ჯგუფებს და შედეგად კომპლექსწარმოქმნის რეაქციები შერჩევითად მიმდინარეობენ. განსაზღვრულ იქნას აგრეთვე დისოციაციის და მდგრადობის მუდმივები ამ კლასის ორგანული რეაგენტების ანალიზური შეფასებისათვის.

რეზიუმე. შესწავლილია სპილენძი(II)-ის კომპლექსწარმოქმნა აცეტილაცეტონის აზონაწარმებთან, რომლებიც სხვადასხვა ფუნქციონალურ ჯგუფებს შეიცავენ.

ფოტომეტრული მეთოდით შესწავლილია გარეშე იონების, შემნიღბავი ნივთიერებების და ფუნქციონალური ჯგუფების გავლენა სპილენძი(II)-ის ბინალური და შერეულ ლიგანდიან

კომპლექსებზე. მონახულია ოპტიმალური პირობები და რეაგენტის ახალი კლასი, რომლის გავლენა მნიშვნელოვნად ზრდის მის შერჩევითობას.

მეთოდები. აღნიშნული ლიგანდები მიღებულ იქნა აზოშეუღლების რეაქციებით სუსტ ტუტე არეში. რეაგენტების სისუფთავეს აკონტროლებდნენ სპექტროფოტომეტრულად L^{1-5}-ის ხსნარების შთანთქმის სპექტრების და თხელფენოვანი ქრომატოგრაფიის მეთოდით. მათი შედგენილობა და აღნაგობა დადგენილია ანალიზის სხვადასხვა ფიზიკურ-ქიმიური მეთოდებით.

დასკვნა. ტაუტომერული წონასწორობის გადანაცვლების ხარჯზე მიღებულია 5 რეაგენტი. განსაზღვრულია მათი დისოციაციის მუდმივები შვარცენბახის განტოლების მიხედვით, შესწავლილია პროტოლიტური თვისებები და ნაჩვენებია, რომ მოლეკულის არომატულ ნაწილში შეყვანილი ფუნქციონალური ჯგუფების უარყოფითი ინდუქციური ეფექტის ზრდისას, იზრდება მათი მჟავური თვისებები. კვანტურ-ქიმიურ მონაცემებზე დაყრდნობით ნავარაუდევია არომატულ ნაწილში OH- და ჰიდრაზონული ფორმის (=N–NH–) ჯგუფის დეპროტონიზაცია. ასევე განსაზღვრულია მდგრადობის საფეხუროვანი მუდმივები ბიერუმის მეთოდით. პოტენციომეტრული გატიტვრის შედეგების შედარებით ნაჩვენებია L^{1-5}-თან Cu(II)-ის კომპლექსების მდგრადობის მუდმივების ცვლილება და ნავარაუდევია L^{1-5} ლიგანდების მაღალი ანალიზური შესაძლებლობა. მორეაგირე კომპონენტების თანაფარდობა კომპლექსებში დადგენილია სტარიკ-ბარბანელის მიახლოებითი გამოსავლიანობის მეთოდით, წონასწორობის გადანაცვლების და იზომოლარული სერიების მეთოდებით.

შესწავლილია გარეშე იონების და შემნიღბავი ნივთიერებების ზეგავლენა კომპლექსწარმოქმნის პროცესზე. შემოთავაზებულია მათი გამოყენების შესაძლებლობები შენადნობებში სპილენძის ფოტომეტრული განსაზღვრისთვის.

საკვანძო სიტყვები: ფუნქციონალური ჯგუფები, ტაუტომერული წონასწორობის გადანაცვლების გავლენა.

THE GEORGIAN CERAMISTS ASSOCIATION JOINED
THE INTERATIONAL CERAMIC FEDERATION SINCE 2008

THE GEORGIAN CERAMISTS ASSOCIATION HAS BEEN A MEMBER
OF THE EUROPEAN CERAMIC SOCIETY SINCE 2002

THE GEORGIAN CERAMIC ASSOCIATION WAS FOUNDED IN 1998
THE MAGAZINE WAS FOUNDED IN 1998

TBILISI, "CERAMICS, SCIENCE AND ADVANCED TECHNOLOGIES", Vol. 25. 2(50). 2023

Reference of magazine is obligatory on reprinting

Print circulation 6,75. Contract amount 50. Printed A4 format.

GEORGIAN CERAMISTS ASSOCIATION. Tbilisi. Str. Kostava 69. Phone: +995 599 151957
E-mail: kowsiri@gtu.ge, Zviad Kovziridze

http://www.ceramics.gtu.ge